

University of Alberta

**Displacement of Water by Gas in Propped Fractures: Effect of Fracture Fluid
Surface Tension, Viscosity, Proppant Wettability and Gravity**

by

Jaskaran Singh Parmar

A thesis submitted to the Faculty of Graduate Studies and Research
in partial fulfillment of the requirements for the degree of

Master of Science
in
Petroleum Engineering

Department of Civil and Environmental Engineering

©Jaskaran Singh Parmar
Fall 2013
Edmonton, Alberta

Permission is hereby granted to the University of Alberta Libraries to reproduce single copies of this thesis and to lend or sell such copies for private, scholarly or scientific research purposes only. Where the thesis is converted to, or otherwise made available in digital form, the University of Alberta will advise potential users of the thesis of these terms.

The author reserves all other publication and other rights in association with the copyright in the thesis and, except as herein before provided, neither the thesis nor any substantial portion thereof may be printed or otherwise reproduced in any material form whatsoever without the author's prior written permission.

ABSTRACT

Inefficient recovery of fracturing water used in multi-stage hydraulic fracturing operations is a growing industrial concern. Non-recovered water can be trapped in the tight rock matrix and/or in the complex fracture network. Trapped water can block the gas flow and damage the reservoir.

This study reports results of various drainage experiments conducted to identify the factors controlling water displacement in propped hydraulic fractures. We conduct two sets of drainage experiments. First set of experiments are conducted by using a proppant packed column which is saturated with frac-fluid. These experiments are used to investigate the role of proppant and fluid characteristics on fluid recovery. Second set of drainage experiments are conducted in a physical fracture model. These experiments are designed to investigate the role of gravity, drawdown, surface tension and proppant wettability on fluid recovery.

The results of this study suggest that gravity plays a dominant role in fracture cleanup and that water cleanup in fractures below well may be inefficient. Increasing the drawdown does not improve water recovery. Reducing surface tension and using treated hydrophobic proppant improves the sweep efficiency and in turn the load recovery.

ACKNOWLEDGEMENTS

First and foremost I would like to thank God for blessing me with this beautiful life. I then pay my sincere thanks and gratitude to my supervisors Dr. Ergun Kuru and Dr. Hassan Dehghanpour for giving me an opportunity to do research under their able supervision. Their constant guidance and support has helped me throughout my degree. Gentlemen, I have learned a lot from your experience. Thanks again.

Special thanks to our lab technician Mr. Todd Kinnee for providing technical assistance in lab and helping me out with my experiments. I also want to thank my lab mates Santhosh Veerabhadrapa, Ankit Doda, Kaiyrzhan, Qing Lan and Mingxiang Xu for assisting me in my experiments. This research was partly supported by Natural Science and Engineering Council of Canada, FMC Technologies and Trican Well Services. Their financial support is highly acknowledged. I would also like to thank Momentive for providing free proppant samples that were used in the experiments.

My deepest regards and thanks to my family, Mummy, Papa, brother Mandip, for their unconditional love and affection. Their support has kept me motivated throughout my life. My heartiest thanks to my dear friends Talwinder, Gleam, Anamika, Gurminder, Arsh and Mani for all the memorable time we spent together.

Last but not the least I want to thank University of Alberta and Department of Civil & Environmental Engineering for great infrastructure and a valuable program in Petroleum Engineering.

TABLE OF CONTENTS

1. INTRODUCTION.....	1
1.1 Overview and Background.....	1
1.2 Problem statement.....	3
1.3 Objectives of the study.....	7
1.4 Methodology.....	8
1.5 Structure of thesis.....	9
2. LITERATURE REVIEW.....	11
2.1 Hydraulic Fracturing Operation.....	11
2.1.1 Introduction.....	11
2.1.2 Multistage Hydraulic Fracturing.....	12
2.1.3 Definitions	13
2.2 Proppants.....	14
2.2.1 Proppant Types.....	14
2.2.2 Proppant Characteristics.....	15
2.3 Fracturing Fluids and Additives.....	16
2.3.1 Properties of Fracture Fluids.....	17
2.3.2 Fracture Fluid Types.....	17
2.3.3 Additives Used In Water Based Fluid.....	18

2.4	Frac- Fluid Recovery: Imbibition of Frac-Fluid Into Rock Matrix.....	20
2.5	Frac Fluid Recovery: Inefficient Fracture Drainage	21
2.5.1	Definitions.....	21
2.5.2	Effect of Capillary Forces.....	23
2.5.3	Effect of Viscous Forces.....	25
2.5.4	Effect of Gravity Forces.....	26
2.5.5	Displacement Instability In Porous Media.....	26
3.	Dimensional Analysis.....	29
3.1	Objective.....	29
3.2	Introduction.....	29
3.3	Procedure.....	29
3.4	Components of Dimensionless Time.....	32
3.5	Sample Calculations of Dimensionless Time.....	32
4.	Column Experiments.....	35
4.1	Material used.....	35
4.1.1	Column.....	35
4.1.2	Mesh.....	35
4.1.3	Frac-fluid.....	36
4.1.4	Proppants.....	36
4.2	Experimental Set Up and Procedure.....	36
4.3	Results.....	39
4.3.1	Effect of Proppant Size.....	39
4.3.2	Effect of Proppant Size Distribution.....	40

4.3.3 Effect of Proppant Type.....	42
4.3.4 Effect of Fracturing Fluid Type.....	45
4.4 Discussion.....	48
4.4.1 Effect of Size.....	48
4.4.2 Effect of Proppant Size Distribution.....	49
4.4.3 Effect of Proppant Type.....	49
4.4.4 Effect of Fracturing Fluid Type.....	49
5. 2D Experiments: Apparatus and Procedure.....	51
5.1 Materials and Equipment.....	51
5.2 Experimental Procedure	55
6. 2D Experiments: Results and Discussion.....	58
6.1 Results.....	58
6.1.1 Effect of Fracture Orientation.....	58
6.1.2 Effect of Drawdown.....	64
6.1.3 Effect of Surface Tension and Proppant Wettability.....	68
6.1.4 Effect of Frac-Fluid Viscosity.....	77
6.2 Discussion.....	80
6.2.1 Experimental Setup Limitations.....	80
6.2.2 Results.....	82
7. Conclusion and Recommendations.....	85
7.1 Conclusions.....	85
7.1.1 Column Experiments.....	85
7.1.2 2D Experiments.....	86

7.2 Recommendations for future work.....	87
8. References.....	88
9. Appendix.....	99

LIST OF FIGURES

Figure 1: Microscopic images showing comparison of pore structure of different reservoir rocks.....	2
Figure 2: Conceptual model showing water drainage in vertical fracture. Water drains with gravity in fractures above the well and against gravity in fractures below the well.....	6
Figure 3: Illustration of vertical and horizontal fracturing.....	12
Figure 4: Schematic showing fracture spacing and half length	14
Figure 5: Illustrates proppant embedment resulting in reduced fracture width	16
Figure 6: Illustration of frac-fluid composition and additives used.....	20
Figure 7: Schematic of the experimental set-up.....	37
Figure 8: Effect of proppant size on water recovery: Normalized cumulative water production versus dimensionless time for different proppant sizes.....	39
Figure 9: Ultimate water recovery vs proppant mean diameter.....	40
Figure 10: Effect of proppant size distribution on water recovery: Normalized cumulative water production versus dimensionless time for coarse, fine and mixed sand.....	41
Figure 11: Effect of different proppant types on fluid recovery: Normalized cumulative water production versus dimensionless time.....	43

Figure 12: Ultimate recoveries for various proppant types.....	43
Figure 13: (a) Contact angle of water on proppant A (b) Contact angle of water on proppant B (c) Contact angle of water on proppant C (d) Contact angle of water on proppant D (e) Contact angle of water on sand.....	44
Figure 14: Effect of fluid type: Normalized fluid recovery versus dimensionless time.....	46
Figure 15: Effect of fluid type: Normalized fluid recovery versus dimensionless time.....	47
Figure 16: Ultimate recovery for different fluid and proppant type.....	48
Figure 17: The picture of experimental cell	51
Figure 18: Light box used to illuminate back side of experimental cell.....	52
Figure 19: Water Trap to capture water sucked during vacuum operation.....	52
Figure 20: DuNouy tensiometer used to measure surface tension.....	53
Figure 21: C-VOR Rheometer.....	53
Figure 22: Experimental setup for drainage in the direction of gravity.....	56
Figure 23: Experimental setup for drainage against gravity direction.....	57
Figure 24: Experimental setup for drainage against gravity direction.....	57
Figure 25: Effect of fracture orientation on water recovery rate.....	59

Figure 26: Images taken during the downward water displacement in the vertical cell show a stable displacement front moving downward at time intervals t1, t2 and t3 (test 1 of set 1).....	61
Figure 27: Images taken during the upward water displacement in the vertical cell show unstable displacement at time intervals t1, t2 and t3 (test 2 of set 1).....	62
Figure 28: Images taken during the horizontal water displacement show unstable displacement front at time interval t1, t2 and t3.....	63
Figure 29: Effect of drawdown on water recovery rate.....	65
Figure 30: Effect of drawdown on drainage pattern at 10 psi drawdown, showing development of fingers at different time intervals t1, t2 and t3.....	66
Figure 31: Effect of drawdown on drainage pattern at 20 psi drawdown, showing development of fingers at time intervals t1, t2 and t3.....	67
Figure 32: Effect of drawdown on drainage pattern at 30 psi drawdown, showing development of fingers at time intervals t1, t2 and t3.....	68
Figure 33: Effect of interfacial tension (Set 3, test 2): Semi-log plot of normalized fluid recovery versus dimensionless time	70
Figure 34: Figure 34: Drainage pattern at time interval t1, t2 and t3 in experimental cell packed with hydrophilic glass beads and saturated with 1 wt% isopropanol solution (test2 of set3).....	72

Figure 35: (a) Contact angle of 1 wt% isopropanol on hydrophobic (treated) glass beads (b) Contact angle of water on hydrophobic (treated) glass beads (c) Contact angle for water on hydrophilic(untreated) glass beads.....	72
Figure 36: Effect of wettability (Set 3, test 2): Semi-log plot of normalized fluid recovery versus dimensionless time.....	73
Figure 37: Drainage pattern at time intervals t1, t2 and t3 in experimental cell packed with hydrophobic glass beads and saturated with water (test3 of set3).....	84
Figure 38: Illustration of formation and growth of gas lumps in a pack of hydrophobic glass beads (t1) Gas lump f1 and f2 is formed (t2) Gas lump f1 becomes discontinuous, gas lump f2 keeps growing (t3) Gas lump f1 disappears and a new gas lump f1' is formed. Gas lump f2 grows and becomes discontinuous.....	75
Figure 39: Effect of surface property (Set 3): Semi-log plot of normalized fluid recovery versus dimensionless time	76
Figure 40: Drainage pattern at time interval t1, t2 and t3 in the experimental cell packed with hydrophobic glass beads and saturated with 1 wt% isopropanol solution (test4 of set 3).....	77
Figure 41: Variation of viscosity of 0.025% xanthan gum solution with shear rate on a log-log plot.....	78
Figure 42: Comparison of the recovery rate for two different fluids	79

Figure 43: Drainage pattern at time interval t1, t2 and t3 in experimental cell saturated with 0.025 wt% xanthan gum solution.....80

Figure 44: Illustration of fracture below horizontal well with reservoir feeding gas into the fracture.....81

Figure 45: Comparing the recovery rate of all the drainage experiments conducted in this study shows three different types of recovery profiles for gravity stable, gravity neutral and gravity unstable tests.....83

LIST OF TABLES

Table 4.1: Fluid properties.....	36
Table 4.2: Experimental conditions to test the effect of proppant size on frac-fluid recovery.....	39
Table 4.3: Experimental conditions to test the effect of proppant size distribution on frac-fluid recovery.....	41
Table 4.4: Experimental conditions to test the effect of proppant type on frac-fluid recovery.....	42
Table 4.5: Experimental conditions to test the effect frac-fluid type on recovery....	45
Table 4.6: Experimental conditions to test the effect frac-fluid type on recovery....	47
Table 6.1: Experimental conditions to test the effect of fracture orientation (Set1).....	59
Table 6.2: Experimental conditions to test the effect of drawdown (Set 2).....	64
Table 6.3: Experimental conditions to test the effect of surface tension and surface property (Set 3).....	69
Table 6.4: Experimental conditions to test the effect of fluid viscosity (Set 4).....	78
Table A.1: Calculation of identity matrix step 1.....	103
Table A.2: Calculation of identity matrix step 2.....	103
Table A.3: Calculation of identity matrix step 3.....	104

Chapter 1

Introduction

1.1 Overview and Background

World's hunger for energy is increasing with each passing year. According to data published by United States Energy Information Administration in 2012, global energy demand has increased by more than 70% in past 30 years. Currently, more than 50% of this energy is supplied by oil and gas industry¹. From past century and a half, conventional oil and gas has been used to meet the ever increasing energy demand. Growing hydrocarbon demand coupled with fast depleting conventional resources has shifted industry's focus towards development of unconventional resources.

Unconventional resources are vast and even greater than conventional resources. But, these resources have been vastly underdeveloped due to high cost associated with its exploitation. Increase in oil and gas prices in mid-2000s coupled with technological advancements pushed back industry's focus towards development of unconventional reservoirs. Lately shale and tight reservoirs, some of the many type of unconventional reservoirs, have caught industry attention. According to a report published by ERCB in 2012 there is 1291 trillion cubic feet (TCF) of shale gas-in-place, in Alberta alone.

Shale reservoirs are composed of fine grained clastic sedimentary rock. Clastic sedimentary rock is composed of shale which is a mixture of flakes of clay mineral and small fragments of other minerals such as quartz and calcite². Shale reservoirs are found at a depth range of 1000 to 13000 ft. Thickness of these reservoirs may vary from 50 to 600 ft with a porosity of 2 to 8% and total organic content ranging from 1 to 14%³. Shale reservoirs have ultra low permeability, in order of nanodarcy. Figure 1 compares the pore structure of different reservoir rocks.

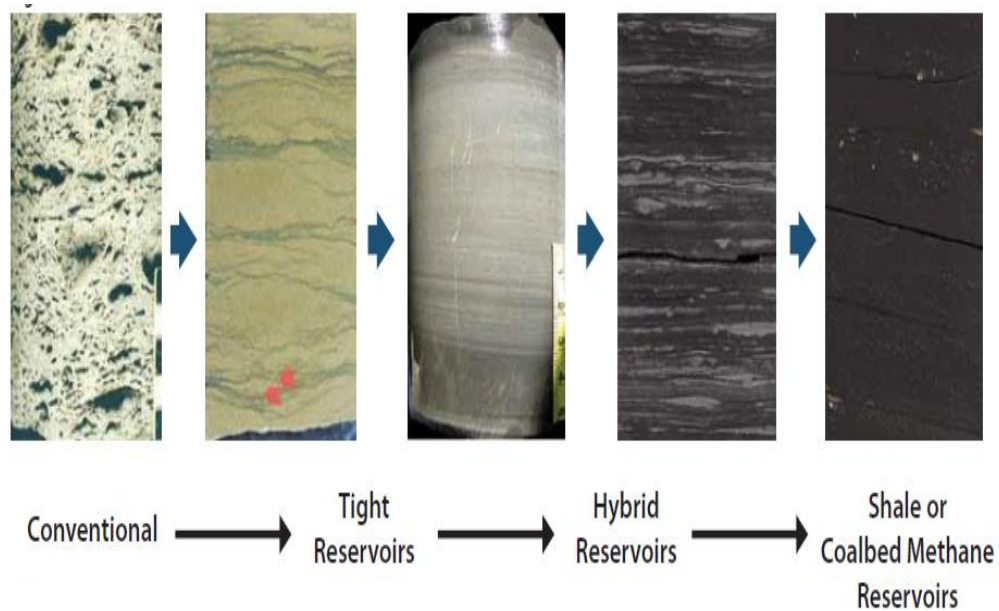


Figure 1: Microscopic images showing comparison of pore structure of different reservoir rocks (source: CSUG hydraulic fracturing brochure)

Due to ultra low permeability, production rate from shale reservoirs is very low and uneconomical.

Hydraulic fracturing, also known as fracking, has proved to be a successful technique for hydrocarbon recovery from shale and tight reservoirs. Hydraulic

fracturing operation involves pumping a mixture of proppants and fracturing fluid into the reservoir through a wellbore, generally horizontal, at a pressure above reservoir fracture pressure. The fracturing fluid is generally water based and water requirement for developing an unconventional reservoir is in order of several million gallons³. Proppant requirement for fracturing can be up to a million pounds per reservoir. The mixture of proppants and water is usually pumped at a rate of 75-150 bbl/min/well³.

1.2 Problem Statement

Hydraulic fracturing involves pumping mixture of fracturing fluid, generally water based, and proppant in large volumes into the formation. Water requirement for fracturing a single well ranges from 1.2 to 3.5 million US gallons^{4,5}. Hydraulically fractured wells often require refracturing in order to maintain economical production rates, thus requiring additional water^{4,5}. It has been estimated that on an average 3 to 8 million US gallons of water is consumed by a single well during its lifetime^{5,6,7}.

Once the reservoir is fractured, the well is shut for certain period of time and then opened for production. Both gas and fracturing fluid are recovered at the surface. The fraction of total injected fracturing fluid, which is recovered during the flowback operation, is referred to as “Load recovered”. Field data shows that usually less than 30% of the total fracturing water is produced back⁸ (i.e. the

load recovery is less than 30%). Recovering the fracturing water is important for two main reasons:

- **Minimizing the formation and fracture face damage:** The water residing in the fracture or rock matrix reduces the hydrocarbon production rate by reducing gas/oil relative permeability^{9,10,11}. This in turn affects the economics of the project.
- **Minimizing the fresh water consumption:** The recovered water can be reused for subsequent fracturing operations, after required treatments. This reduces the total water consumption for developing a specific unconventional field.

Two possible reasons that may be responsible for in-efficient load recovery are:

- Fracturing fluid invasion into the rock matrix due to forced or spontaneous imbibition
- Fracturing fluid retention in the propped fracture due to capillary, gravity and relative permeability effects.

In this research we study the fracturing fluid retention in the fractures or inefficient fracture drainage. Various mechanisms have been proposed for fracturing fluid retention in fractures including capillary pressure, relative permeability, and stress sensitive fracture conductivity¹². Furthermore, the displacement efficiency in propped hydraulic fractures may depend on interfacial tension, viscosity ratio, density ratio, and proppant wettability.

Various column experiments have been conducted ^{13, 14, 15} to study two- and three-phase gravity drainage. Studies done by Howard et al. ²¹ on proppant packed columns shows improved water recovery when surfactants are added to the fracturing fluid. Another study done by Shahidzadeh et al. ¹⁶ shows that wettability significantly influences the drainage behavior¹⁶. They conducted experiments on hydrophobic and hydrophilic glass beads and observed a higher water recovery rate in case of hydrophobic glass beads.

In this study, third reason is proposed, which relates low frac fluid recovery rate to unstable displacement of water by hydrocarbon in the propped fractures. Experimental studies done on packed^{17, 18} and open¹⁹ Hele-Shaw cells show that unfavorable mobility ratio results in unstable displacement front by formation of fingers¹⁸. Fingering causes early breakthrough of non-wetting fluid. This results in large residual saturation of wetting phase in porous media.

In addition to mobility ratio, the direction of displacement relative to gravity direction can influence the sweep efficiency. As shown in Figure 2, in horizontal wells fractures are generated above and below the well. These fractures are generally vertical due to minimum horizontal stress. For fractures above the well, drainage is in the gravity direction and for fractures below the well drainage is against the gravity direction.

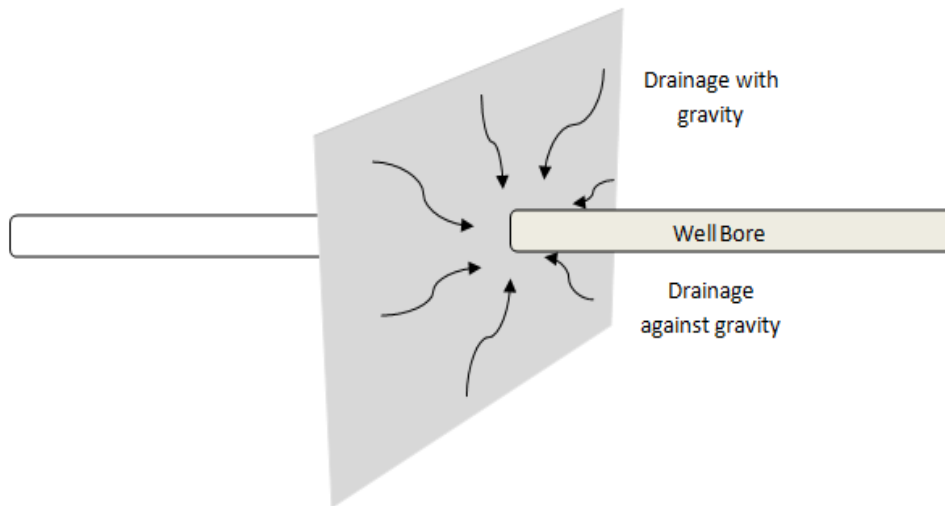


Figure 2: Conceptual model showing water drainage in vertical fracture. Water drains with gravity in fractures above the well and against gravity in fractures below the well

Recently, a simulation study⁵⁷ showed there is inefficient water drainage in fractures below well due gravity effects. Furthermore, in a field study⁵⁶ it was observed that wells placed at the bottom of the formation had better fracture cleanup due to gravity drainage as compared to wells placed at the top of the formation. These studies indicate the dominant role played by gravity in fracture drainage, which needs to be experimentally verified.

Studies conducted in the past mainly focus on viscous and capillary forces to understand drainage and instability in porous media^{19, 20}. Very limited research has been done on instability during drainage against gravity direction, in porous media²³. Most of the studies carried out using Hele-shaw models and by packing sand between glass plates do not take gravity into consideration. Some drainage experiments that have been conducted against gravity direction^{22, 23} are not aimed at studying the factors such as drawdown, surface tension, wettability and viscosity.

In this study, two types of experiments were conducted. One being, one dimensional column experiments to investigate the role of proppant characteristics and fluid properties on fluid recovery.

The second being, 2D fracture model experiments in which glass beads were packed between two glass plates to investigate the effect of fracture orientation, drawdown, interfacial tension, wettability and viscosity on displacement efficiency and stability.

1.3 Objectives of the Study

The objectives of this study are

- To study the effect of proppant characteristics and fluid properties on fracture drainage using column experiments
- To study the effect of gravitational, viscous and capillary forces on fracture drainage using 2D propped hydraulic fracture model
- Develop dimensionless scaling parameter (in this case dimensionless time) using variables involved in experiments, to upscale the results from lab to field scale.

1.4 Methodology

The objectives mentioned above were accomplished by using the following methodology

- 1) Dimensional analysis of the experimental variables was conducted by using the procedure proposed by Peters²⁴. An expression of dimensionless time was developed as a function of the variables considered in the experimental study.
- 2) Effect of proppant characteristics was studied by changing the size, size distribution and type of proppants using column experiments.
- 3) Effect of fluid characteristics was studied by comparing the results of normal water and oil as fracturing fluids, using column experiments
- 4) Effect of gravitational force on the fracture drainage was studied by changing the orientation of the 2D propped fracture model to
 - (a) Horizontal, with gas injection from the side
 - (b) Vertical, with gas injection at the bottom of the cell (Gravity unstable)
 - (c) Vertical, with gas injection at the top of the cell (Gravity stable)
- 5) Effect of viscous forces was studied with the help of two experiments conducted by using 2D fracture model. In first experiment, gas was injected at a pressure of 10, 20 and 30 psi while keeping the production end open to atmosphere. In second experiment, viscosity of water, used as frac-fluid, was increased by adding 0.025 wt% Xanthan gum. Results from this test were then compared with normal water test to understand viscosity effect. In both experiments drainage direction was against gravity direction.

6) Effect of capillary forces was studied in two ways. In first experiment surface tension of frac-fluid was reduced by adding isopropanol. In second experiment, wettability of the glass beads, being used as proppants, was altered from hydrophilic to hydrophobic. Results of both the experiments were then compared with normal water test. In both the experiments drainage direction was against gravity direction.

1.5 Structure of Thesis

Chapter 1 gives a brief overview about unconventional resources, introduces to the problem and discusses the aim of conducting the study and methodology used to solve the problem

Chapter 2 introduces the hydraulic fracturing process. It then discusses the previous studies relating to low frac-fluid recovery during the flow back operations.

Chapter 3 explains the dimensional analysis approach used to obtain dimensionless time

Chapter 4 presents the experimental procedure and results for column experiments

Chapter 5 discusses experimental apparatus and procedures used for 2D fracture model experiments

Chapter 6 presents and discusses the results of 2D fracture model experiments

Chapter 7 presents conclusions based on the experimental results along with some recommendations for future work

Chapter 2

Literature Review

This chapter introduces the hydraulic fracturing process. It then discusses the previous studies related to low frac-fluid recovery during flow back operation.

2.1 Hydraulic Fracturing Operation

2.1.1 Introduction

Hydraulic fracturing is a very common technique used to enhance hydrocarbon recovery from shale and tight reservoirs. Fracturing operation involves pumping millions of barrels of fracturing fluid³, generally water based, mixed with proppants at pressures above the reservoir fracture pressure. High injection pressure causes the reservoir to fracture, creating large interface between reservoir and the well bore. Proppants keep the fracture open, thus maintaining the conductive paths.

Hydraulic fracturing can be carried out following the completions of both vertical and horizontal wells. Figure 3 illustrates the types of well completions. Due to recent technological advances in horizontal drilling, horizontal well completion has been used increasingly for low to very low permeability reservoirs²⁶. Moreover, horizontal well have following advantages over vertical wells²⁵

- The interface created between rock matrix and well bore is much higher in a horizontal well as compared to a vertical well. Thus, more hydrocarbons can be

produced from a single well in horizontal well completion.

- In horizontal drilling, the same surface location can be used to drill multiple wells. This in turn reduces the ground surface footprint of the horizontal wells compared to vertical wells to produce same amount of hydrocarbon.

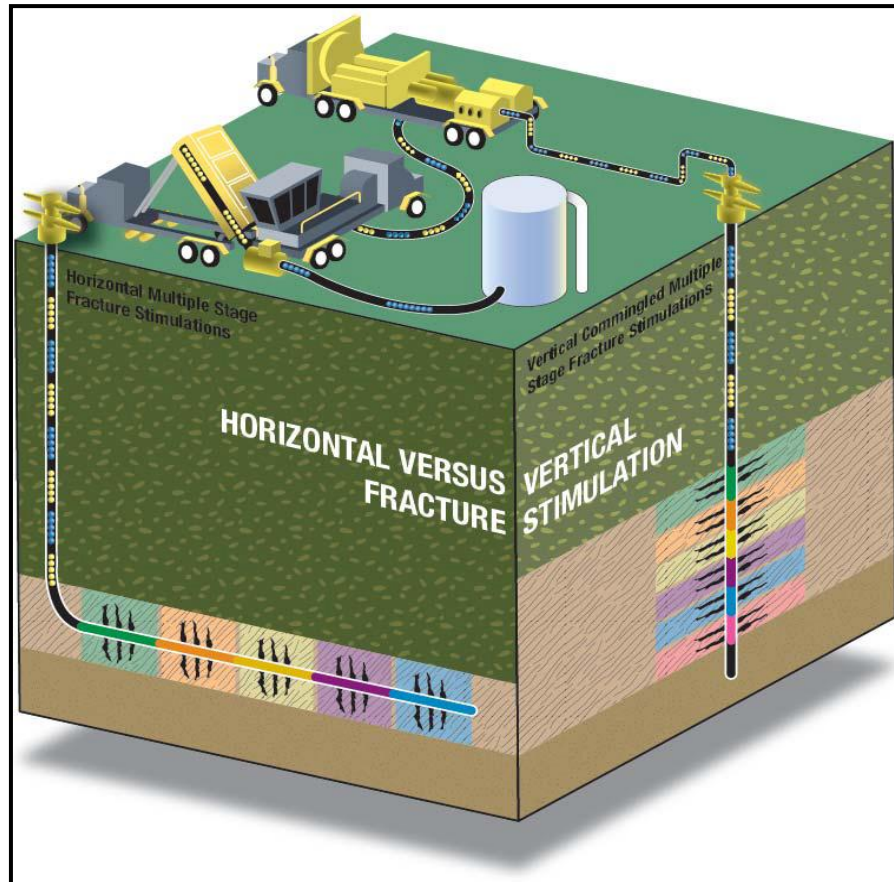


Figure 3: Illustration of vertical and horizontal fracturing (Source: June Warren Publishing, 2008)

2.1.2 Multistage Hydraulic Fracturing

Hydraulic fracturing in horizontal well completions is usually carried out in multiple stages, also known as multi-stage hydraulic fracturing. Multistage hydraulic fracturing is carried out using plug and perf technique.

In plug and perf technique, initially perforation is carried out at the toe end of the horizontal well bore. High pressure frac-fluid is then pumped into the wellbore, causing the reservoir to fracture in that section (also called stage). After completion of the first stage, the fractured section is temporarily plugged and isolated and a new section is perforated and fractured. This process goes on until the entire length of the horizontal wellbore has been fractured²⁶.

2.1.3 Definitions

This section outlines some common definitions used in hydraulic fracturing. Moreover, it will help the reader to better understand physics of hydraulic fracturing.

- **Fracture spacing:** It is the distance between two consecutive fractures. In Figure 4 it is represented by “D”.
- **Fracture half length:** It is the half of the total length of the fracture. In Figure 4 fracture length is represented by “ x_f ” and $x_f/2$ would be fracture half length.
- **Fracture conductivity:** It is defined as the product of fracture permeability and fracture width.

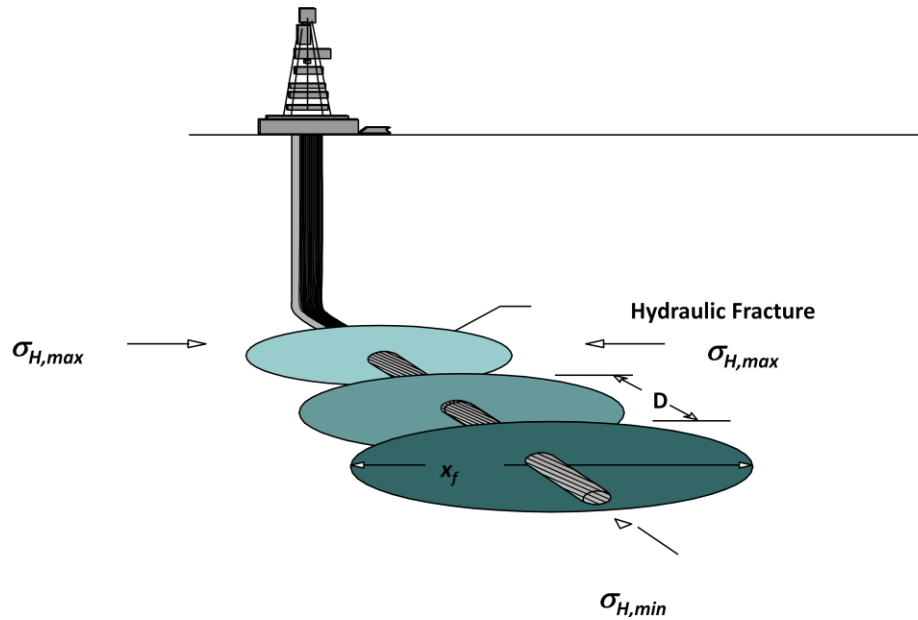


Figure 4: Schematic showing fracture spacing and half length (Source: Valko²⁷)

2.2 Proppants

Stresses in the reservoir rock tend to close the fracture²⁸. This in turn reduces the matrix well bore interaction. Proppants pumped with the fracturing fluid keep the fracture open by overcoming the fracture closure stresses. For most of the fracturing operations sand with small size, in the range of 100 mesh, is used as proppant. Large sizes of proppant (40/70, 30/50 and 20/40) are used when conductivity is important³².

2.2.1 Proppant Types

In addition to sand, industry is using many other types of proppants. Broadly, they can be classified into three types³³.

1. Normal sand: It is composed of quartz. Due to its low cost and ease of availability, sand is the most commonly used proppant in the industry.

Studies show that cyclic stresses results in crushing of normal sand resulting in lower fracture conductivity as compared to resin coated proppants.³⁴

2. Resin coated proppant: It is normal sand uniformly coated with different resins. When used as proppant, it results in better conductivity, compared to normal sand³⁴. But they are expensive.
3. Ceramics: It is composed of ceramic particles. They have very high fracture strength which results in high fracture conductivity³³. Also, they are environmentally friendly. Similar to resin coated ceramics, they are expensive.

2.2.2 Proppant Characteristics

Proppants are constantly subjected to stresses due to fracture closure stress and cyclic stresses caused by shut-ins and workovers²⁹. Stresses cause the proppant particles to break into small particles or embed into the formation²⁹, also known as proppant fine generation and proppant embedment respectively. In a study³⁰, it was found that 5% proppant fine generation cause, 54% loss in fracture conductivity. Furthermore, proppant embedment results in reduced fracture width and can also result in lower fracture conductivity³¹.

Therefore, proppants must be carefully selected to ensure maximum fracture flow capacity. Following are some of the proppant characteristics that may help in achieving the desired goal²⁸

1. Sufficient compressive stress and malleability to overcome fracture closure stresses and ensure maximum fracture conductivity

2. Maximum size and narrow size distribution range which ensures easy injection into the fracture
3. Sphericity of the particles should be close to one so that stress distribution is uniform
4. Inert to formation fluids and fracturing fluid additives
5. Specific gravity ranging from 0.8-3.0
6. Low cost and readily available

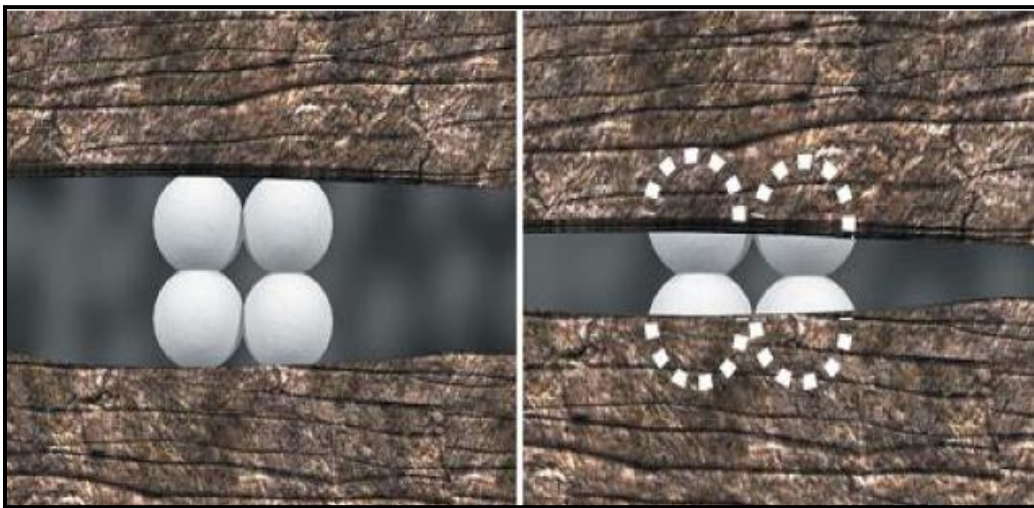


Figure 5: Illustrates proppant embedment resulting in reduced fracture width
(Source: Terracina et al., 2010)

2.3 Fracturing Fluids and Additives

Fracturing fluid along with proppants is pumped into the reservoir to fracture the reservoir rock. Fracturing fluid helps to keep the fracture open and transport the proppants into the fractures. This goal is mainly achieved due to viscous properties of the fracturing fluid. In addition to viscous properties, there are many other properties that needs to be taken care in order ensure good fracking job. Desired

properties of fracturing fluid are listed in the following section

2.3.1 Properties of Fracture Fluids

Some key properties of the fracturing fluid which ensure good fracture job are^{28,35}

- Low leak-off rate into the formation so that it does not affect hydrocarbon production
- Ability to effectively transport proppants in the fractures
- Low friction loss during pumping
- Should be easy to remove from the formation

2.3.2 Fracture Fluid Types

Based on the above mentioned properties different type of fracturing fluid can be used for frac-job. The two most common type of fracturing fluids used by the industry are:

1) Hydrocarbon based: First frac-fluid used to fracture reservoir was oil based²⁸. It was prepared by thickening gasoline with Napalm, an aluminum fatty acid salt. Studies show that hydrocarbon based fluids results in higher production rates^{36,37}. Also, they have better flow back efficiency as compared to water based fluids³⁷. These fluids are particularly used for the hydrocarbon bearing formations which are sensitive to water. Safety issues³⁸ and high cost are the two drawbacks of the hydrocarbon based fluids.

2) Water based: More than 90% of the frac-fluid being used by the industry is water based³⁹. This is so because water is cheap and easily available. Moreover, as

opposed to hydrocarbon based fluids there are no fire hazards associated with water based fluids. One key problem associated with water based fluid is the low recovery of water used in fracturing operation⁸. Non recovered water causes formation damage and thus resulting in low hydrocarbon production rates^{9,10,11}.

2.3.3 Additives Used In Water Based Fluid

As shown in Figure 6, 99% of the frac-fluid is composed of water and sand (proppant). Less than 1% of the frac-fluid is composed of additives. These additives perform number of functions in order to make the fracture treatment effective. Some of these additives along with their functions are listed below.

- 1. Friction reducers:** They are used to reduce the friction in the system and ensure that low pumping pressure is required to pump the fluid into the reservoir. Common example of friction reducer is poly acrylamide with a concentration in the range of 0.01-0.1 wt%⁴¹.
- 2. Biocides:** Their function is to prevent the growth of organic material, such as algae and bacteria, in the system. Common example of biocide, used in fracturing job, is quaternary amine with a concentration in the range of 0.005 to 0.1 wt%^{40,41}.
- 3. Scale inhibitors:** Some minerals are produced from the shale reservoirs. Minerals such as Calcium Sulfate, Calcium Carbonate, and barium sulfate can cause scaling problems. It is further aggravated by high pressure differential and low temperatures. Dissolved minerals are deposited on the sides of well which can be detrimental to production⁴¹.

- 4. Clay stabilizers:** Shale reservoirs having significant amount of clay needs clay stabilizer. Normally KCl is used to stabilize the clay present in the reservoirs.
- 5. Surfactants:** Surfactants are the most common frac-fluid additive. Their main purpose is to reduce interfacial tension and increase flow back efficiency. In some cases, they can also be used to provide foam stabilizing action²⁸.
- 6. Gelling agents:** Gelling agents are used to increase the viscosity of the frac-fluid. This in turn reduces the fluid leak off into the rock matrix and help in better transportation of the proppants. The most commonly used gelling agent is guar gum²⁸.
- 7. Cross linkers:** Cross linkers are used in small quantities. They help to join the polymer in three dimensional space⁴². Most commonly used cross linkers are Boron and Zirconium.
- 8. Breakers:** Once the proppants have been placed in fractures by the frac-fluid, viscosity needs to be reduced in order to increase the flow back efficiency. Breakers break the viscosity of the cross linked polymer and help to increase recovery of frac-fluid³⁵. Breakers are generally acids, oxidizers, or enzymes. Commonly used breakers are ammonium persulfate and ammonium sulfate.

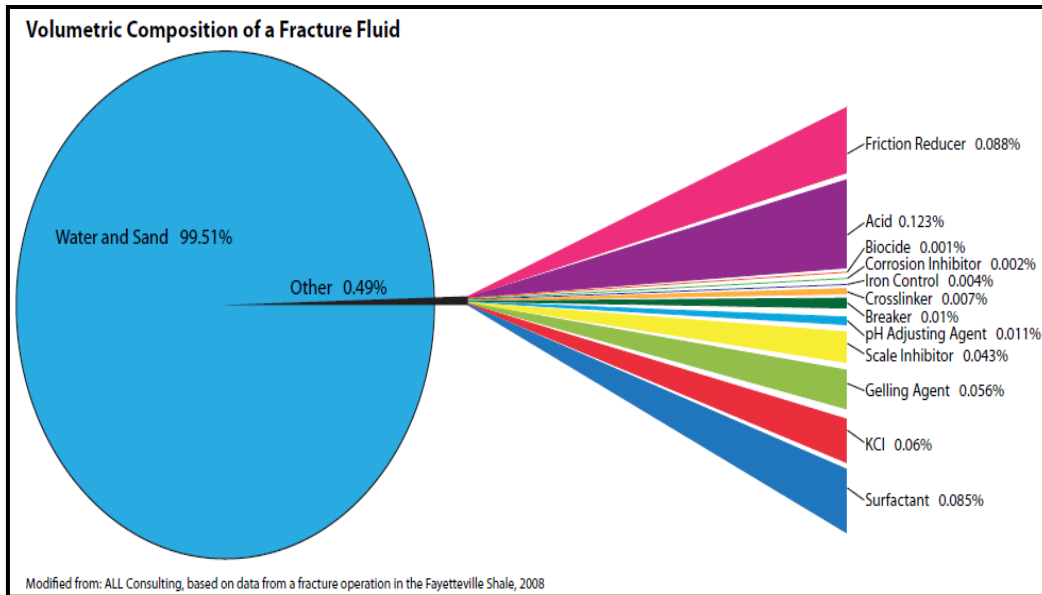


Figure 6: Illustration of frac-fluid composition and additives used ((source: CSUG hydraulic fracturing brochure)

As mentioned earlier water based fluids have poor flow back efficiency. Two possible reasons for low flow back efficiency can be:

1. Imbibition of frac-fluid into rock matrix
2. Inefficient fracture drainage

2.4 Frac-Fluid Recovery: Imbibition of Frac-Fluid into Rock Matrix

One school of thought supports the idea that water injected into the formation imbibes into the rock matrix. Shale reservoirs have very low permeability and it has been shown that as the permeability of the porous media decreases, capillary pressure increases⁴³. High capillary pressure in shale reservoirs results in spontaneous imbibition of fracturing water, which is usually the wetting phase, into the rock matrix. Imbibition of the fluid into the rock matrix causes high water saturation (25-40%)³² near the fracture region. This results in significant reduction

of gas permeability in the invaded zone, also known as fracture face damage^{48,49}, and thus loss in hydrocarbon production rate⁴⁷.

Imbibition of fluid into the rock matrix can be minimized by reducing capillary forces in the rock matrix. These forces can be minimized by using surfactants⁴⁴ or non water wetting agents (used to alter the wettability of rock) in fracturing treatment⁴³. Studies show that fluorochemicals can be used to reduce capillary pressure in rock matrix by altering the wettability of the formation from liquid wet to gas wet^{45,46}. Moreover, for drawdown greater than capillary pressure during flow back, water imbibition into the rock matrix doesn't take place^{10,47}.

Similarly, the rheological properties of the fluid may also be modified to reduce the fluid leak off into the rock matrix⁵⁰. The desired goal can be achieved in two ways:

- Increasing the viscosity of the frac-fluid by using high concentration of gelling agents or cross linkers^{51,52}
- Developing thick filter cake on the fracture face using fluid additives such as starch, mica, silica flour etc⁵³.

Both above mentioned techniques can result in loss of permeability to gas, once the production is started⁵⁰.

2.5 Frac Fluid Recovery: Inefficient Fracture Drainage

Apart from fluid leak off into the rock matrix, fluid may also stay in the fractures. This is also the main focus of this study. Before proceeding to the factors that

impact fracture cleanup, let us familiarize ourselves with some definition which will help understand the discussion presented in the later part of this section.

2.5.1 Definitions

- **Mobility ratio (M):** It is defined as the ratio of mobility of the displacing fluid to the mobility of displaced fluid. In gas water drainage it is defined as

$$M = \frac{\lambda_g}{\lambda_w} = \frac{\left(\frac{k_g}{\mu_g} \right)}{\left(\frac{k_w}{\mu_w} \right)} \quad (2.1)$$

Where,

λ_g, λ_w : Mobility of gas and water respectively in porous media

k_g, k_w : Effective permeability of gas and water respectively in porous media

μ_g, μ_w : Viscosity of gas and water respectively

- **Displacement efficiency⁶⁸:** It is defined as the fraction of displaced fluid recovered (water in our case) by flooding the displacing fluid (gas in our case). Sometimes it is also referred to as local sweep efficiency⁶⁵. In gas water drainage it will be

$$E_D = \frac{V_i - V_r}{V_i} \quad (2.2)$$

Where,

E_D = Displacement Efficiency

V_i : Volume of water before starting gas flood

V_r : Volume of water after the gas flood

- **Areal sweep efficiency⁶⁵**: It is defined as the area swept by the displacing fluid front to the total area of the porous media.

2.5.2 Effect of Capillary Forces

Capillary pressure in porous media is defined by Young-Laplace equation (2.3)

$$P_c = \frac{2\sigma \cos\theta}{r} \quad (2.3)$$

Where,

P_c : Capillary pressure

σ : Surface tension

θ : Contact angle

r : Pore radius

Capillary pressure is also defined as the pressure difference between the non-wetting and wetting phase. Capillary pressure is a pore scale phenomenon which makes it significant with respect to other forces that governs displacement⁵⁴. For displacement of wetting phase by non-wetting phase (drainage) capillary forces act against the flow. Therefore, to increase displacement efficiency during drainage it becomes important to minimize capillary forces.

Individual effect of each of the variables, constituting capillary pressure, on drainage in porous media is discussed below

- **Surface tension**: From equation 2.3 it can be deduced that capillary pressure decreases with decrease in surface tension. Surfactants are generally used in the frac-fluid to reduce surface tension. A study conducted on flowback aid

using proppant packed column shows improved frac-fluid recovery when surfactants are added to frac-fluid.

- **Wettability:** Equation 2.3 suggests that as the contact angle increases, capillary pressure decreases. If contact angle of a fluid on porous media is less than ninety degrees it is called preferential wetting phase and if contact angle is greater than ninety degrees it is called non-wetting phase . In a previous study¹⁶ done by saturating proppant packed column with water, an increase in water recovery was observed by changing the wettability of glass beads from hydrophilic to hydrophobic. In another study⁵⁵ conducted by water flooding oil saturated cores, it was observed that oil recovery of water wet cores was higher than that of oil wet cores. These studies indicate that for better recovery of the saturating fluid, displacing fluid should be the wetting phase.

- **Pore size:** Equation 2.3 suggests that as the pore size (r) decreases, capillary pressure increases. This means that large pores can be easily invaded by the displacing fluid⁵⁴. Moreover, in a study³⁶ conducted on proppant pack column, it was shown that coarse proppants had better fluid recovery than fine proppants due to greater pore size. This indicates at the importance of proppant size in fracture cleanup.

Studies^{12,29} show that cyclic stresses, due to shut-ins and high production rates, results in crushing of proppants. This in turn decreases the pore size and increases the capillary pressure. This means that strength of the proppants also play a critical role in fracture cleanup.

2.5.3 Effect of Viscous Forces

Two parameters which contribute to viscous forces during drainage in porous media are:

- **Viscosity:** Viscosity of the frac-fluid is increased by adding gelling agents for better transportation of proppants into the fractures. Fracture closure stresses cause the filtration of frac-fluid. Due to small pore size of tight reservoir only water molecules are able to invade into the rock matrix and polymer molecules accumulate in the fracture. This increases polymer concentration in the fracture¹⁷. In a study³¹ it was shown that polymer concentration in the fracture was 5 to 7 times the initial concentration. Increased polymer concentration in fractures lead to reduced porosity. Moreover, it has been found that 10% reduction in porosity results in 35% loss in permeability¹⁷. This in turn makes it difficult to displace the frac-fluid in the fractures. This in turn reduces hydrocarbon production rate.
- **Drawdown:** For fast displacements, where viscous forces exceed capillary forces, displacement is controlled by viscous forces⁵⁴. In a study²⁰ gas was injected into water saturated sand pack and it was observed that increase in differential pressure did not result in any increase in water recovery. The reason discussed by the author was that the minimum differential pressure applied for the tests exceeded capillary pressure gradient. Therefore, for drawdown greater than capillary pressure, capillary forces have no effect^{10,47}.

2.5.4 Effect of Gravity Forces

Gravity can significantly impact drainage in fractures. In a field study⁵⁶, a comparison of wells placed at the top and bottom of the formation was done. The wells compared had the same completion, same lithology and were placed in the same reservoir. It was found that the well placed at the bottom of the formation had better fracture cleanup and had high ultimate gas recovery as compared to well placed at the top. The reason discussed by the author was that when well is placed at the bottom of the formation, gravity assists frac-fluid drainage in fracture. This results in better fracture cleanup. Consistently, a simulation study⁵⁷ showed that fractures created above the horizontal well bore cleanup up better as compared to fractures created below the well. The reason discussed by the author was that in fractures below the well water drainage is against gravity hence fracture cleanup is poor. Whereas for fractures above well water drainage is in the direction of gravity, which in turn facilitates more water drainage and improved water recovery.

2.5.5 Displacement Instability in Porous Media

Interplay of all the forces discussed earlier can make displacement of one fluid by another in a porous media either stable or unstable. Displacement in a porous media is said to be stable if there is a uniform displacement front without formation of preferential paths or fingers. Unstable front leads to fingering, which in turn results in early breakthrough of displacing fluid, hence low sweep efficiency. Various experimental (mostly using Hele shaw models) and numerical studies have been conducted to understand the interplay of these forces and their effect on instability⁵⁸⁻⁶³. Onset of instability in porous media was described by Chouke's theory⁶³. For

displacement of fluid 1 by fluid 2, a system is unstable for all displacement velocities (V) greater than a critical displacement velocity (V_c).

$$V_c = \frac{(\rho_1 - \rho_2)g \cos \alpha}{\left(\frac{\mu_2}{k_2} - \frac{\mu_1}{k_1}\right)} \quad (2.4)$$

Provided that perturbation, caused due to unbalanced forces, contains a wavelength which is greater than critical wavelength (λ_c) given by the equation (2.5)

$$\lambda_c = 2\pi \sqrt{\frac{\sigma^*}{\left(\frac{\mu_2}{k_2} - \frac{\mu_1}{k_1}\right)(V - V_c)}} \quad (2.5)$$

This means that $V > V_c$ is the necessary condition for instability and $\lambda > \lambda_c$ is the necessary and sufficient condition.

Where,

μ_1, μ_2 : Viscosity of fluid 1 and 2 respectively

k_1, k_2 : Absolute permeability of fluid 1 and 2 in porous media respectively

ρ_1, ρ_2 : Density of fluid 1 and 2 respectively

g : Gravitational constant

α : Angle of the model from the vertical (0° for displacement of fluid 1 by fluid 2 vertically against gravity)

σ^* : Effective surface tension

σ : Bulk surface tension

λ_c : Critical wavelength of perturbation

V_c : Critical displacement velocity

V: Displacement velocity

Also, σ^* is proportional to σ

Chapter 3

Dimensional Analysis

3.1 Objective

Objective of this section is to develop a systematic dimensional analysis of variables involved in frac-fluid displacement by gas in propped fractures and obtain dimensionless time for propped fracture model. Results of all the following experiments are expressed in terms of dimensionless time (t_d).

3.2 Introduction

We wish to develop dimensionless groups based on our experimental variables. These dimensionless groups will be arranged to develop dimensionless time. The resulting dimensionless time will be used to scale up the experimental results to field cases. Field values of different parameters will be substituted in the dimensionless time to obtain the equivalent of lab time in field conditions.

3.3 Procedure

Step 1

Reduce the number of variables by combining some variables. For example gravity segregation is expressed as $\Delta\rho g$. Therefore we can replace ρ_w , ρ_{air} and g with one variable $\Delta\rho g$

The following are the experimental variables:

ΔP = Drawdown

d_p = Proppant diameter

t = Time

L = Length of experimental cell

W = Width of experimental cell

h = Thickness of experimental cell

μ_g = Injection gas viscosity

μ_L = Frac-fluid viscosity

$\Delta\rho g$ = Gravitational forces

$\sigma \cos \theta$ = Capillary forces

Step 2

Form the power product of all the variables listed above to obtain a dimensionless constant

$$(\Delta P)^{x_1} * (d_p)^{x_2} * (t)^{x_3} * (L)^{x_4} * (\Delta\rho g)^{x_5} * (\sigma \cos \theta)^{x_6} * (\mu_g)^{x_7} * (\mu_L)^{x_8} * (h)^{x_9} * (W)^{x_{10}} = \text{Dimensionless constant} \quad (3.1)$$

Step 3

Express each of the variables in terms of basic dimensional variables i.e. mass (M), length (L) and time (T).

$$[ML^{-1}T^{-2}]^{x1} * [L]^{x2} * [T]^{x3} * [L]^{x4} * [ML^{-2}T^{-2}]^{x5} * [ML^{-2}]^{x6} * [ML^{-1}T^{-1}]^{x7} ** \\ [ML^{-1}T^{-1}]^{x8} * [L]^{x9} * [L]^{x10} = \text{Dimensionless constant} \quad (3.2)$$

Step 4

Since the right side of equation 3.2 is a dimensionless constant. Therefore, it can be represented as $[M^0L^0T^0]$. Now, equating the powers of mass, length and time on both sides gives us following linear homogenous equations. Equation 3.3, 3.4 and 3.5 are obtained by equating the powers of mass, length and time on both sides.

$$M: x1 + x5 + x6 + x7 + x8 = 0 \quad (3.3)$$

$$L: -x1 + x2 + x4 - 2x5 - 2x6 - x7 - x8 + x9 + x10 = 0 \quad (3.4)$$

$$T: -2x1 + x3 - 2x5 - x7 - x8 = 0 \quad (3.5)$$

There is a detailed theory available to obtain non-trivial solution for set of linear homogenous equation such as 3.6. However, we use a small part of that theory to obtain solution to our linear homogenous equation (3.6). The solution gives us a complete set of independent dimensionless groups. One of these dimensionless groups is dimensionless time (t_d).

$$t_d = \left(\frac{d_p^3}{L * W * h} \right) * \left(\frac{\mu_g}{\mu_L} \right) * \left(\frac{d_p * \Delta \rho g}{\Delta P} \right) * \left(\frac{\Delta P}{d_p * (\sigma \cos \theta)} \right)^{0.5} * t$$

Detailed calculations used to obtain dimensionless time (t_d) are available in appendix.

3.4 Components of Dimensionless Time

Various components of dimensionless time can be described as follows:

$\left(\frac{d_p^3}{L*W*h}\right)$: Accounts for geometrical properties of fracture

For column experiments this component will be $\left(\frac{d_p^3}{D^2*L}\right)$

For 2D experiments this component will be $\left(\frac{d_p^3}{L*W*h}\right)$

Where,

D: Diameter of column

L: Length of column

$\left(\frac{\mu_g}{\mu_L}\right)$: Ratio of viscosity of displacing fluid and displaced fluid

$\left(\frac{d_p*\Delta\rho g}{\Delta P}\right)$: Ratio of gravity to viscous forces

$\left(\frac{\Delta P}{d_p*(\sigma \cos \theta)}\right)$: Ratio of viscous to capillary forces

3.5 Sample Calculations of Dimensionless Time

An example calculation to show how the lab time scale can be correlated to field time scale is given below:

We know,

$$t_d = \left(\frac{d_p^3}{L*W*h}\right) * \left(\frac{\mu_g}{\mu_L}\right) * \left(\frac{d_p*\Delta\rho g}{\Delta P}\right) * \left(\frac{\Delta P}{d_p*(\sigma \cos \theta)}\right)^{0.5} * t$$

For lab conditions

Proppant size = 16/30

Mean diameter for given mesh size was calculated using following formula

$$\text{Mean diameter (in)} = 0.4114 * \left(\frac{1}{(\text{small mesh size})^{1.06}} + \frac{1}{(\text{large mesh size})^{1.06}} \right)^{0.64}$$

Length of cell = 1 ft

Width of cell = 1 ft

Thickness of cell = 0.375 in

Viscosity of gas = 0.000165 Poise @ STP

Density of gas = 4.614 kg/m³ @ STP

Viscosity of frac-fluid = 0.01 Poise

Density of frac-fluid = 1000 kg/m³

Drawdown = 20 psi

Surface tension = 72 dynes/cm

Contact angle = 0°

$$t_d = 3.13349E-08 * t_{lab} \quad (3.11)$$

If the following data is assumed for field conditions

Proppant size = 40/70

Fracture height = 100 ft

Fracture half-length = 1000 ft

Fracture width = 0.01 in

Gas viscosity (methane) = 0.000011 cP @STP

Gas density (methane) =

Frac-fluid viscosity = 10 cP

Frac-fluid density = 1000 kg/m³

Drawdown = 100 psi

Surface tension between fluids = 72 dynes/cm

Contact angle = 0°

$$t_d = 1.82E-12 * t_{field} \quad (3.12)$$

Equating equations 3.11 and 3.12

$$3.13349E-08 * t_{lab} = 1.82E-12 * t_{field}$$

$$t_{field} = 17217.69705 t_{lab} \quad (3.13)$$

If we substitute $t_{lab} = 1$ sec in equation 3.13, then 1 sec in lab equals 4.78 hours in field.

Chapter 4

Column Experiments

Experiments in this chapter are designed to test the effect of different proppant and frac-fluid characteristics on fluid recovery. A column is packed with proppants, saturated with frac-fluid and allowed to drain under the influence of gravity. The amount of fluid recovered is plotted against dimensionless time, developed in previous chapter.

These experiments will serve as base case for 2D experiments presented in the following chapters. It is important to note here that, experiments in this chapter are designed for a comparative study and may not represent the actual fracture drainage. Recovery values of these experiments should not be compared with field values because capillary rise effect in column is significant compared to total length of the column used.

4.1 Material used

The material used for the experiments is discussed in this section.

4.1.1 Column

A cylindrical column made up of plexi-glass was used in the experiments to model fracture. The dimensions of the column were 12” in height and 1” in diameter. It was then packed with proppants and saturated with frac-fluid.

4.1.2 Mesh

A screen with 120 mesh size was fixed at the bottom of the column so that the

proppants were properly confined within the column.

4.1.3 Frac-fluid

Two different frac-fluids, water and mineral oil, were used in the experiments. The physical properties of these fluids are listed in Table 4.1.

Table 4.1: Fluid properties

Fluid	Plastic Viscosity(cP)	Surface tension (mN/m)	Specific Gravity
Water	1	72	1
Mineral Oil	18	24	0.8

4.1.4 Proppants

Four commercially available resin coated proppants and normal sand were used as proppants. The commercially available proppants had different surface properties. However, complete detail of surface coating of each proppant was not available.

4.2 Experimental Set Up and Procedure

Column experiments were conducted by using the set-up shown in Figure 7 to investigate the role of various parameters on the recovery rate. Different parameters studied in these experiments were:

- a) Proppant Size
- b) Proppant Type
- c) Proppant Size Distribution
- d) Frac-fluid surface tension and viscosity

The experimental procedure is as follows

- Seal the column from the bottom

- Fill the column with proppants
- Record the mass of the proppants in the column
- Calculate the volume of proppants in the column by knowing the density of proppants.
- Calculate the packing pore volume by subtracting volume of proppants from the column volume.
- Apply vacuum and saturate the packed column with water
- Cover the top of the column with a mesh and turn it upside down
- Open the seal at the top to allow the inflow of air into the column
- Allow the column to drain under the influence of gravity and measure the effluent mass.

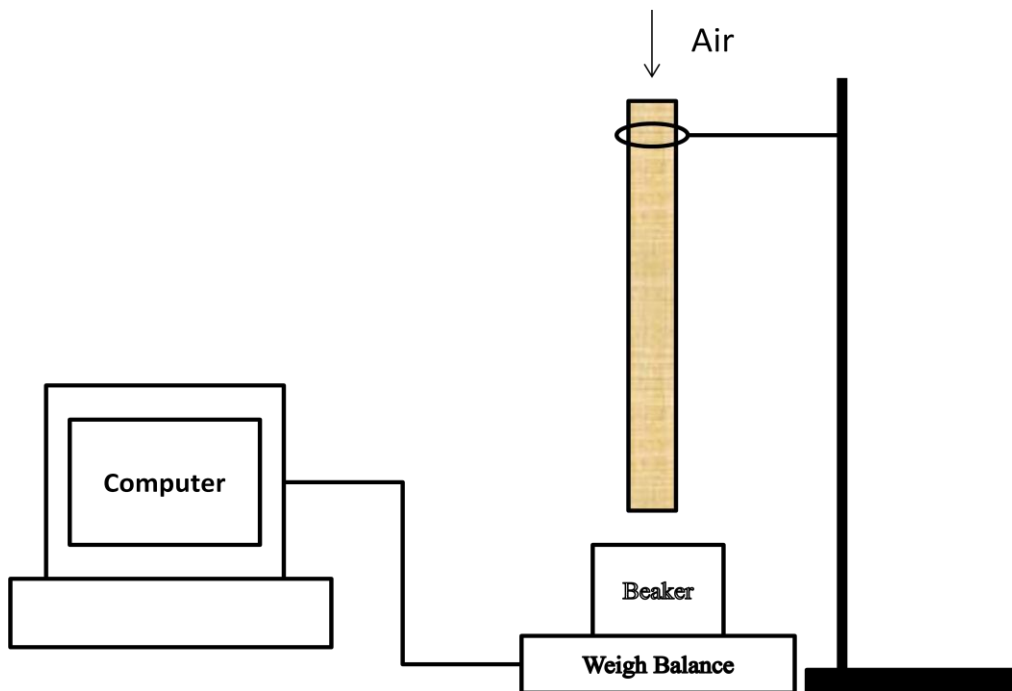


Figure 7: Schematic of the experimental set-up. The cylindrical column is 12” long and 1” in diameter.

4.3 Results

In this section results of different set of experiments are presented. For each experiment, weight percentage of recovered fluid versus time was measured. The recovery curves of different experiments were compared to study the role of proppant and frac-fluid properties on proppant pack cleanup.

4.3.1 Effect of Proppant Size: Experimental conditions for this set of experiments are listed in Table 4.2. Figure 8 compares the recovery curves of proppants with four different mesh sizes commonly used in fracturing operations. It is observed that the production rate (specified by the slope of the recovery curve) is initially high and then quickly decreases with time. Each curve reaches to a plateau determining the final water recovery, which strongly depends on proppant size. Figure 9 shows, ultimate recovery versus the proppant mean diameter, calculated by using equation (4.1)⁶⁴.

$$\text{Mean diameter (in)} = 0.4114 * \left(\frac{1}{(\text{small mesh size})^{1.06}} + \frac{1}{(\text{large mesh size})^{1.06}} \right)^{64} \quad (4.1)$$

Ultimate recovery increases by increasing the proppant size by a non-linear relationship. Increasing the proppant diameter decreases the capillary pressure, according to Young-Laplace equation (2.3), which in turn increases the wetting phase trapping.

Table 4.2: Experimental conditions to test the effect of proppant size on frac-fluid recovery

Property	Test 1	Test 2	Test 3	Test 4
Fracturing fluid	100% Water	100% Water	100% Water	100% Water
Viscosity	1 cp	1cp	1cp	1cp
Interfacial tension	72 dynes/cm	72 dynes/cm	72 dynes/cm	72 dynes/cm
Displacing fluid	Air	Air	Air	Air
Drawdown	Spontaneous drainage	Spontaneous drainage	Spontaneous drainage	Spontaneous drainage
Type of proppants	Normal Sand	Normal Sand	Normal Sand	Normal Sand
Proppant size	20/40	16/20	30/50	40/70
Wettability	Hydrophilic	Hydrophilic	Hydrophilic	Hydrophilic

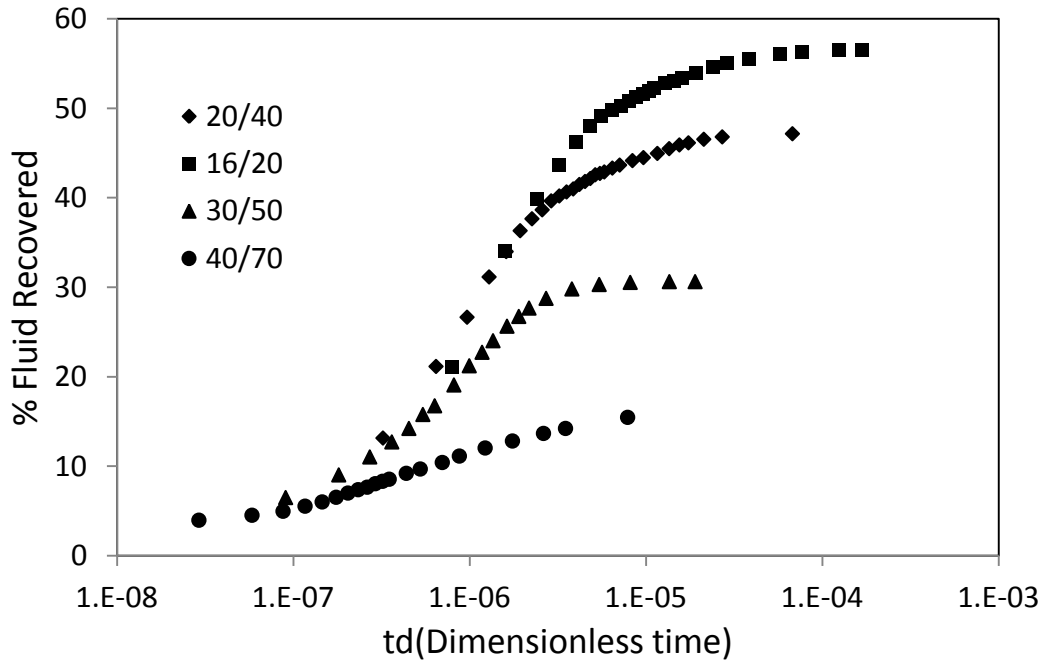


Figure 8 Effect of proppant size on water recovery: Normalized cumulative water production versus dimensionless time

The slope of the curve at each point represents the fractional production rate. As

shown in Figure 8, the production rate for the finest sand is the lowest and remains constant for a long duration of time. As the proppant size increases the production rate increases initially with time but then starts to decrease and eventually becomes zero. Figure 9 illustrates the ultimate recovery changes as a function of mean diameter of proppants. Mean diameter of proppant is calculated by using equation (4.1).

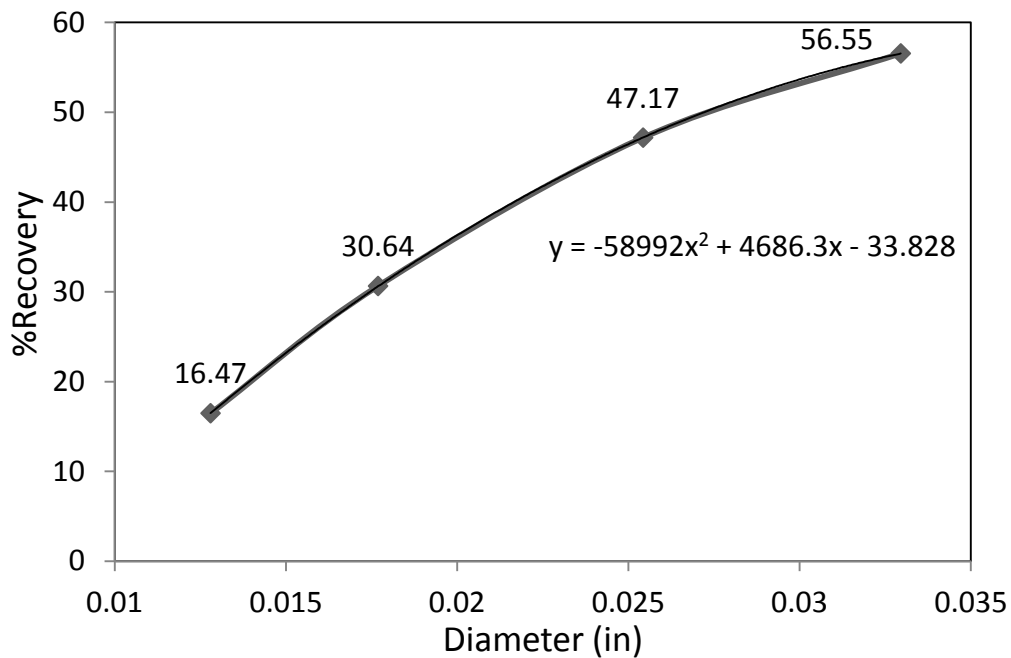


Figure 9: Ultimate water recovery vs proppant mean diameter

4.3.2 Effect of Proppant Size Distribution: To model the effect of proppant size distribution, the column was packed with a mixture of fine (mesh size 40/70) and coarse (20/40) sand with a ratio of 1:4. Experimental conditions for this set of experiments are presented in Table 4.3. Figure 10 compares the recovery curves of the mixed sand with that of the two uniform sands. Ultimate water recovery in coarse sand decreases by more than 20% by adding 25% of fine sand

Table 4.3: Experimental conditions to test the effect of proppant size distribution on frac-fluid recovery

Property	Test 1	Test 2	Test 3
Fracturing fluid	100% Water	100% Water	100% Water
Viscosity	1 cp	1cp	1cp
Interfacial tension	72 dynes/cm	72 dynes/cm	72 dynes/cm
Displacing fluid	Air	Air	Air
Drawdown	Spontaneous drainage	Spontaneous drainage	Spontaneous drainage
Type of proppants	Normal Sand	Normal Sand	Normal Sand
Proppant size	20/40	40/70	25% 40/70 + 75% 20/40
Wettability	Hydrophilic	Hydrophilic	Hydrophilic

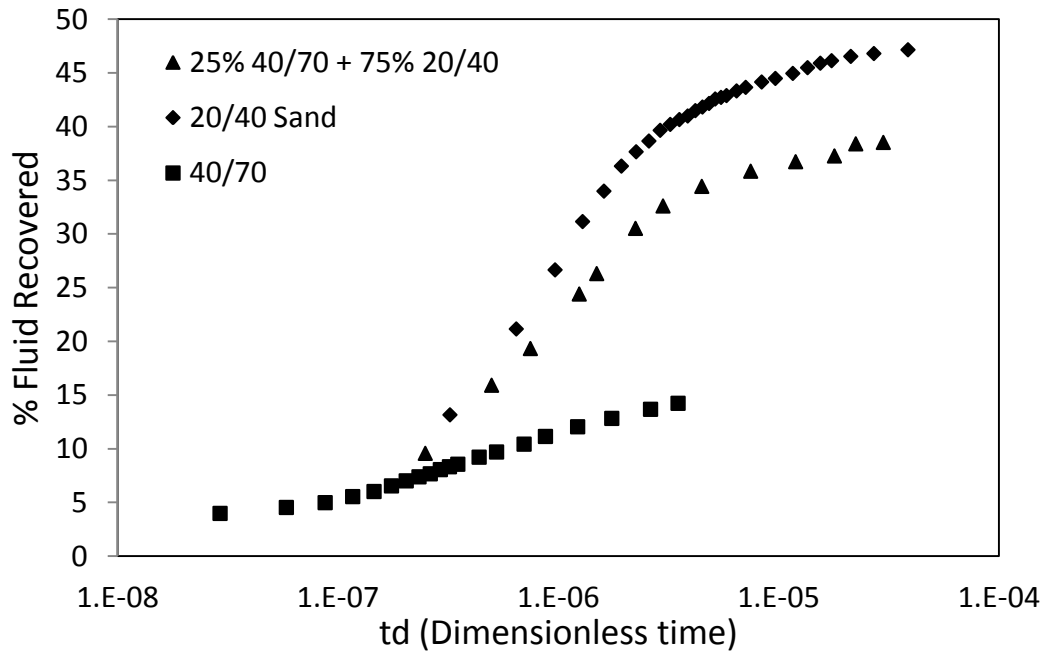


Figure 10 Effect of proppant size distribution on water recovery: Normalized cumulative water production versus dimensionless time for coarse, fine and mixed sand

4.3.3 Effect of Proppant Type: In this section, the drainage behavior of proppants packs with similar size (20/40) but different surface properties are compared. Experimental conditions for this set of experiments are presented in Table 4.4. Drainage experiments are conducted by using four different types of commercially available proppants named as A, B, C, and D. Recovery curve of the four proppants and ordinary sand are compared in Figure 11.

Table 4.4: Experimental conditions to test the effect of proppant type on frac-fluid recovery

Property	Test 1	Test 2	Test 3	Test 4	Test 5
Fracturing fluid	100% Water				
Viscosity	1 cp	1cp	1cp	1cp	1cp
Interfacial tension	72 dynes/cm				
Displacing fluid	Air	Air	Air	Air	Air
Drawdown	Spontaneous drainage				
Type of proppants	Proppant A	Proppant B	Proppant C	Proppant D	Normal Sand
Proppant size	20/40	20/40	20/40	20/40	20/40
Wettability	Hydrophilic	Hydrophobic	Hydrophilic	Hydrophilic	Hydrophilic

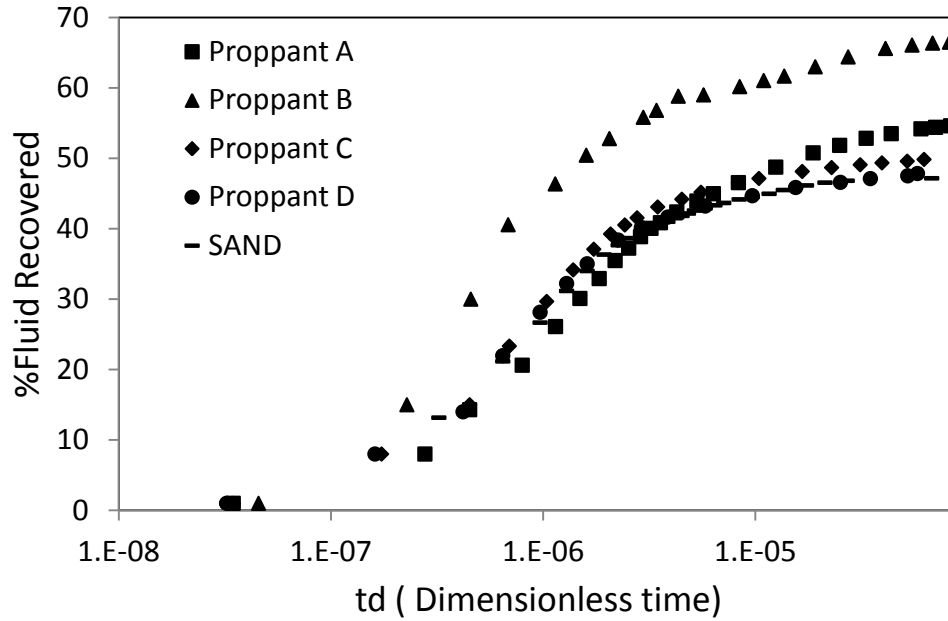


Figure 11 Effect of different proppant types on fluid recovery: Normalized cumulative water production versus dimensionless time

Although the recovery curves of proppants A, C, and D are similar to that of normal sand, that of proppant A is significantly higher than others. This is also shown in Figure 12, which compares the ultimate recovery of the five samples.

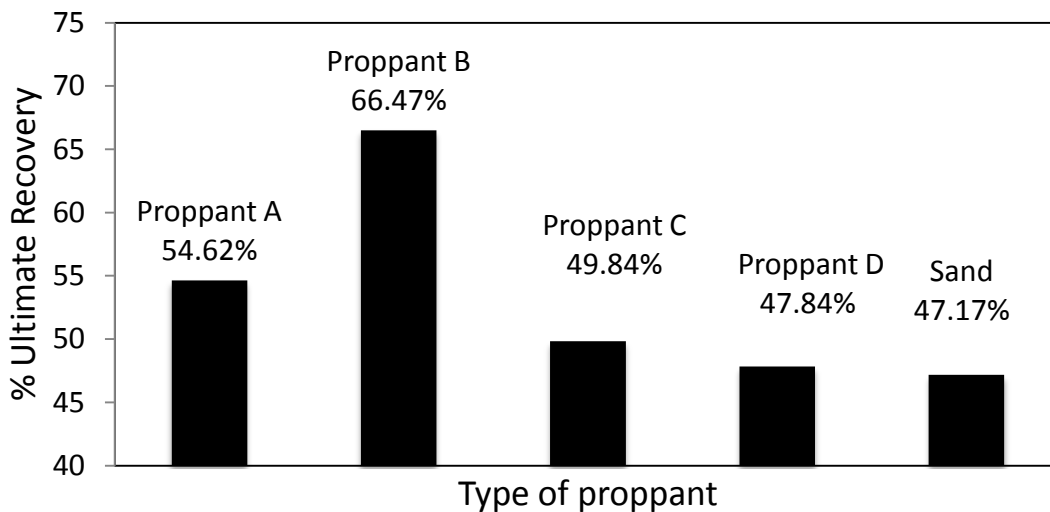


Figure 12 Ultimate recoveries for various proppant types

Wettability of proppant B was compared with other samples by measuring the

contact angle. Figure 13 shows the contact angle of water on the surface of different proppants. From Figure 13(b) contact angle for proppant B is clearly greater than 90 degrees, which shows the hydrophobic nature of this proppant. Contact angle for proppant D and sand is zero. Contact angle for Proppant A and C is greater than zero but less than 90 degrees.

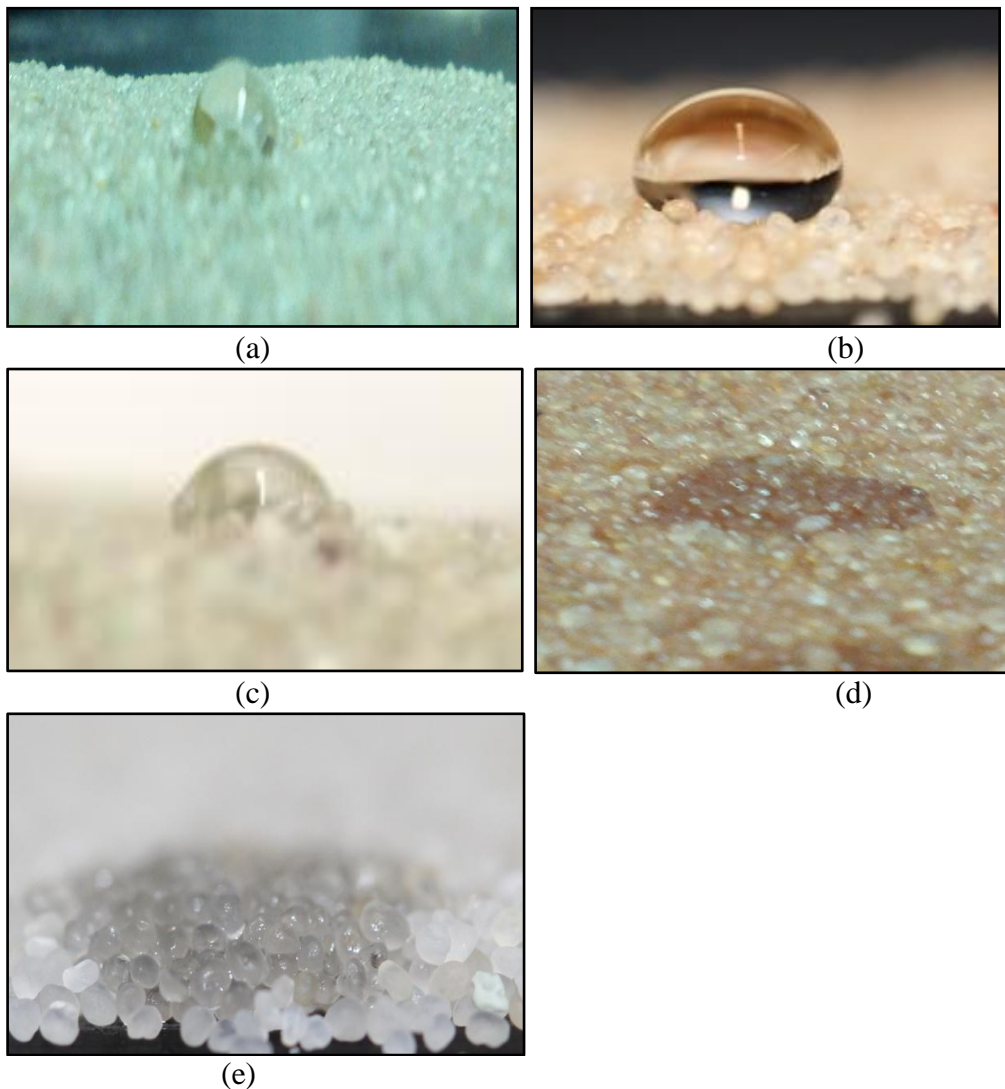


Figure 13: (a) Contact angle of water on proppant A (b) Contact angle of water on proppant B (c) Contact angle of water on proppant C (d) Contact angle of water on proppant D (e) Contact angle of water on sand

4.3.4 Effect of Fracturing Fluid Type: To study the effect of fluid type, drainage behavior of oil and water in 20/40 mesh size proppant pack is compared. Two different proppant types are used to compare the effect of fracturing fluid type. Firstly sand is used as proppant pack and then proppant B is used as proppant pack.

With Sand Used to Pack the Column: Operating conditions for this experiment are summarized in Table 4.5. Figure 14 shows that ultimate oil recovery (67%) is significantly higher than ultimate water recovery (47%). This can be explained by higher surface tension of water compared to oil. However, the early-time production rate for oil is much lower than that of water. This can be explained by higher viscosity of oil compared to water.

Table 4.5: Experimental conditions to test the effect frac-fluid type on recovery

Property	Test 1	Test 2
Fracturing fluid	100% Water	100% Mineral oil
Viscosity	1 cp	18 cp
Interfacial tension	72 dynes/cm	24 dynes/cm
Displacing fluid	Air	Air
Drawdown	Spontaneous drainage	Spontaneous drainage
Type of proppants	Normal Sand	Normal Sand
Proppant size	20/40	20/40
Wettability	Hydrophilic	Hydrophilic

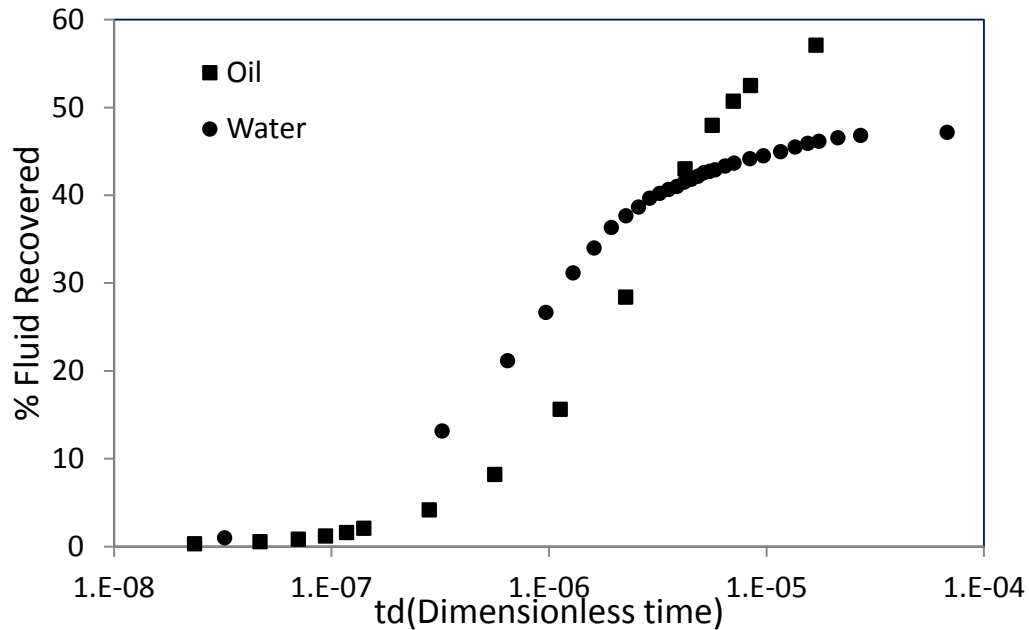


Figure 14 Effect of fluid type: Normalized fluid recovery versus dimensionless time

With proppant B used to pack the column The effect of fluid type is also studied using Proppant B. This proppant outperformed other proppants in terms of fluid recovery when water was used as frac-fluid. Operating conditions for this experiment are summarized in Table 4.6. Figure 15 shows that production rate for two fluids is different but ultimate recovery is comparable.

Figure 16 shows that ultimate oil recovery (73%) is slightly higher than ultimate water recovery (67%). Increase in water recovery with proppant B as compared to normal sand is due to hydrophobic nature of proppant B. The contact angle of water on proppant B is greater than 90 degrees but that of oil is zero. The reason for better recovery of oil is due to its lower surface tension compared to water. However, the initial production rate of oil is lower than that of water due to higher viscosity of oil.

Table 4.6: Experimental conditions to test the effect frac-fluid type on recovery

Property	Test 1	Test 2
Fracturing fluid	100% Water	100% Mineral oil
Viscosity	1 cp	18 cp
Interfacial tension	72 dynes/cm	24 dynes/cm
Displacing fluid	Air	Air
Drawdown	Spontaneous drainage	Spontaneous drainage
Type of proppants	Proppant B	Proppant B
Proppant size	20/40	20/40
Wettability	Hydrophilic	Hydrophilic

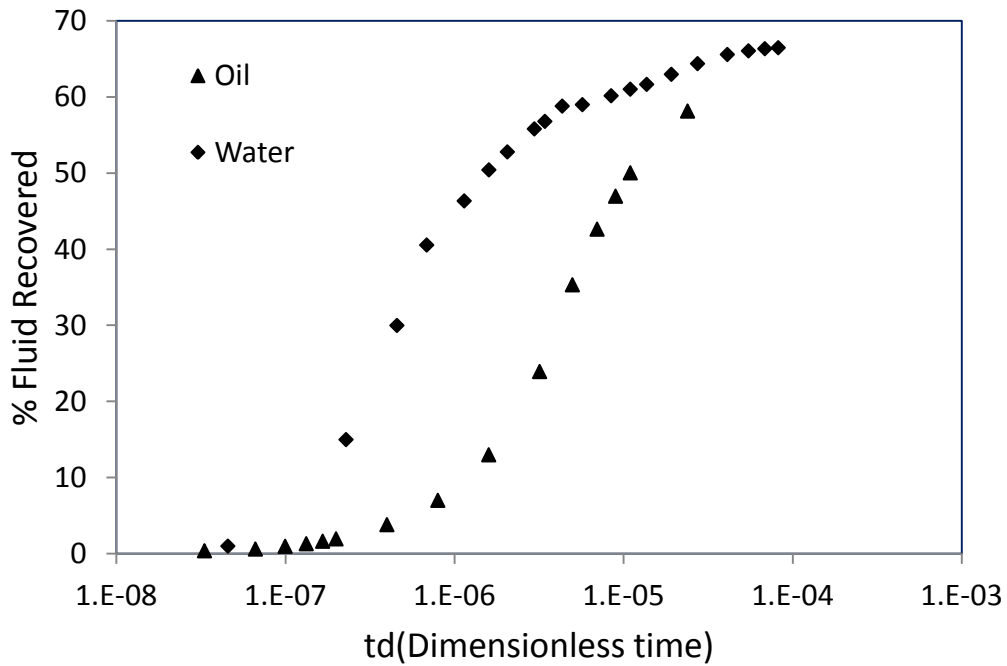


Figure 15: Effect of fluid type: Normalized fluid recovery versus dimensionless time

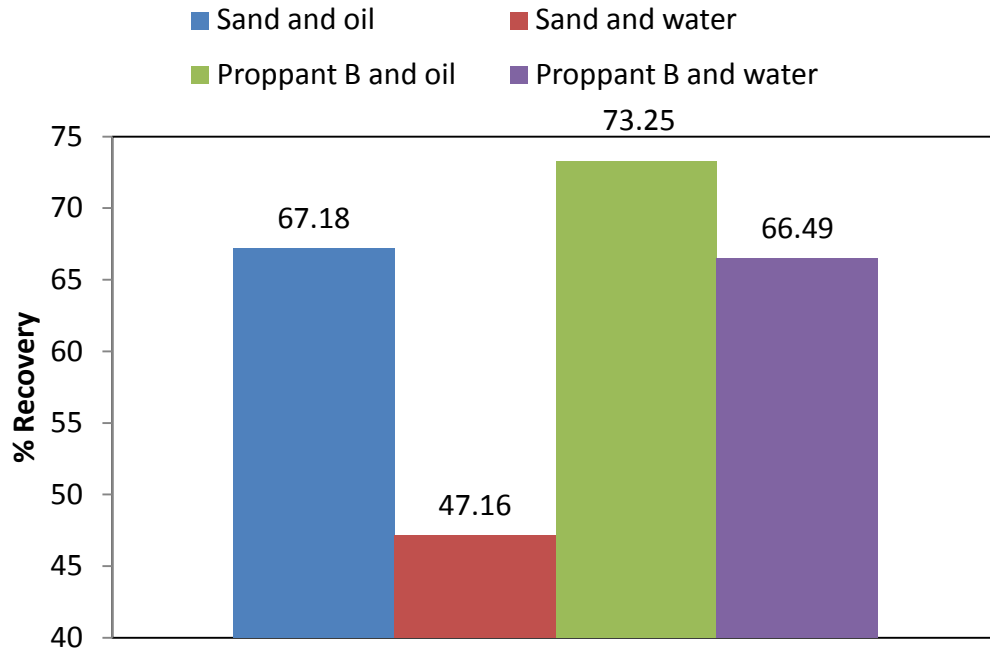


Figure 16: Ultimate recovery for different fluid and proppant type

4.4 Discussion

This section presents the discussion of the results.

4.4.1 Effect of size: Our results show that with increasing proppant size both production rate and ultimate recovery increased. This is mainly because of the fact that capillary forces decrease with increase in proppant size. As the proppant size increases, size of pore spaces also increases. Since capillary pressure is inversely proportional to pore size, considering Young-Laplace equation, increasing the pore size results in reduced capillary forces. In our experiments capillary force is mainly responsible for water holdup. Therefore, lesser the capillary force higher the recovery. The relation between average proppant size and water recovery is observed to be non-linear. While selecting proppant size one must go for coarse size. Coarse size proppants will not only allow the better fracturing fluid recovery

but also result in wider fracture opening, hence better production. Consistently, a field⁶⁶ study also reported better production rate by using coarse size proppants.

4.4.2 Effect of Proppant Size Distribution: Cyclic stresses in reservoir results in crushing of the proppants^{12,29}. This changes the pore size distribution of fractures in the reservoir. Crushed sand occupies the pore spaces initially present. From the experimental data it is seen that variation in pore size distribution significantly affects the water recovery. This implies that before selecting a proppant for fracturing it should be tested for the nature of stresses it is anticipated to undergo in the reservoir. Selected proppant should be able to bear the anticipated stresses without being crushed. Crushing of the proppants result in change in size distribution of the proppants in the fracture. Thus affecting the fracture cleanup.

4.4.3 Effect of Proppant Type: From the experimental results it is seen that surface properties of proppants has a significant impact on water recovery. Out of various proppants used Proppant B (hydrophobic in nature) was found to be very effective in fracture fluid cleanup. Water recovery for Proppant B (66.5%) was significantly higher than other proppant types (48% approx). Thus surface properties of the proppant should be tested before selecting a proppant. Hydrophobic characteristic of the surface helps better cleanup of the fractures.

4.4.4 Effect of Fracturing Fluid Type: Type of fluid does play an important role in fracture cleanup. The ultimate recovery of oil was higher than water when used as

fracturing fluid. This is because of the low surface tension between oil and air as compared to water and air. According to Young-Laplace equation capillary pressure is directly proportional to surface tension. Lower surface tension results in lower capillary pressure. This in turn results in less liquid hold up in proppants. However it was observed that production rate in case of oil was much lower than that of water. This is because of the high viscosity of the oil (18cP) as compared to water (1cP).

Chapter 5

2D Experiments: Apparatus and Procedure

This chapter describes the apparatus and experimental set up used for 2D fracture model experiments.

5.1 Materials and Equipment

Following section explains materials and equipment used for 2-D experiments.

Experimental cell: Figure 17 illustrates the experimental cell used to model water displacement by gas in a propped hydraulic fracture. Experimental cell consisted of two transparent plates made of plexiglass. The space between the two plates (0.375 in) was packed with proppants and then tightened using nuts and bolts. There were three inlets for fluid injection and one outlet for fluid production. The dimensions of the experimental cell are 12 in by 12 in by 0.375 in.

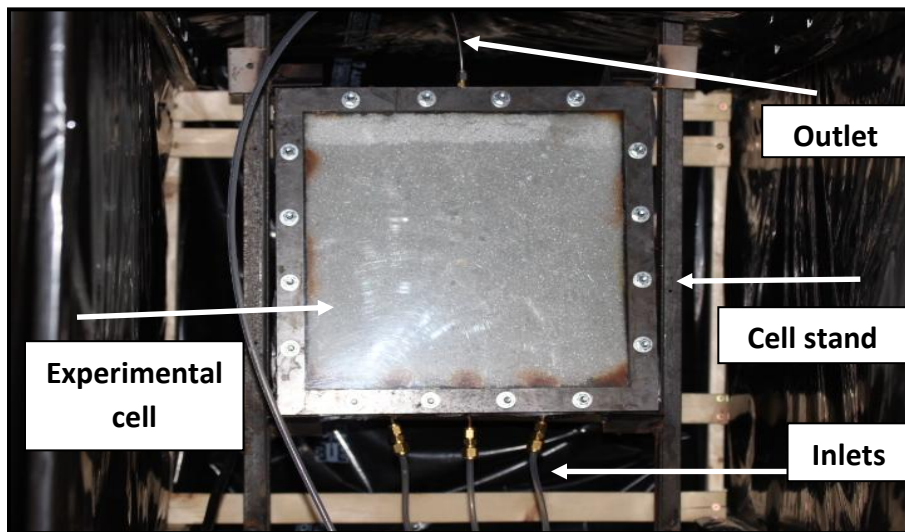


Figure 17: The picture of experimental cell

Experimental Cell Holder: To hold the cell in the vertical position, it was placed in a cell holder shown in Figure 17.

Light box: It consisted of five fluorescent lamps equally spaced in two rows as shown in Figure 18. This arrangement ensured uniform distribution of light behind the cell.

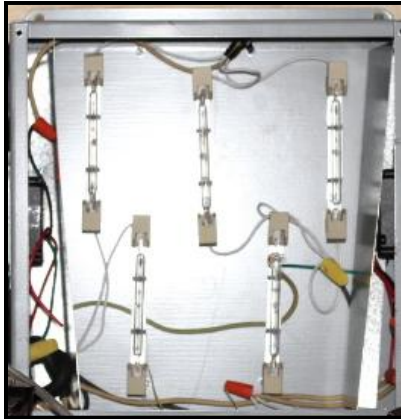


Figure 18: Light box used to illuminate back side of experimental cell

Water Trap: Figure 19 illustrates the water trap used in experiments. It was built to collect water sucked out of the experimental cell during vacuum operation. Both water and gas enters the collector from inlet line. Water being heavier gets trapped in water collector, whereas gas being lighter rises up and leaves the collector through the outlet.

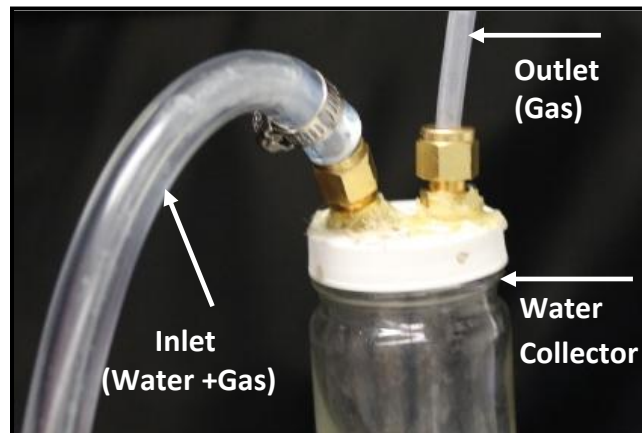


Figure 19: Water Trap to capture water sucked during vacuum operation

DuNouy tensiometer: To measure the interfacial tension of fluid, DuNouy tensiometer was used as shown in Figure 20. It measures the surface tension based on force required to pull the ring free of air water interface²⁴.

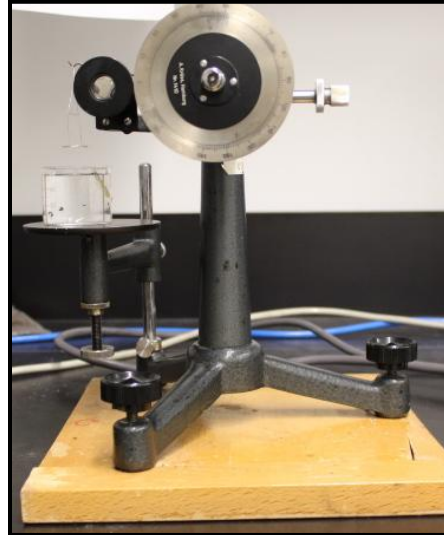


Figure 20: DuNouy tensiometer used to measure surface tension

Rheometer: To study the rheological properties of polymer solution, Bohlin C-VOR Cone and Plate type rheometer (Figure 21) was used. The fluid viscosity was measured for different shear rates changing from 0.01 to 100 sec⁻¹.



Figure 21: C-VOR Rheometer

Data acquisition system: The amount of produced water was recorded automatically by an electronic weight balance. The weight values were continuously digitized and recorded by connecting the weight balance to a computer via RS-232 cable.

Cotton cloth: To ensure uniform gas influx from the three inlets during the displacement experiments, a double-layered cotton cloth was placed between the inlet ports and the end part of the sand pack.

Proppants: Two types of proppants were used in the experiments

- a) Untreated glass beads of mesh size 20/30 and 16/30
- b) Treated glass beads of mesh size 16/30

Treated glass beads were hydrophobic as opposed to normal glass beads which were hydrophilic. To change the wettability of the glass beads, the procedure suggested by Shahidzadeh-Bonn et. al ¹⁶ was used. Step by step procedure to alter the wettability is as follows:

- Prepare 1 wt% n-octyl triethoxysilane in isopropanol
- Add 2 wt% of distilled water and 0.2 wt% of HCl (37 wt.%)
- Stir mixture for 5 hrs
- Soak Beads in mixture for 1 hr
- Remove excess mixture and dry beads in oven at 100° C

Frac-fluids: Three types of fluids were used as frac-fluids

- a) **Water:** Most of the experiments were conducted by using tap water as frac-fluid.
- b) **1 wt% Isopropanol in water:** Surface tension of normal water was reduced

by adding 1 wt% isopropanol in water. Interfacial tension of the resulting fluid was measured using DuNouy tensiometer (Figure 20).

- c) **0.025 wt% Xanthan gum:** Viscosity of water was increased by adding 0.025 wt% Xanthan gum. Rheological properties of resulting fluid were measured using C-VOR rheometer (Figure 21).

Gas Phase: 97% pure nitrogen was used for injection in all the experiments.

Syringe Pump: Experimental cell was saturated by injecting frac-fluid with the help of syringe pump. Some features of syringe pump are listed below

1. Flow rates: 0.00001 μ l/min to 250ml/min
2. Maximum capacity 250 ml
3. Can be used for both injecting and withdrawing fluid

5.2 Experimental Procedure

Experiments were conducted at three different orientations of the cell. Step by step procedure for conducting experiments is listed below.

- Pack the 0.375-in space between two glass plates by glass beads
- Fix the cell in the vertical position by using a holder
- Saturate experimental cell by injecting frac-fluid from the bottom of the cell using a syringe pump
- Simultaneously apply vacuum at the end opposite to frac-fluid injection end
- Calculate the mass of frac-fluid in the cell by subtracting the fluid mass collected in the vacuum line from the injected fluid mass
- Once cell is saturated with frac-fluid, inject nitrogen gas at fixed pressure

- (a) From the top of the cell to simulate drainage in the direction of gravity (Figure 22)
- (b) From the bottom of the cell to simulate drainage against gravity direction (Figure 23)
- (c) From the side of horizontal cell to simulate gravity neutral test (Figure 24)
- Record the mass of fluid drained from the production end by using a balance connected to the computer
 - Turn on the fluorescent lamps at the back side of the cell and take images frequently to observe the drainage pattern

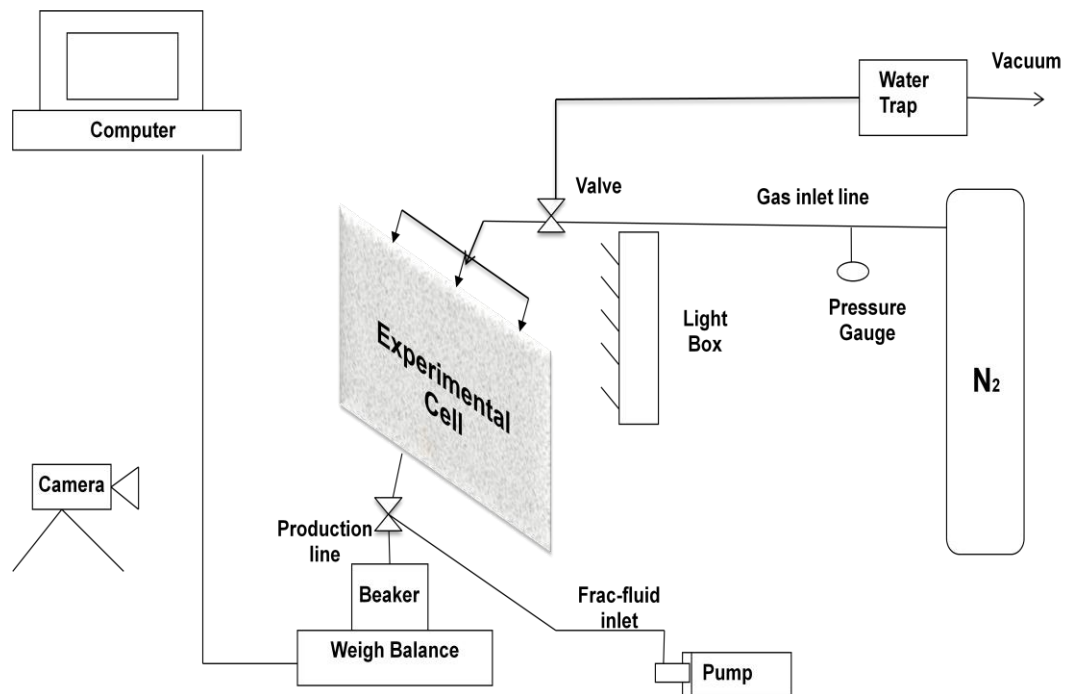


Figure 22: Experimental setup for drainage in the direction of gravity

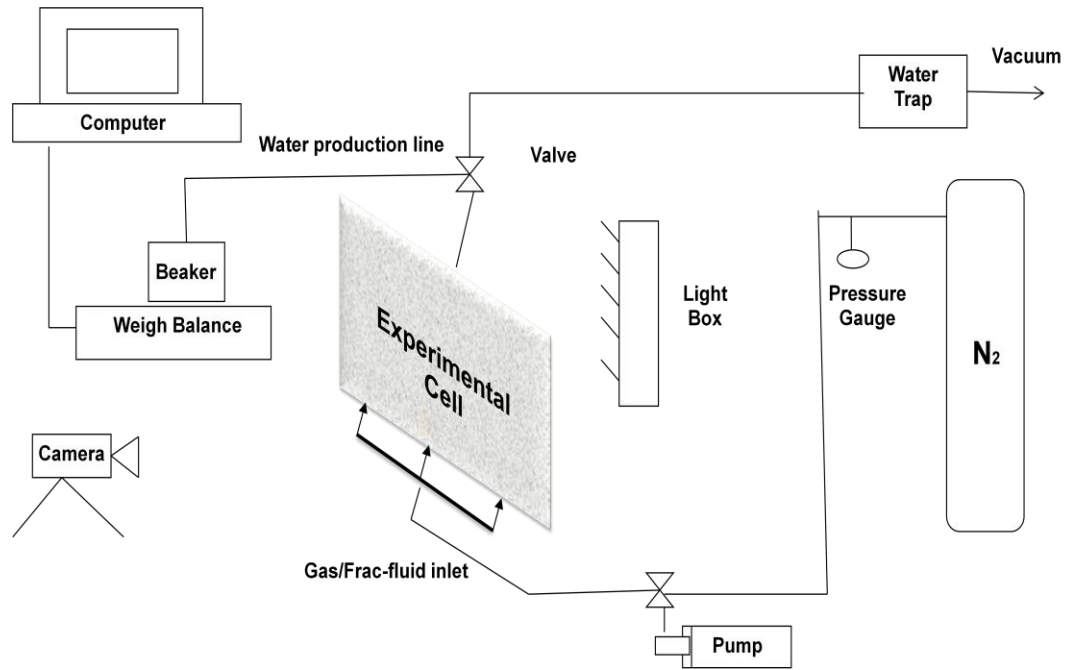


Figure 23: Experimental setup for drainage against gravity direction

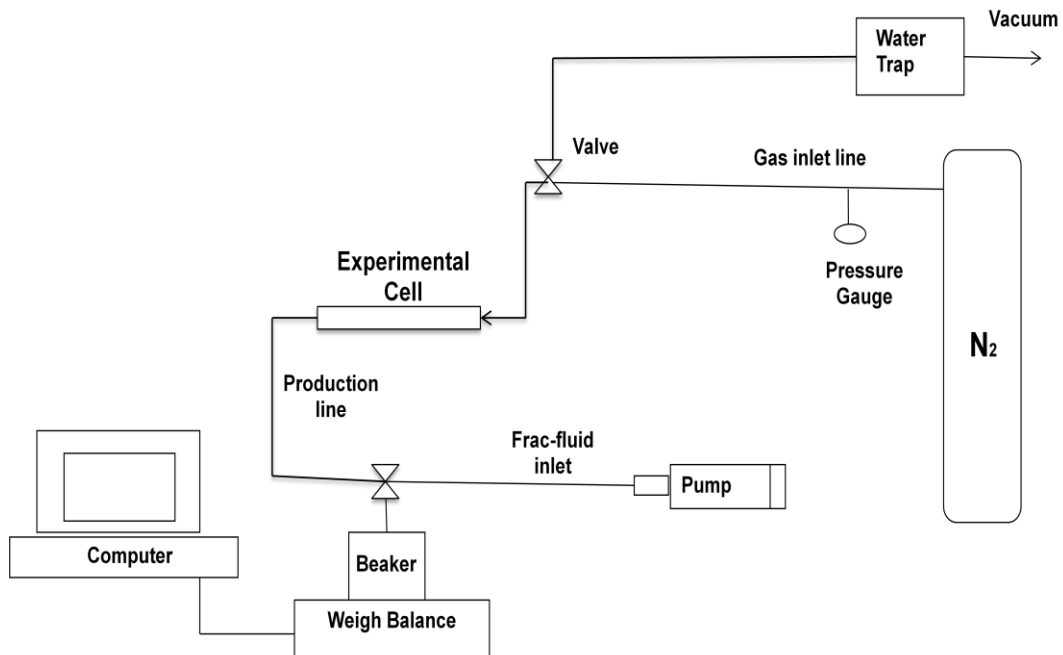


Figure 24: Experimental setup for drainage against gravity direction

Chapter 6

2D Experiments: Results and Discussion

This chapter presents results and discussion of experiments conducted in 2D propped hydraulic fracture model.

6.1 Results

For each experiment we measure the weight of the fluid recovered versus time while pictures of the experimental cell are being taken at regular intervals. The recovery curves of different experiments are compared to study the role of fracture orientation, drawdown, surface tension, proppant wettability and viscosity on water recovery. Also, the images taken during the experiments are compared to study the drainage pattern.

6.1.1 Effect of Fracture Orientation (Set 1): To study the effect of fracture orientation, we conduct drainage tests by injecting nitrogen at a fixed pressure of 15 psi into

- a) The top of the vertical cell: To simulate drainage in the direction of gravity
- b) The bottom of the vertical cell: To simulate drainage against the direction of gravity
- c) The side of the horizontal cell: To simulate drainage without gravity effects

Operating conditions for this set of experiments are listed in Table 6.1. Figure 25 presents the comparison of the recovery curves obtained from these tests. The ultimate water recovery in test 2, where water drains upward against gravity, is

extremely low (10.8%). The ultimate recovery in test 1, where water drains downward in the gravity direction, is very high (79.3%). The ultimate recovery in test 3 (37.94 %) is higher than test 2, but still much lower than test 1.

Table 6.1: Experimental conditions to test the effect of fracture orientation (Set1)

Property	Test 1	Test 2	Test 3
Type of fracturing fluid	100% Water	100% Water	100% Water
Viscosity	1 cp	1cp	1cp
Interfacial tension	72 dynes/cm	72 dynes/cm	72 dynes/cm
Gas injected	Nitrogen	Nitrogen	Nitrogen
Gas injection direction	Gravity stable	Gravity unstable	Neutral
Drawdown	15 psi	15 psi	15 psi
Type of proppants	Normal glass beads	Normal glass beads	Normal glass beads
Proppant size	20/30	20/30	20/30
Wettability	Hydrophilic	Hydrophilic	Hydrophilic

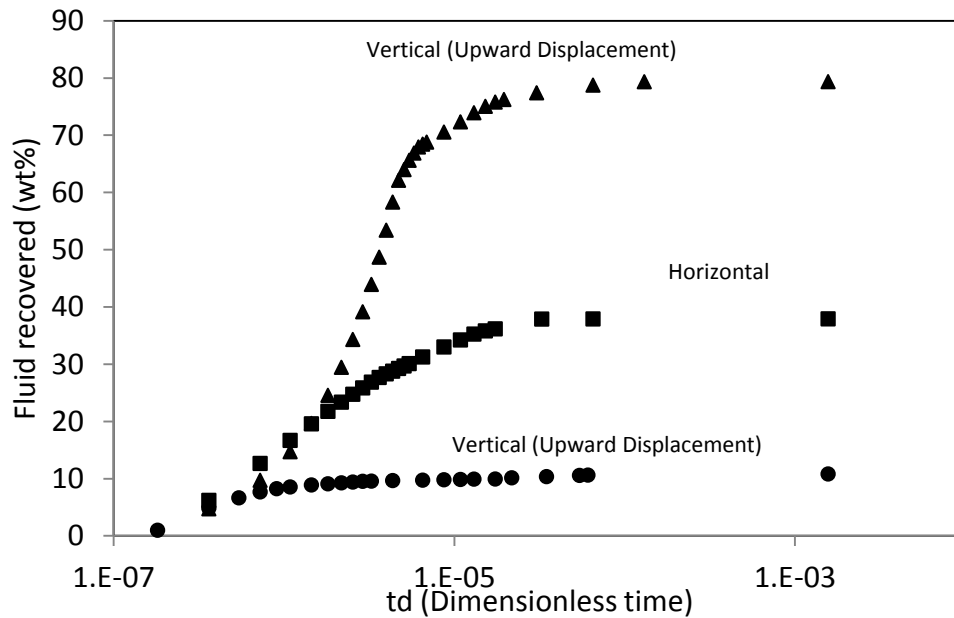


Figure 25 Effect of fracture orientation on water recovery rate

To investigate the observed difference, we compare the pictures taken during the drainage tests. Figure 26 shows how drainage front progresses during the test 1 where gas is injected in the direction of gravity in a vertical cell. The dark colored region in the pictures represents high gas saturated area and light colored region represents high water saturated area. It is observed that the drainage front during test 1 is very stable and most of the water is recovered behind this front.

Figure 27 shows the drainage pattern of test 2 where gas is injected against gravity direction in a vertical cell. Comparing Figures 26 and 27, it can be observed that the drainage pattern in test 2 is very different than that of test 1. In test 2, fingers (preferential flow path) are observed, which grow in number with time (Figure 27). Most of the gas flows through these preferential paths and is produced at the top. Formation of these fingers is detrimental to water recovery since only a small portion of the porous medium is swept by gas. In other words, the areal sweep efficiency is very low in this case. Figure 27 shows that even after a relatively long time a significant amount of water is left in the cell.

Figure 28 shows the drainage pattern of test 3 where gas is injected perpendicular to gravity direction in a horizontal cell. We observe that the drainage front in test 3 is less stable than that of test 1. Although an unstable front is observed, the areal sweep efficiency in this case is higher than that in test 2.

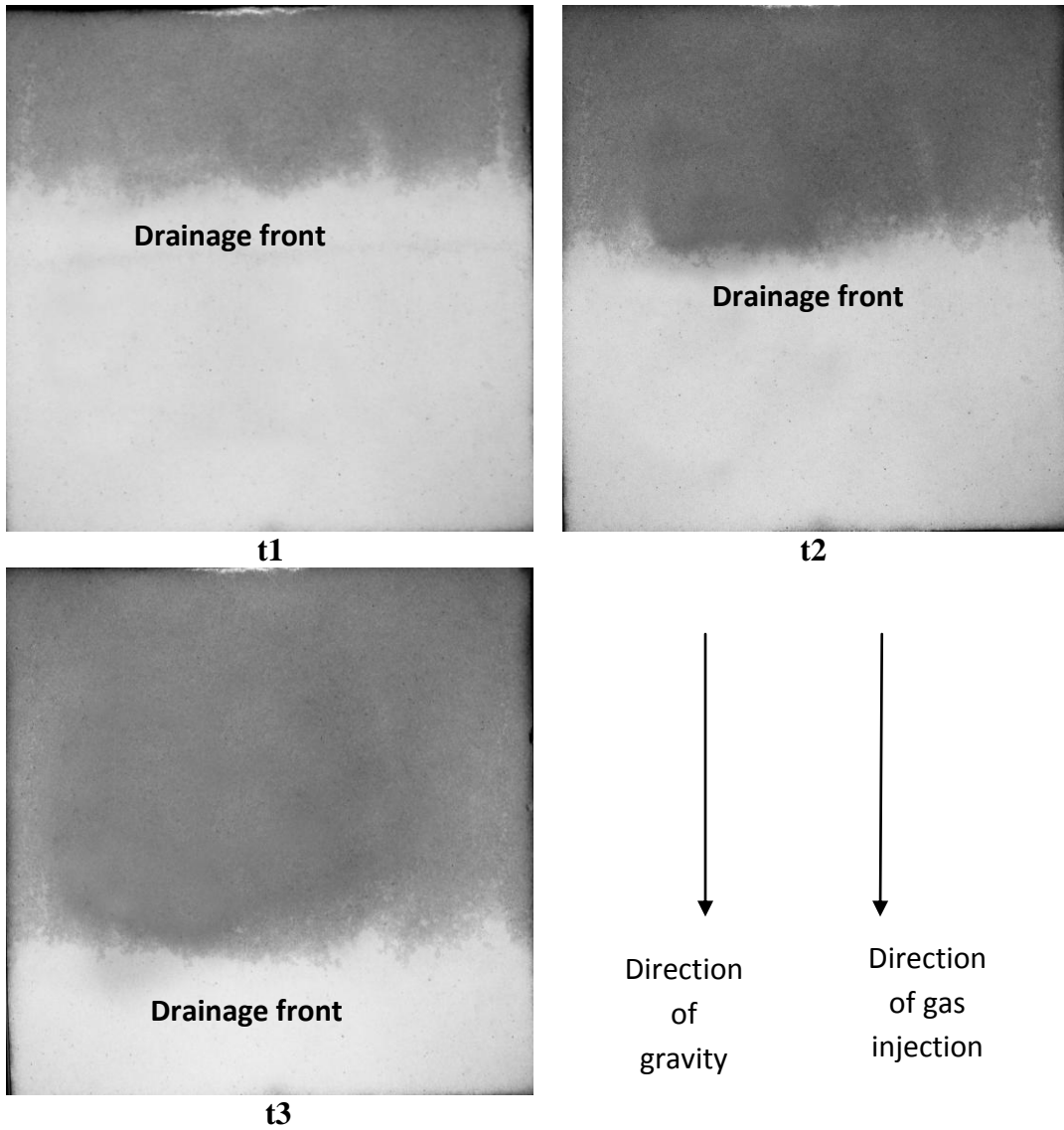


Figure 26 Images taken during the downward water displacement in the vertical cell show a stable displacement front moving downward at time intervals t1, t2 and t3 (test 1 of set 1)

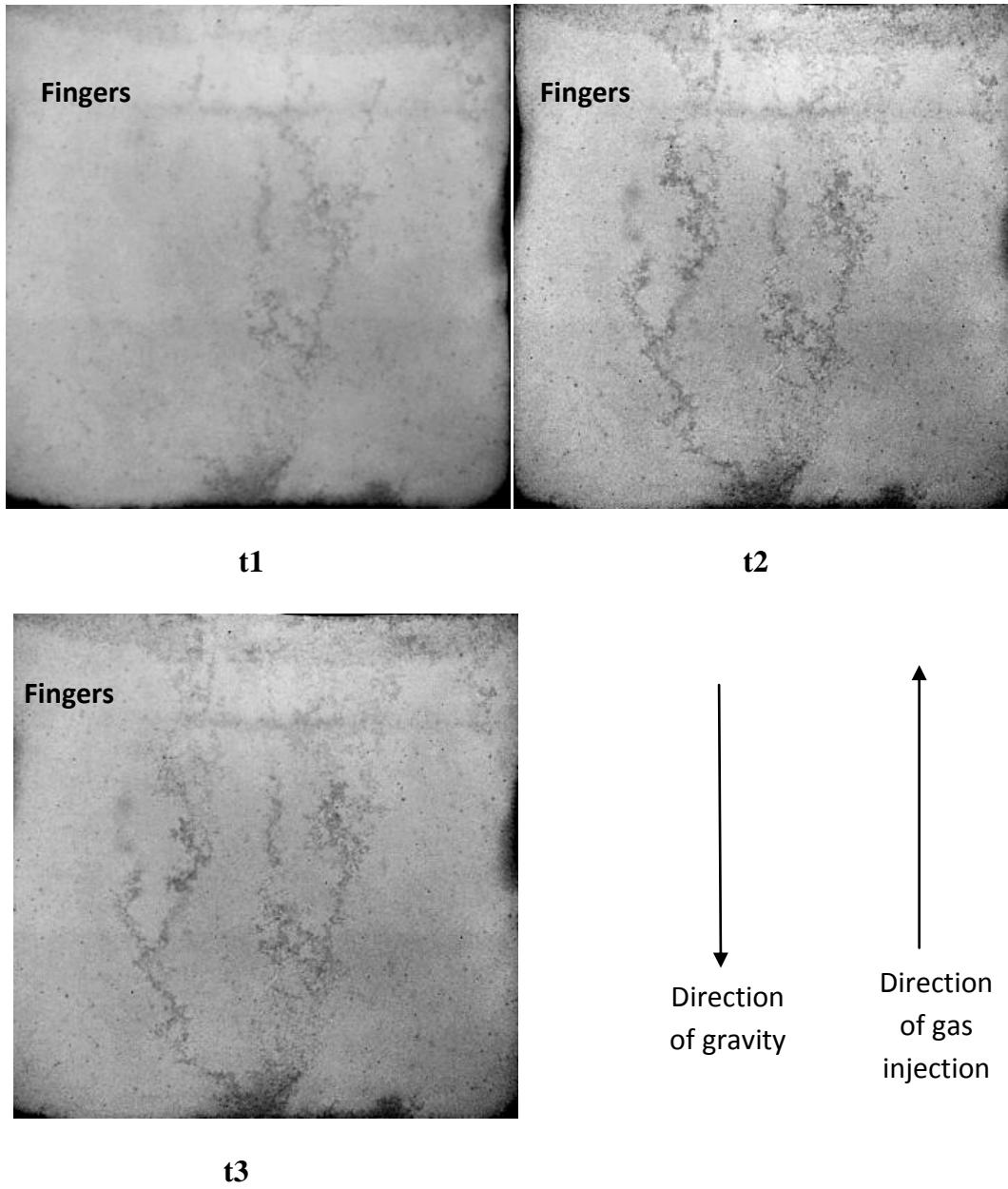


Figure 27 Images taken during the upward water displacement in the vertical cell show unstable displacement at time intervals t1, t2 and t3 (test 2 of set 1)

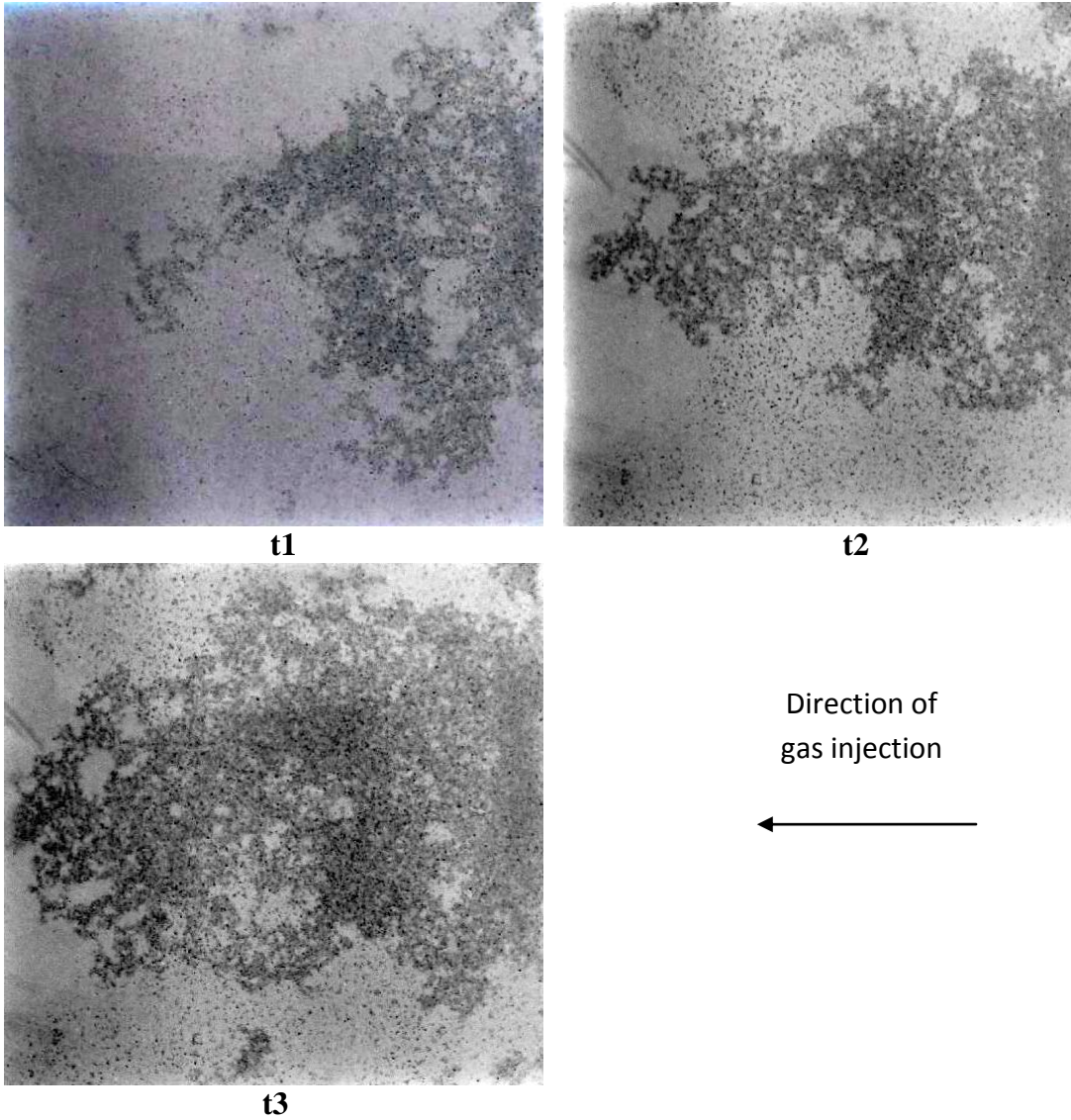


Figure 28 Images taken during the horizontal water displacement show unstable displacement front at time interval t1, t2 and t3

6.1.2 Effect of Drawdown (Set 2): To study the effect of drawdown on drainage we use three different injection pressures of 10, 20 and 30 psi while keeping the production open to atmosphere. Gas is injected at the bottom of the vertical cell. Table 6.2 lists the detailed operating conditions used for these experiments.

It is found that the recovery rate and ultimate recovery are almost the same for all three injection pressures. As shown in Figure 29, the ultimate recovery is found to be nearly 8% for all the three injection pressures. Production rate, which is represented by the slope of the curve, is initially high but decreases with time. This indicates the decrease in production rate of water with time.

Table 6.2: Experimental conditions to test the effect of drawdown (Set 2)

Property	Test 1	Test 2	Test 3
Type of fracturing fluid	100% Water	100% Water	100% Water
Viscosity	1 cp	1cp	1cp
Interfacial tension	72 dynes/cm	72 dynes/cm	72 dynes/cm
Gas injected	Nitrogen	Nitrogen	Nitrogen
Drawdown	10 psi	20 psi	30 psi
Type of proppants	Normal glass beads	Normal glass beads	Normal glass beads
Proppant size	16/30	16/30	16/30
Wettability	Hydrophilic	Hydrophilic	Hydrophilic

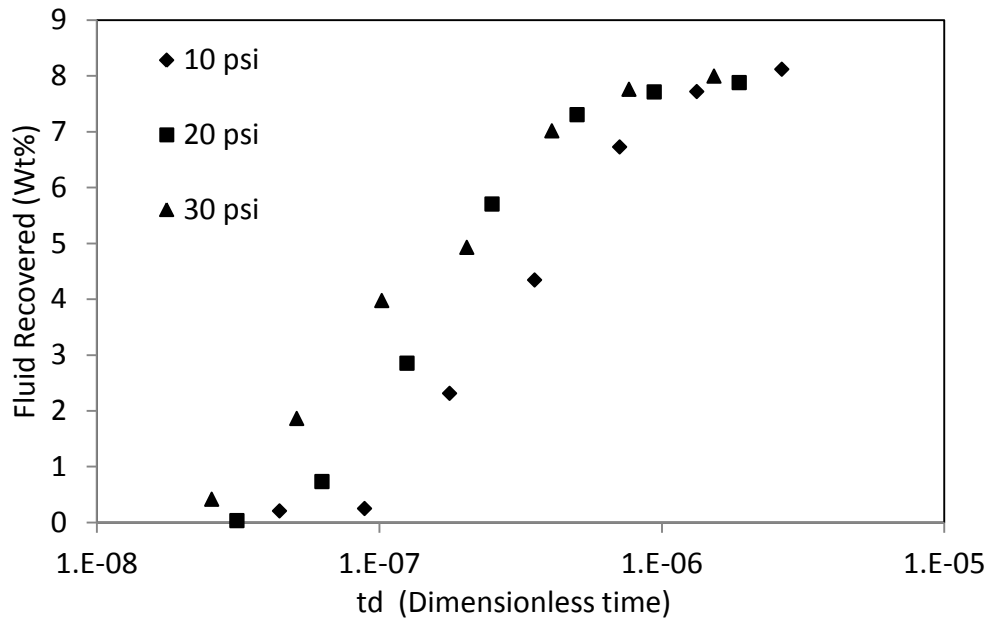


Figure 29 Effect of drawdown on water recovery rate

Drainage patterns observed at 10, 20 and 30 psi injection pressures are shown in Figures 30, 31 and 32 respectively. At 10 psi drawdown we observe only one finger which breaks through the production end. At 20 and 30 psi drawdown, multiple fingers, forming a branch at the bottom of the cell, are observed. Interestingly, water depletion occurs at the top part of the cell, which can be explained by the density difference between the gas and water. Due to gravity segregation water replaces the gas in the developed fingers, and gas moves upward.

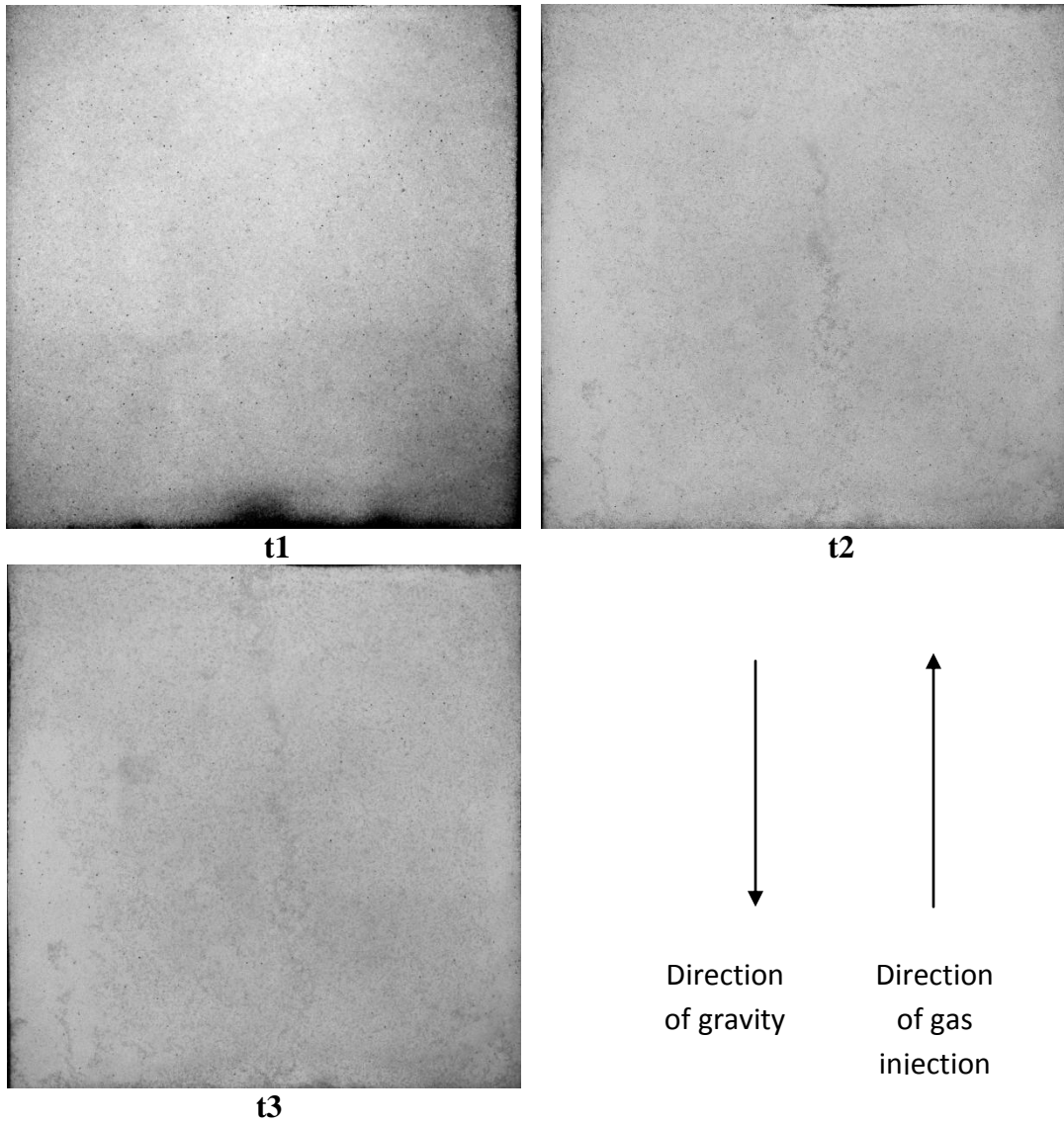


Figure 30: Effect of drawdown on drainage pattern at 10 psi drawdown, showing development of fingers at different time intervals t1, t2 and t3

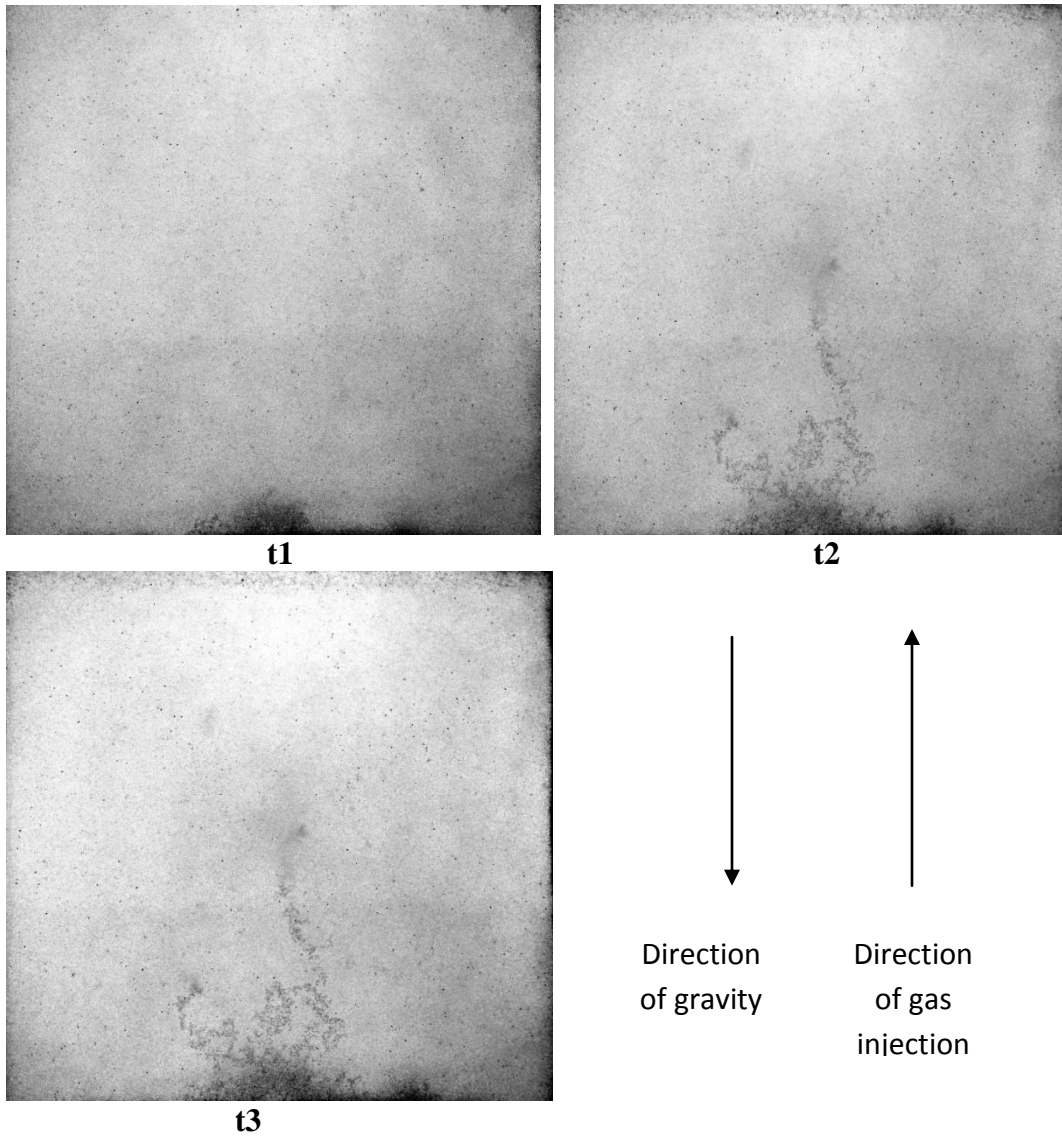


Figure 31: Effect of drawdown on drainage pattern at 20 psi drawdown, showing development of fingers at time intervals t1, t2 and t3

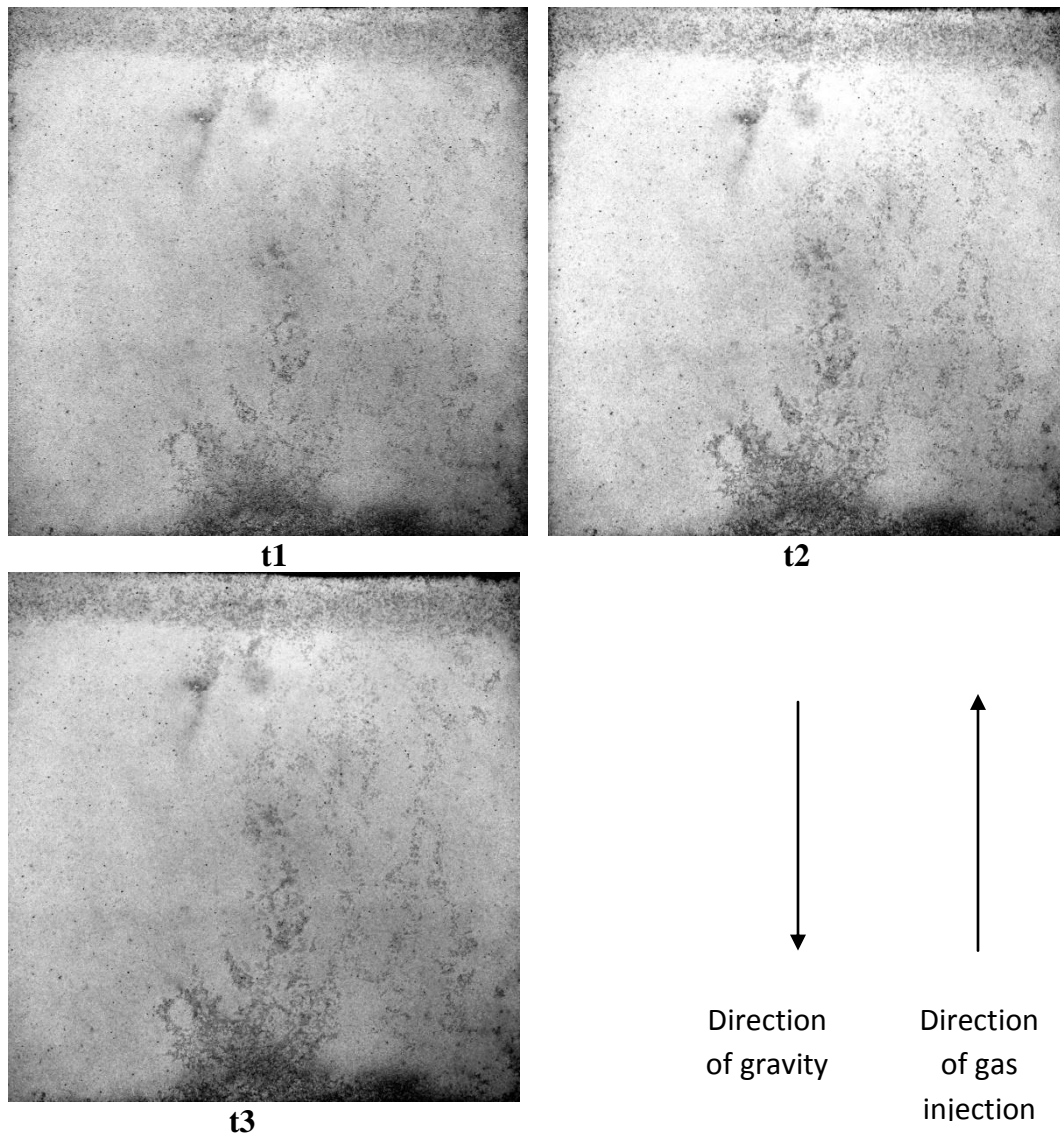


Figure 32: Effect of drawdown on drainage pattern at 30 psi drawdown, showing development of fingers at time intervals t1, t2 and t3

6.1.3 Effect of Surface Tension and Proppant Wettability (Set3): To study the effect of surface tension and proppant wettability characteristics on the frac fluid recovery, we change the interfacial tension of the frac-fluid and wettability of the glass beads used as proppant.

Table 6.3: Experimental conditions to test the effect of surface tension and surface property (Set 3)

Property	Test 1	Test 2	Test 3	Test 4
Type of fracturing fluid	100% Water	1 Wt% Isopropanol in Water	100% Water	1 Wt% Isopropanol in Water
Viscosity	1 cp	1 cp	1 cp	1 cp
Interfacial tension	72 dynes/cm	42 dynes/cm	72 dynes/cm	42 dynes/cm
Gas injected	Nitrogen	Nitrogen	Nitrogen	Nitrogen
Drawdown	20 psi	20 psi	20 psi	20 psi
Type of proppants	Normal glass beads	Normal glass beads	Treated glass beads	Treated glass beads
Proppant size	16/30	16/30	16/30	16/30
Wettability	Hydrophilic	Hydrophilic	Hydrophobic	Hydrophobic

Effect of Surface Tension (Test 2 of set 3): We study the effect of surface tension by using isopropanol. A solution of 1wt% of isopropanol in water was prepared. Surface tension of the resulting fluid is measured using DuNouy tensiometer. The operating conditions for these set of experiments are listed in Table 6.3.

Figure 33 compares the recovery profiles of isopropanol solution and water. It is observed that the ultimate recovery of isopropanol solution is almost 30% higher than that of water.

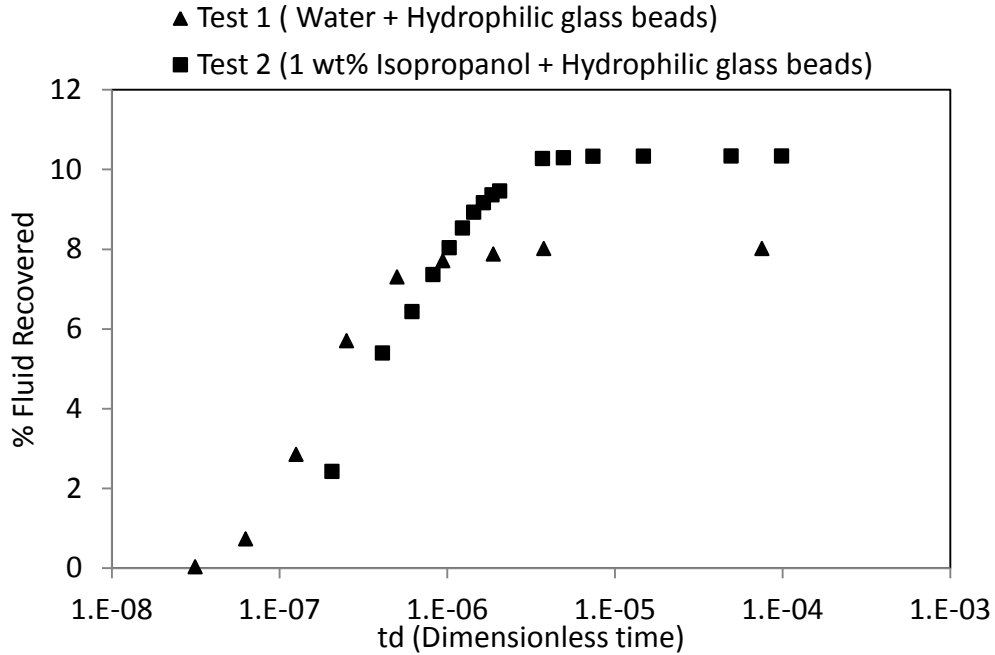


Figure 33: Effect of interfacial tension (Set 3, test 2): Semi-log plot of normalized fluid recovery versus dimensionless time

Drainage patterns observed during the displacement experiments with isopropanol solutions are shown in Figure 34. Comparing the drainage pattern of isopropanol solution (Figure 34) with that of water (Figure 31), indicates that more fingers are generated in the case of isopropanol solution (i.e. frac-fluid with low surface tension) as compared to normal water. More fingers mean higher areal sweep efficiency and, hence, higher fluid recovery.

Dependency of finger thickness on surface tension has been studied experimentally and the following expression has been proposed^{28,29}

$$h = 1 - \left(\frac{\mu U}{\sigma} \right)^{1/2} \quad (6.1)$$

Where,

h = Thickness of finger

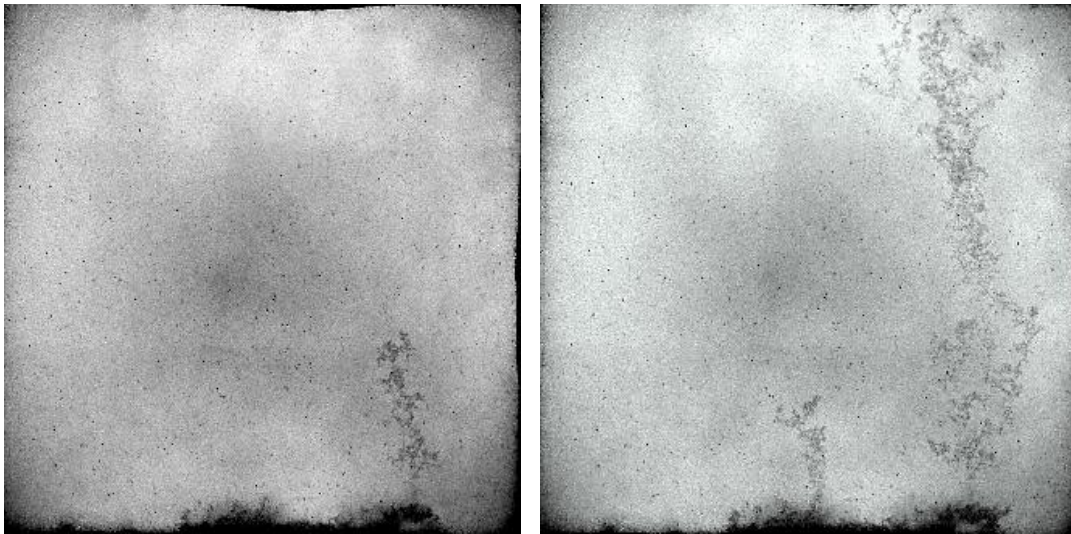
μ = Viscosity of displaced fluid

U = Velocity of finger

σ = Surface tension

Equation (5) suggests a decrease in finger thickness with reduction in surface tension. But, in our case we don't observe any significant change in the size of the fingers by reducing surface tension, comparing Figures 31 and 34.

Another study³⁰ conducted by using random walk model shows that with reduction in surface tension, fingers generated begin to split as they travel through porous media. Consistently, Figure 34 shows that fingers generated at the center and right side of experimental cell break into multiple fingers as they travel through the length of the porous medium.



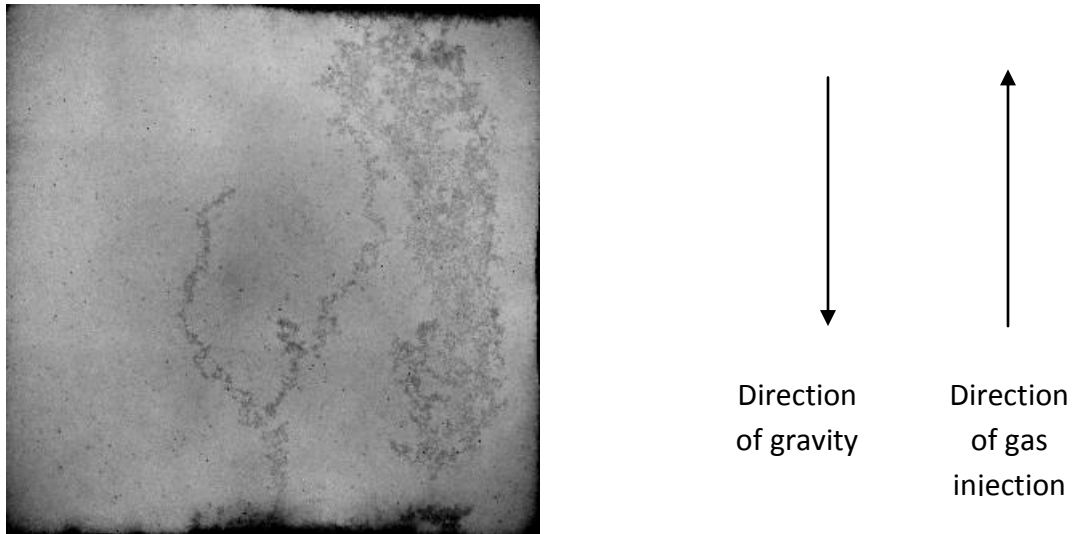


Figure 34: Drainage pattern at time interval t1, t2 and t3 in experimental cell packed with hydrophilic glass beads and saturated with 1 wt% isopropanol solution (test2 of set3)

Effect of Wettability (test 3 of set 3): To change the wettability of the glass beads, we use the procedure suggested by Shahidzadeh-Bonn et. al ²². Step by step procedure to alter the wettability is explained in chapter 3.

The resulting glass beads were hydrophobic with the contact angle greater than 90° as shown in Figure 35 (b). These chemically treated glass beads were then packed in the experimental cell. Detailed experimental conditions for this test are presented in Table 6.3.

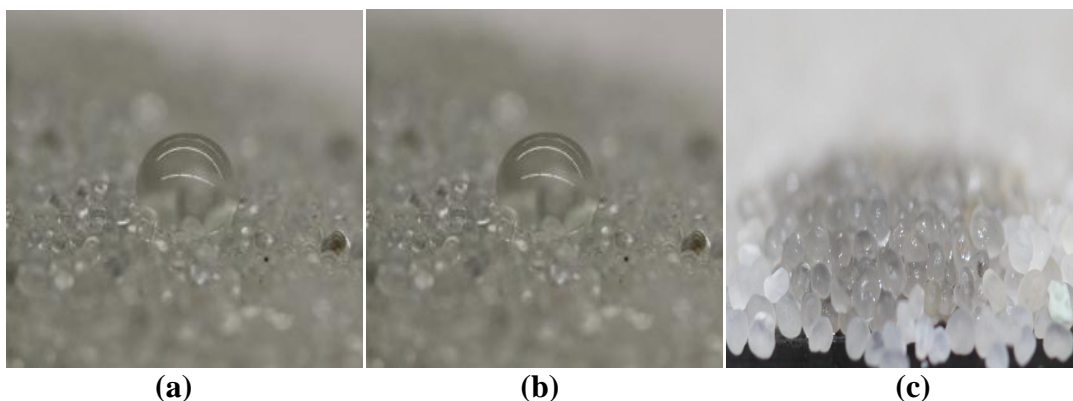


Figure 35: (a) Contact angle of 1 wt% isopropanol on hydrophobic (treated) glass beads (b) Contact angle of water on hydrophobic (treated) glass beads (c) Contact angle for water on hydrophilic (untreated) glass beads

As shown in Figure 36, ultimate recovery of frac-fluid from hydrophobic pack (18.61%) is more than two times higher than that from hydrophilic pack (8.01%).

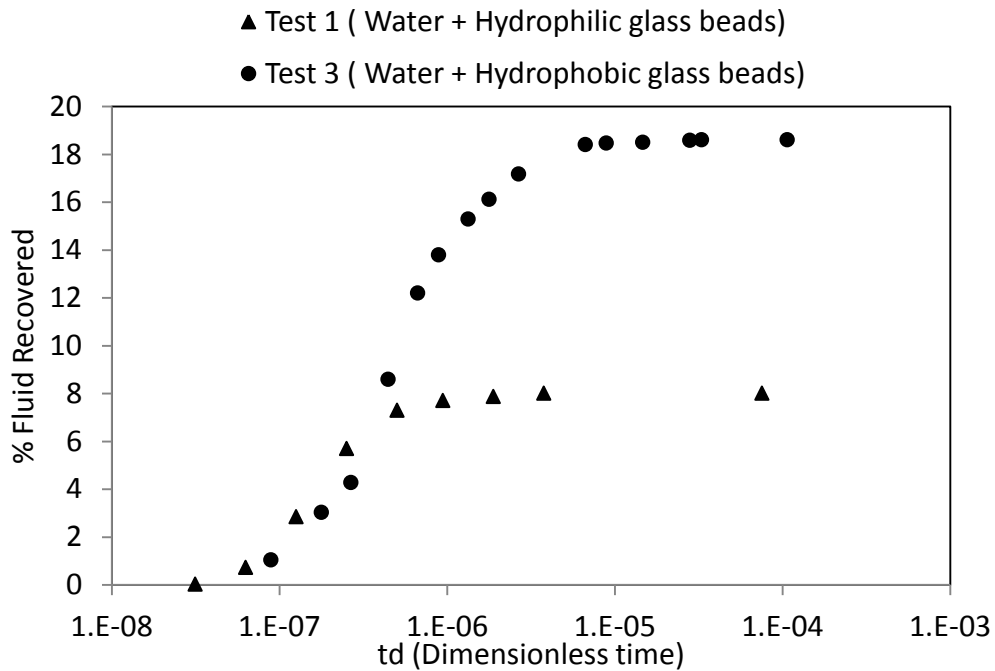


Figure 36: Effect of wettability (Set 3, test 2): Semi-log plot of normalized fluid recovery versus dimensionless time

As shown in Figure 37, channels of gas are observed to be formed with hydrophobic glass beads. The thickness of these channels is higher than thickness of fingers observed with hydrophilic pack (Figure 31 and 34). This indicates that the sweep efficiency is better in porous media packed with hydrophobic proppants. This observation shows the strong effect of surface properties on sweep efficiency during fracture clean-up. However, the effect of gravity is still dominant, as the ultimate recovery does not exceed 20 %.

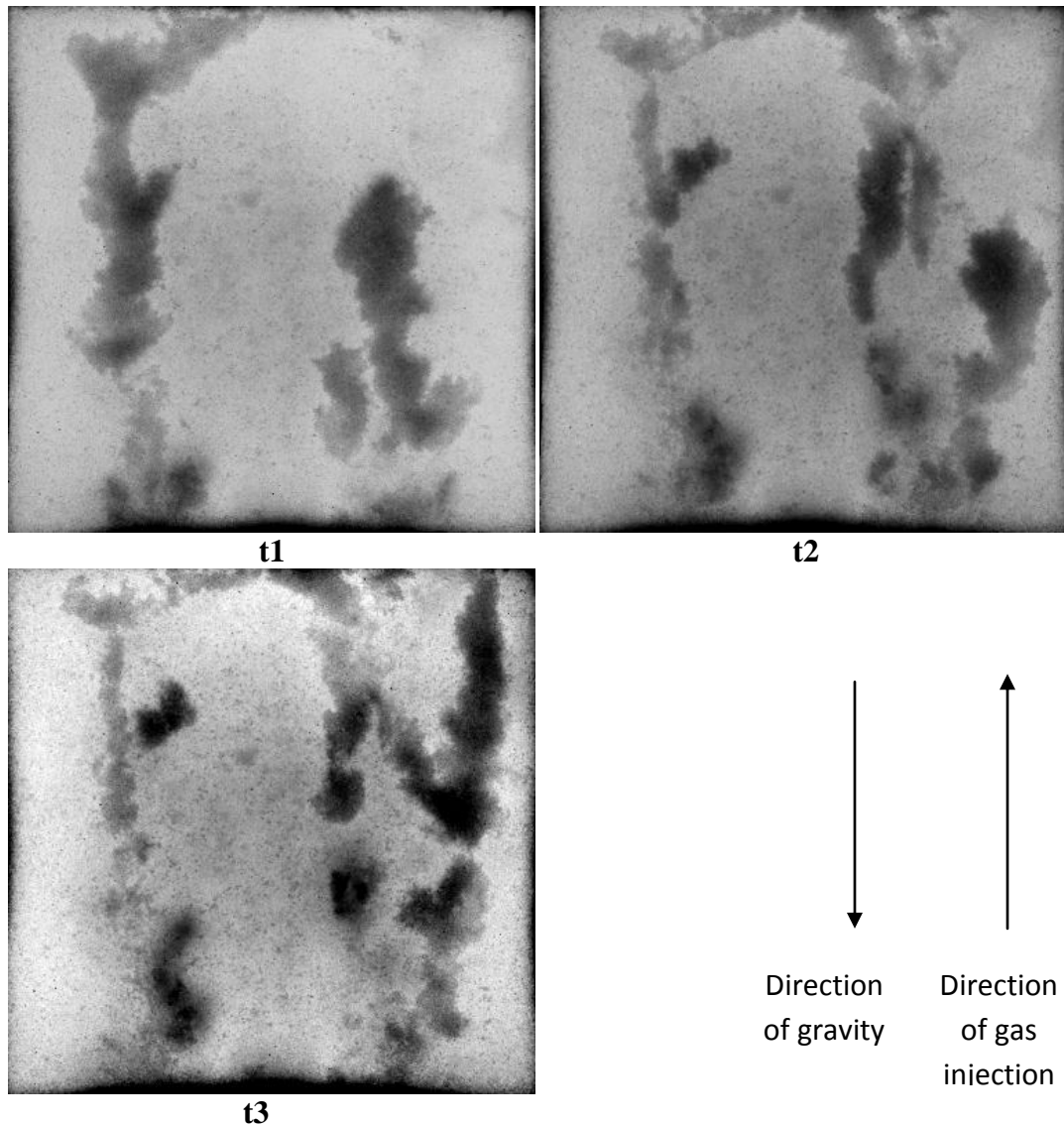


Figure 37: Drainage pattern at time intervals t1, t2 and t3 in experimental cell packed with hydrophobic glass beads and saturated with water (test3 of set3)

In a previous study²², done by draining proppant packed columns saturated with water, an increase in water recovery was observed by changing the wettability of glass beads from hydrophilic to hydrophobic. In another study¹³, of water flooding experiments conducted in oil saturated cores, higher oil recovery rates were observed in water wet cores as compared with oil wet cores. For oil wet cores, the instability is higher and results in early breakthrough of water and low oil recovery. From these studies, it can be concluded that for better sweep efficiency, the porous

media should be preferentially wetted by displacing fluid rather than displaced fluid.

When using hydrophobic glass beads, we also observe discontinuous gas lumps, which move upward and displace water rather than gas traveling in continuous fingers. These lumps disappear when they reach the production end and new lumps are formed at the gas injection end. Figure 38 illustrates the formation and growth of such gas lumps.

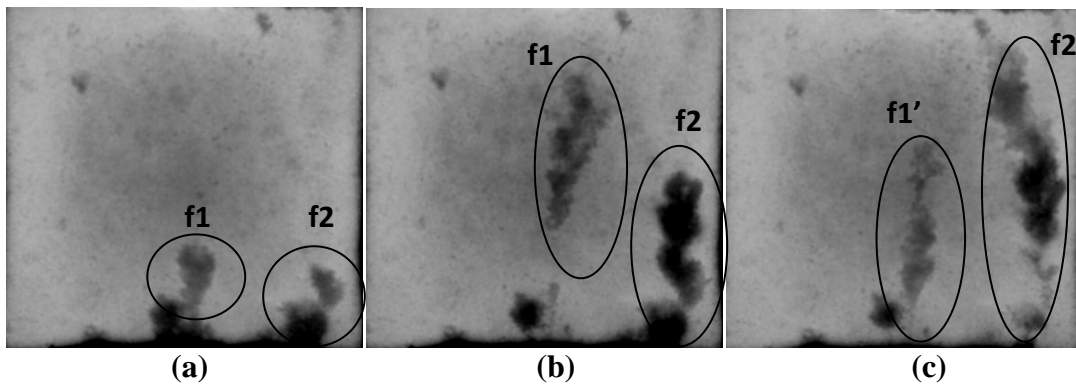


Figure 38: Illustrates formation and growth of gas lumps at three different time interval (a) Gas lumps f1 and f2 are formed (b) Gas lump f1 becomes discontinuous and gas lump f2 keeps growing (c) Gas lump f1 disappears and a new gas lump f1' is formed. Gas lump f2 grows and becomes discontinuous.

There are two ways of looking at this phenomenon

(a) At the microscopic scale, imbibition and drainage occur simultaneously. When a new gas lump is formed, it drains the water and creates low water saturated area. But, soon water, from the surrounding high water saturated area, imbibes into the drained area and replaces the gas.

(b) At macroscopic scale, counter current flow of water and gas occur due to buoyancy effect. Gas with a lower density moves upward due to buoyancy effect and water drains downwards.

Combined Effect of Surface Tension and Wettability (test 4 of set 3): This test is

aimed to study combined effect of surface tension and wettability. Table 6.3 lists the operating conditions used for this set of experiments. As shown in Figure 39, it is observed that recovery in test 4 (Isopropanol solution+Hydrophobic proppants) is higher than that in test 1 (Water + hydrophilic proppants) and test 2 (isopropanol solution + hydrophilic proppants) but it is slightly less than that in test 3 (water+hydrophobic proppants). Figure 40 shows that wide channels are formed in test 4 resulting in a higher water recovery.

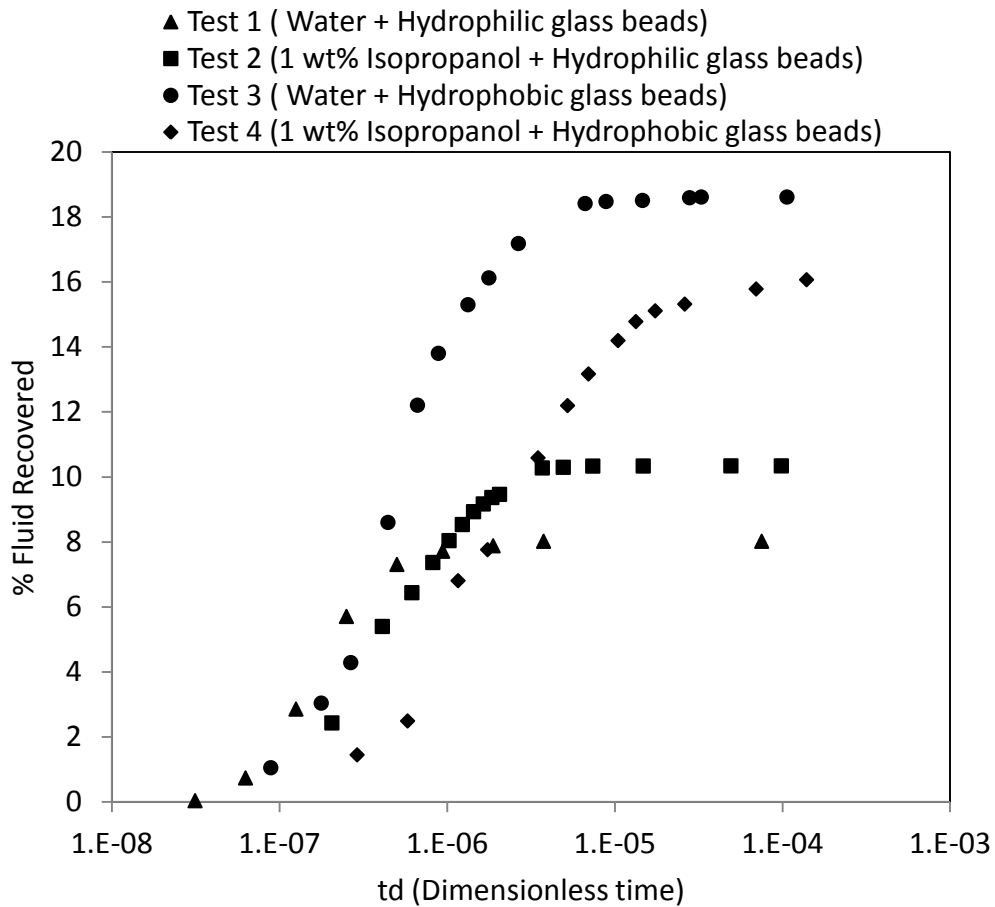


Figure 39: Effect of surface tension and wettability (Set 3): Semi-log plot of normalized fluid recovery versus dimensionless time

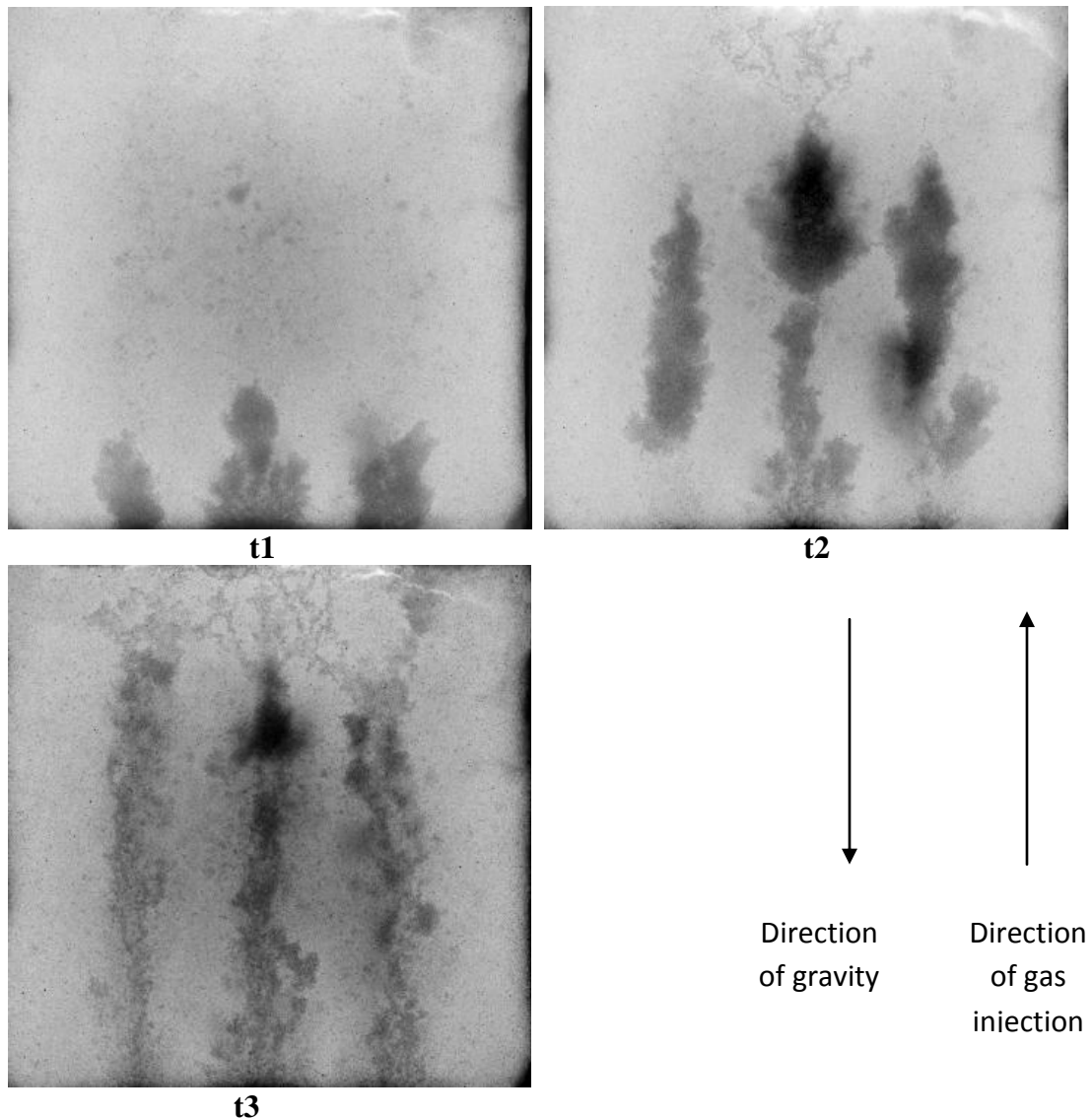


Figure 40: Drainage pattern at time interval t1, t2 and t3 in the experimental cell packed with hydrophobic glass beads and saturated with 1 wt% isopropanol solution (test4 of set 3)

6.1.4 Effect of Viscosity: We study the effect of viscosity on fracture drainage by adding 0.025 Wt% of Xanthan Gum to water. Variation of the resulting fluid viscosity with shear rate is shown in Figure 41. This fluid is then used to saturate the proppant pack. The operating conditions for this experiment are listed in table 6.4. As shown in Figure 42, the recovery of this fluid is almost negligible, 0.8%. Drawdown of 20 psi is not sufficient to overcome the increased viscous forces due

to high frac fluid viscosity. Also, since there is no drainage of the fluid, no drainage pattern is observed in Figure 43.

Table 6.4: Experimental conditions to test the effect of fluid viscosity (Set 4)

Property	Test 1	Test 2
Type of fracturing fluid	0.025 Wt% Xanthan gum in water	100% Water
Viscosity	10 cp @ 1 (1/s) shear rate	1 cp
Gas injected	Nitrogen	Nitrogen
Drawdown	20 psi	20psi
Type of proppants	Normal glass beads	Normal glass beads
Proppant size	16/30	16/30
Wettability	Hydrophilic	Hydrophilic

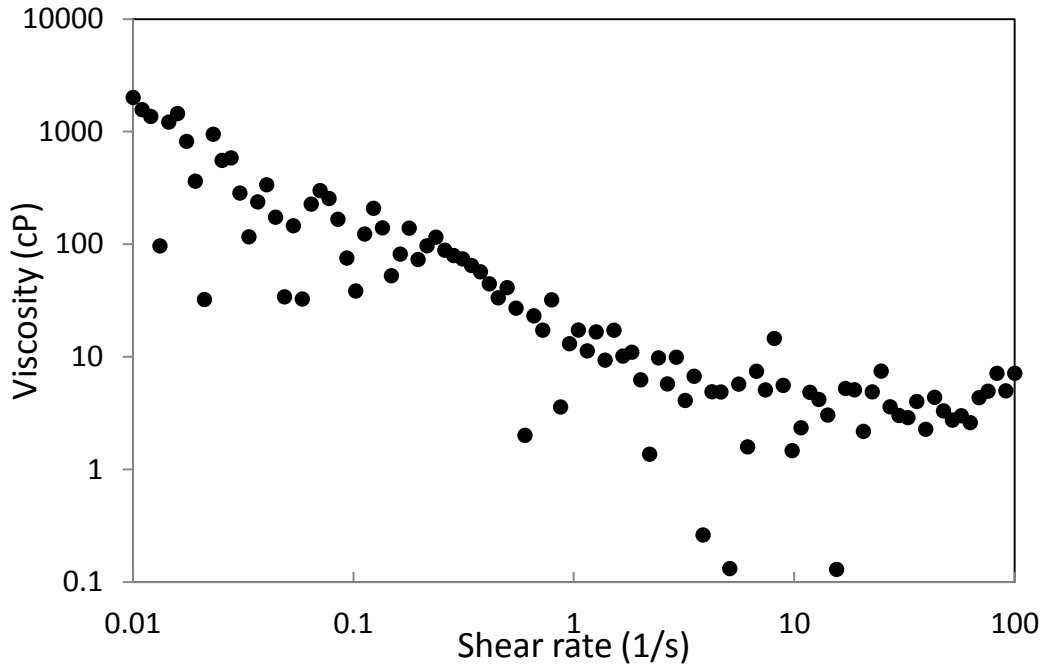


Figure 41: Variation of viscosity of 0.025% xanthan gum solution with shear rate on a log-log plot

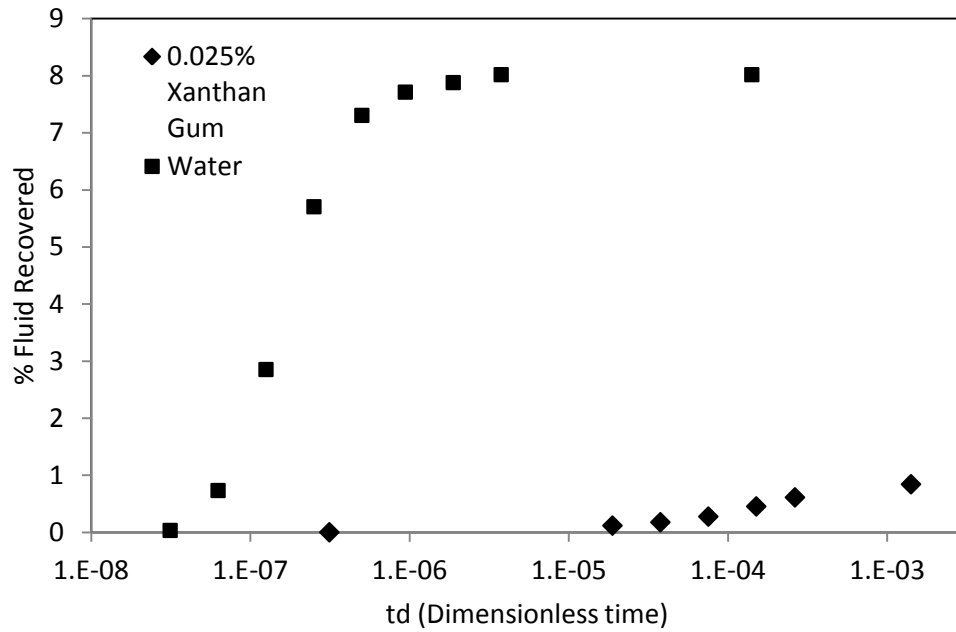
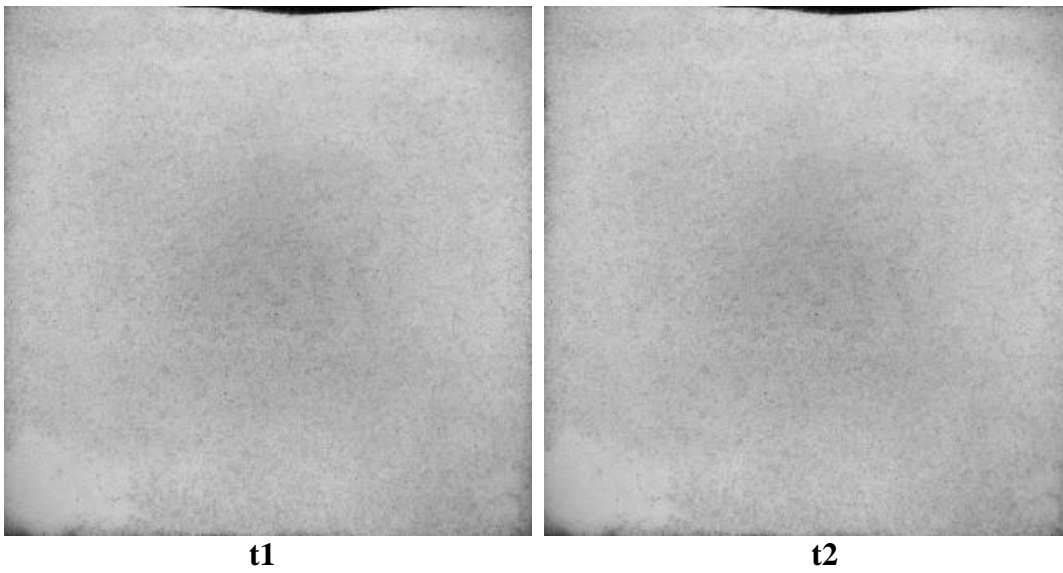
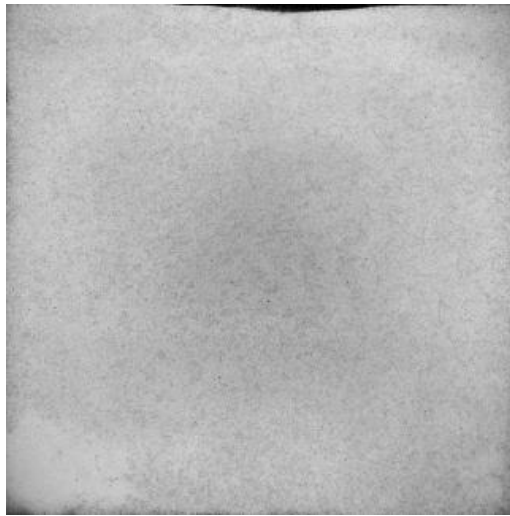


Figure 42: Comparison of the recovery rate for two different fluids





t3

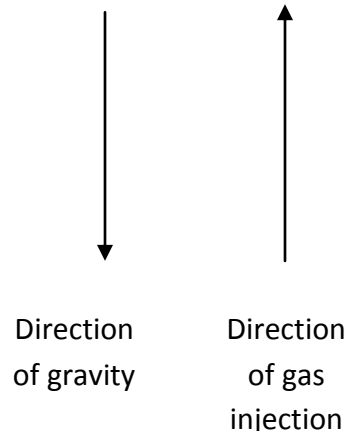


Figure 43: Drainage pattern at time interval t1, t2 and t3 in experimental cell saturated with 0.025 wt% xanthan gum solution

6.2 Discussion

6.2.1 Experimental Setup Limitations

The fracture model used may have some possible limitations which are discussed below:

- 1) Point Injection: Gas was injected in the fracture model through three inlet ports which were quarter inch in diameter. A cotton cloth was used to cover the inlet ports to ensure uniform gas injection. Uniform gas front was observed in vertical downward displacement of water by gas, indicating uniform gas distribution in the cell. Thus, the fingers observed in the gravity unstable tests were due to displacement instability and not due to point injection.
- 2) Fracture Pack: Our fracture model was tightly packed with proppants but reservoir fractures may or may not be completely packed with proppants. In case the fractures are not tightly packed, water recovery from fractures may be different from what we see in our results.

3) Spontaneous Imbibition: Proppants in the fracture model were enclosed between two plexi glass sheets instead of rock matrix. Hence there was no frac-fluid loss due to spontaneous imbibition in our experimental setup.

4) Gas influx from fracture face: In reservoir conditions gas influx is from fracture face while in our physical model, gas was injected from one side of the fracture model. The reason for using this approach is explained using Figure 44. Also, in our explanation we assume that flow in fractures is in one direction i.e. from reservoir towards wellbore.

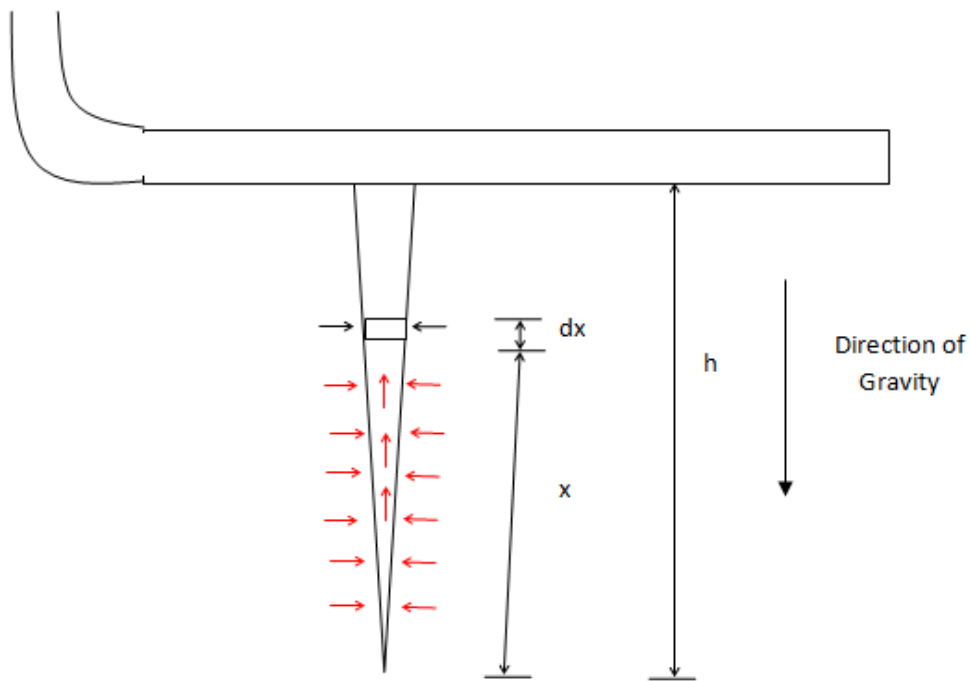


Figure 44: Illustration of fracture below horizontal well with reservoir feeding gas into the fracture

Where,

h = fracture height

dx = small fraction of fracture (our fracture model represents this part)

x = Part of the fracture feeding element dx

Our fracture model was 1 feet in height whereas fracture height in the reservoir may be as high as 100 feet. Thus our fracture model represents small part of the fracture represented by dx in Figure 44.

As shown in Figure 44, reservoir feeds gas into the fracture from its face. After entering the fracture gas flows upward towards the wellbore. The cumulative gas influx from the lower portion of fracture (represented by x) enters the bottom of the fracture element dx . This gas influx (shown in red in Figure 44) is much higher than the gas influx coming from fracture face of element dx (shown in black in Figure 44). Thus for element dx gas influx from the fracture face can be neglected. Since the small element dx represents our fracture model, we can conclude that absence of gas influx from fracture face, in our physical model, does not have much impact on the general results.

6.2.2 Results

Figure 45 summarizes the results of all the experiments performed in the study, and demonstrates the strong effect of gravity on water recovery. Three distinct clusters for gravity stable, gravity neutral and gravity unstable behavior can be observed.

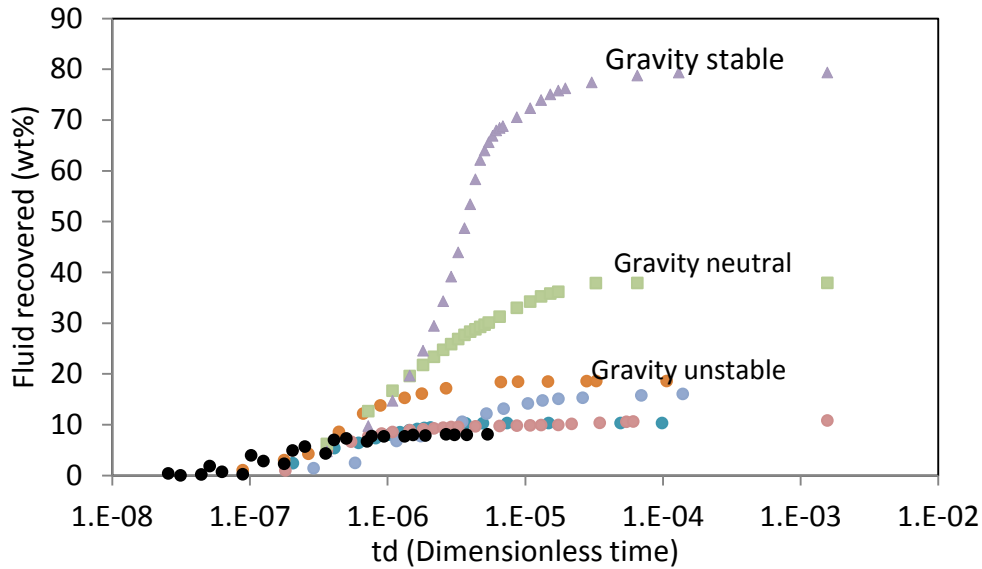


Figure 45: Comparison of recovery rate of all the drainage experiments conducted in this study shows three different types of recovery profiles for gravity stable, gravity neutral and gravity unstable tests

Based on the results of this study, it can be concluded that upward displacement of water by gas in a porous media is unstable. Fingering results in poor sweep efficiency and thus, low water recovery. Furthermore, for upward displacement, it is observed that drawdown has a minor effect on water recovery. However, using surfactant in frac-fluid resulted in 30% increase in ultimate recovery. Also, changing the wettability of porous media from hydrophilic to hydrophobic doubled the water recovery. Changing the wettability resulted in formation of wider fingers and thus, higher sweep efficiency and ultimate water recovery.

The results of this study can be used to explain low frac-fluid recovery observed during flowback operation after hydraulic fracturing treatments. Some of the fractures created by multi-stage hydraulic fracturing are below the horizontal well. Clean-up of these fractures require displacement of water by gas against gravity

direction. Our results suggest that this displacement is not efficient and water recovery is very low due to poor sweep efficiency. Results observed in our study are in agreement with the results of field⁵⁶ and simulation⁵⁷ studies conducted by other researchers. Similar to our results their studies show inefficient cleanup of fractures below well.

Assuming 50% of fractures are created above and 50% fractures are created below the horizontal well, results of this study suggest that only 45% of the total fluid present in the fractures is recovered back during flow back operation. Therefore, the well is opened for flow back some of the water leaks into the formation due to spontaneous imbibitions. Imbibed water is not accounted in our calculations.

Finally, most of the simulation studies being conducted use relative permeability curves to model fracture drainage. This can be misleading since relative permeability curves can be used only when displacement is stable and uniform. Results from this study demonstrate that for upward displacement drainage takes place by channeling and fingering.

Chapter 7

Conclusions and Recommendations

7.1 Conclusions

Based on experimental results of this study, following conclusions can be drawn

7.1.1 Column Experiments

- Increase in proppant size resulted in increased production rate and ultimate recovery. Thus, coarse proppants should be used to ensure better fracture cleanup
- From the experimental data it is seen that variation in pore size distribution results in reduction in water recovery. Thus, proppants which can withstand the stresses, that they are anticipated to undergo in the reservoir, should be selected for fracturing job.
- Certain resin coated proppants, due to their hydrophobic nature, outperformed normal sand, in terms of fluid cleanup. This indicates that surface property of the proppant has an important role to play in fracture cleanup.
- Type of fluid does play an important role in fracture cleanup. The ultimate recovery with oil was higher than that of with water. However it was observed that production rate in case of oil was much lower than that of water. This is because of the high viscosity of the oil (18cP) as compared to water (1cP).

7.1.2 2D Experiments

- Water recovery from propped fractures is very low when the flow direction is against gravity. Based on the results, less than 45% of the fluid present in the fractures is recovered back (assuming 50% of all fractures are created above the well and 50% of all fractures are created below well).
- Drawdown pressure has negligible effect on ultimate water recovery from propped fractures.
- Use of surfactant in frac fluids results in almost 30% improvement in the ultimate fluid recovery.
- Number and size of fingers generated during frac fluid displacement by gas increased by reducing capillary forces (i.e., reduction of frac fluid surface tension). Therefore, using surfactants in fracturing fluids improves the sweep efficiency.
- Proppant wettability significantly influences the drainage pattern, sweep efficiency, and ultimate water recovery in fractures. Using hydrophobic proppants improves the sweep efficiency and in turn, increase the ultimate fluid recovery
- Fluid viscosity significantly influences the drainage rate and ultimate recovery. Addition of 0.025 wt% of Xanthan Gum results in almost negligible recovery of the frac fluid from the propped fractures.
- Finally, most of the simulation studies being conducted use relative permeability curves to model fracture drainage. This can be misleading since relative permeability curves can be used only when displacement is stable

and uniform. Results from this study demonstrate that for upward displacement drainage takes place by channeling and fingering.

7.2 Recommendations for Future Work

All the objectives set in the beginning of this study were achieved but in order to better understand fluid loss during hydraulic fracturing following may be carried out

- Fracture drainage model can be combined with fluid imbibition into the rock matrix. This will give a better understanding of amount of fluid that imbibes and fluid that stays in fractures.
- Effect of frac-fluid density can be tested on fracture drainage against gravity. Since gravity forces are mainly responsible for poor fracture drainage, decrease in density of frac-fluid should help improve fracture cleanup.
- Effect of fluid evaporation on fluid cleanup can be tested by raising the temperature of fracture model to reservoir conditions.

References

- 1) BP energy outlook 2030, London, January 2012
- 2) Blatt, H. and Robert J. T., (1996) *Petrology: Igneous, Sedimentary and Metamorphic*, 2nd ed., Freeman, pp. 281–292 ISBN 0-7167-2438-3
- 3) Cipolla, C.L., Lolon, E.P., Erdle, J.C., and Rubin, B. 2010. Reservoir Modeling in Shale-Gas Reservoirs. *SPE Res Eval & Eng* 13 (4): 638-653. SPE-125530-PA. <http://dx.doi.org/10.2118/125530-PA>
- 4) Andrews, A. et al. (30 October 2009) (PDF). *Unconventional Gas Shales: Development, Technology, and Policy Issues (Report)*. Congressional Research Service. p. 7; 23. Retrieved 22 February 2012
- 5) Abdalla, C. W.; Drohan, J. R. (2010) *Water Withdrawals for Development of Marcellus Shale Gas in Pennsylvania. Introduction to Pennsylvania's Water Resources (Report)*. The Pennsylvania State University. Retrieved 16 September 2012
- 6) Arthur, J. D.; Uretsky, M.; Wilson, P. (May 5–6, 2010). "Water Resources and Use for Hydraulic Fracturing in the Marcellus Shale Region". Meeting of the American Institute of Professional Geologists. Pittsburgh: ALL Consulting. p. 3. Retrieved 2012-05-09.

- 7) Cothren, J., Modeling the Effects of Non-Riparian Surface Water Diversions on Flow Conditions in the Little Red Watershed (Report). U. S. Geological Survey, Arkansas Water Science Center Arkansas Water Resources Center, American Water Resources Association, Arkansas State Section Fayetteville Shale Symposium 2012. p. 12. Retrieved 16 September 2012
- 8) Pagels.M, Hinkel, Hinkel.J.J, Willberg,D.M, 2012, Measuring Capillary Pressure Tells More Than Pretty Pictures, SPE Form Eval, SPE 151729-MS doi 10.2118/151729-MS
- 9) Tannich, J.D., 1975. Liquid Removal From Hydraulically Fractured Gas Wells, Journal of Petroleum Technology, Volume 27, Number 11, pg 1309-1317doi: 10.2118/5113-PA
- 10) Parekh,B., Sharma,M.M., 2004, Cleanup of Water Blocks in Depleted Low-Permeability Reservoirs, SPE 89837-MS DOI 10.2118/89837-MS
- 11) Fahimpour, J.,Jamiolahmady,M., Severac,S., Sohrabi,M., 2012 Optimization of Fluorinated Wettability Modifiers for Gas-Condensate Carbonate Reservoirs, SPE Primary and Enhanced Recovery Processes, SPE 154522-MS DOI 10.2118/154522-MS
- 12) Cheng, Y. 2012. Impact of Water Dynamics in Fractures on the Performance of Hydraulically Fractured Wells in Gas-Shale Reservoirs. J Can Pet Technol 51 (2): 143-151. SPE-127863-PA

- 13) Dehghanpour,H., DiCarlo,D.A, Aminzadeh.B., and Mirzaei,M., 2010, Two-Phase and Three-Phase Saturation Routes and Relative Permeability During Fast Drainage, SPE Improved Oil Recovery Symposium, SPE 129962-MS, DOI: 10.2118/129962-MS
- 14) Howard,P.R., Mukhopadhyay,S., Moniaga,N., Schafer,L.,Penny,G., Dismuke,K., 2010 Comparison of Flowback Aids: Understanding Their Capillary Pressure and Wetting Properties, SPE Production & Operations, SPE 122307-PA, DOI: 10.2118/122307-PA
- 15) Dehghanpour,H., Aminzadeh, B., Mirzaei, M. and DiCarlo, D. A., 2011, Flow coupling during three-phase gravity drainage, Phys. Rev. E 83, 065302(R), DOI: 10.1103/PhysRevE.83.065302
- 16) Shahidzadeh-Bonn, N., Tournié, A., Bichon, S., Vié, P., Rodts, S., Faure, P., Bertrand, F., Azouni, A. 2004, Effect of wetting on the dynamics of drainage in porous media, Transport in Porous Media, Volume 56, Number 2, pg 209-224, DOI:10.1023/B:TIPM.0000021876.70521.bc
- 17) Pope, D.S., Leung, L.K., Gulbis, J., and Constien, V.G., 1996 Effects of Viscous Fingering on Fracture Conductivity, SPE Production & Facilities, SPE 28511-PA, DOI: 10.2118/28511-PA
- 18) Cottin,C., Bodiguel,H., and Colin,A., 2010, Drainage in two-dimensional porous media: From capillary fingering to viscous flow, Phys. Rev. E 82, 046315, Volume 82, Issue 4, DOI: 10.1103/PhysRevE.82.046315

- 19) Benham, A.L., Olson, R.W., 1963, A Model Study of Viscous Fingering, SPE J., SPE 513-PA, DOI: 10.2118/513-PA
- 20) Tidwell, V., Parker, M., Laboratory Imaging of Stimulation Fluid Displacement from Hydraulic Fractures, SPE 36491-MS, SPE Annual Technical Conference and Exhibition, 6-9 October 1996, Denver, Colorado, <http://dx.doi.org/10.2118/36491-ms>
- 21) Shariatpanahi, S.F., Dastyari, A., Bashukooh, B., Haghghi, M., Sahimi, M., Ayatollahi, S.S., Shiraz U, Visualization Experiments on Immiscible Gas and Water Injection by Using 2D-Fractured Glass Micromodels, SPE Middle East Oil and Gas Show and Conference, Mar 12 - 15, 2005 2005, Kingdom of Bahrain, 2005, <http://dx.doi.org/10.2118/93537-ms>
- 22) Glass, R.J., Conrad, S.H., Peplinski, W., Gravity-destabilized nonwetting phase invasion in macroheterogeneous porous media: Experimental observations of invasion dynamics and scale analysis , Water Resources Research, Vol 36 Issue 11 <http://dx.doi.org/10.1029/2000wr900152>
- 23) Ji,W. Dahmani, A., Ahlfeld, D.P., Lin, J.D., Laboratory Study of Air Sparging: Air Flow Visualization, Edward Hill III , Groundwater Monitoring & Remediation, Vol 13 Issue 4, <http://dx.doi.org/10.1111/j.1745-6592.1993.tb00455.x>
- 24) Peters, E.J., Advanced petrophysics, Vol.1
- 25) What are horizontal drilling and hydraulic fracturing?, <http://www.dec.ny.gov/energy/46288.html#horizontal>

- 26) McDaniel, B.W., Marshall, E., East, L. and Surjaatmadja, J., CT-Deployed Hydrjet Perforating in Horizontal Completions Provides New Approaches to Multi-Stage Hydraulic Fracturing Applications SPE/ICoTA Coiled Tubing Conference & Exhibition, 4-5 April 2006, The Woodlands, Texas, USA DOI 10.2118/100157-MS
- 27) Valkó, P.P., Fracture Design Fracture Dimensions Fracture Modeling, Hydraulic fracturing short course notes, Texas A&M university
- 28) Howard, G.C., Hydraulic fracturing, 1970
- 29) Ouabdesselam, M., Hudson, P.J., An Investigation of the Effect of Cyclic Loading on Fracture Conductivity, SPE 22850-MS, SPE Annual Technical Conference and Exhibition, 6-9 October 1991, Dallas, Texas, <http://dx.doi.org/10.2118/22850-ms>
- 30) Lacy, L.L., Rickards, A.R., Bilden, D.M., Fracture Width and Embedment Testing in Soft Reservoir Sandstone, SPE Drilling & Completion, Volume 13, Number 1, Pages 25-29, DOI: 10.2118/36421-PA
- 31) Penny, G.S., An Evaluation of the Effects of Environmental Conditions and Fracturing Fluids Upon the Long-Term Conductivity of Proppants, SPE Annual Technical Conference and Exhibition, 27-30 September 1987, Dallas, Texas, DOI: 10.2118/16900-MS
- 32) King, G.E., Thirty Years of Gas Shale Fracturing: What Have We Learned?, SPE Annual Technical Conference and Exhibition, 19-22 September 2010, Florence, Italy, DOI:10.2118/133456-MS

33) Online presentation by Carbo ceramics, An Introduction to Proppants and Their Properties, http://www.slideshare.net/SS_CARBO-ceramics/proppant-101-atce2012

34) Terracina, J.M., Turner, J.M., Collins, D.H. and Spillars, S.E., Proppant Selection and Its Effect on the Results of Fracturing Treatments Performed in Shale Formations, SPE Annual Technical Conference and Exhibition, 19-22 September 2010, Florence, Italy, DOI: 10.2118/135502-MS

35) Rahim, Z., Al-Anazi, H. and Al-Kanaan, A., Selecting Optimal Fracture Fluids, Breaker System, and Proppant Type for Successful Hydraulic Fracturing and Enhanced Gas Production - Case Studies, 2013 SPE Middle East Unconventional Gas Conference & Exhibition, Jan 28 - 30, 2013 2013, Muscat, Sultanate of Oman, DOI: 10.2118/163976-MS

36) Gupta, D.V.S. and Leshchyshyn, T.T. , CO₂-Energized Hydrocarbon Fracturing Fluid: History and Field Application in Tight Gas Wells, SPE Latin American and Caribbean Petroleum Engineering Conference, 20-23 June 2005, Rio de Janeiro, Brazil, DOI: 10.2118/95061-MS

37) Gupta, D.V.S. and Hlidek, B.T., Frac-Fluid Recycling and Water Conservation: A Case History, SPE Production & Operations, Volume 25, Number 1, pp. 65-69, 2010, DOI: 10.2118/119478-PA

38) Hlidek, B.T., Meyer, R.K., Yule, K., and Wittenberg, J., A Case for Oil-Based Fracturing Fluids in Canadian Montney Unconventional Gas Development, SPE Annual Technical Conference and Exhibition, 8-10 October 2012, San Antonio, Texas, USA, DOI: 10.2118/159952-MS

- 39) Fink, J. K. 2003. Oil field chemicals, Amsterdam: Gulf Professional Publications
- 40) Johnson, K., French, K., Fichter, J.K., and Oden, R., Use Of Micro biocides In Barnett Shale Gas Well Fracturing Fluids To Control Bacteria Related Problems, CORROSION 2008, March 16 - 20, 2008 , New Orleans LA
- 41) Kaufman, P., Penny, G.S., and Paktinat, J., Critical Evaluation of Additives Used in Shale Slickwater Fracs, SPE Shale Gas Production Conference, 16-18 November 2008, Fort Worth, Texas, USA, DOI: 10.2118/119900-MS
- 42) Understanding hydraulic fracturing, Candian society for unconventional gas.
- 43) Penny, G.S., and Pursley, J.T., CESI Chemical, and T.D. Clawson, Field Study of Completion Fluids To Enhance Gas Production in the Barnett Shale, SPE Gas Technology Symposium, 15-17 May 2006, Calgary, Alberta, Canada, DOI: 10.2118/100434-MS
- 44) Panga, M.K.R., Ooi, Y.S., P.L. Koh, Teknologi, U., Chan, K.S., Enkababian, P., Chenevière, P., Samuel, M., 2006 Wettability Alteration for Water Block Prevention in High Temperature Gas Wells, Society of Petroleum Engineers, ISBN 978-1-55563-230-4, DOI 10.2118/100182-MS
- 45) Tang, G., and Firoozabadi, A., Relative Permeability Modification in Gas/Liquid Systems Through Wettability Alteration to Intermediate Gas Wetting, SPE Reservoir Evaluation & Engineering, Volume 5, Number 6, pp 427-436, DOI: 10.2118/81195-PA

- 46) Tang, G., and Firoozabadi, A., Wettability alteration to intermediate gas wetting in porous media at elevated temperature in porous media, 52, 185-211, 2003
- 47) Holditch, S.A, 1979, Factors affecting water blocking and gas flow from hydraulically fractured gas wells, Journal of Petroleum Technology, Volume 31, Number 12. Pg 1515-1524, DOI: 10.2118/7561-PA
- 48) Yu, X. and Guo, B., How Much Can Fracturing Fluid Damage Productivity of Oil Wells?, SPE International Symposium and Exhibiton on Formation Damage Control, 10-12 February 2010, Lafayette, Louisiana, USA, DOI: 10.2118/125905-MS
- 49) Fletcher, A.J.P., Lamb, S.P., Clifford, P.J., Formation Damage From Polymer Solutions: Factors Governing Injectivity, , SPE Reservoir Engineering Journal, Volume 7, Number 2, 1992, <http://dx.doi.org/10.2118/20243-PA>
- 50) Navarrete, R. C., Himes, R. E., Seheult, J. M., Applications of Xanthan Gum in Fluid-Loss Control and Related Formation Damage, SPE Permian Basin Oil and Gas Recovery Conference, 21-23 March 2000, Midland, Texas, DOI: 10.2118/59535-MS
- 51) Navarrete, R.C., Mitchell, J. P., Fluid-Loss Control for High-Permeability Rocks in Hydraulic Fracturing Under Realistic Shear Conditions, SPE Production Operations Symposium, 2-4 April 1995, Oklahoma City, Oklahoma, DOI: 10.2118/29504-MS

- 52) Parlar, M., Nelson, E.B., Walton, I.C. Park, E., DeBonis, V., An Experimental Study on Fluid-Loss Behavior of Fracturing Fluids and Formation Damage in High-Permeability Porous Media, SPE Annual Technical Conference and Exhibition, 22-25 October 1995, Dallas, Texas, DOI: 10.2118/30458-MS
- 53) Ross, C.M., and Todd, B.L., Current Materials and Devices for Control of Fluid Loss, SPE Formation Damage Control Conference, 18-19 February 1998, Lafayette, Louisiana, DOI: 10.2118/39593-MS
- 54) Lovell, G., Meheust, Y., Maloy, K.J., Aker, E.: Competition of gravity, capillary, and viscous forces during drainage in a two-dimensional porous medium, a pore scale study. *Energy* 30(6), 861–872 (2005)
- 55) Peters, E. J., Flock, D. L., The Onset of Instability During Two-Phase Immiscible Displacement in Porous Media, *SPE Journal*, Volume 21, Number 2, <http://dx.doi.org/10.2118/8371-PA> (1981)
- 56) Taylor, R.S, Barree, R., Aguilera, R., Hoch, O., Storozhenko, K., Why Not to Base Economic Evaluations on Initial Production Alone, Canadian Unconventional Resources Conference, 15-17 November 2011, Alberta, Canada, SPE 148680-MS
- 57) Agrawal, S., Sharma, M.M, 2013, Impact of Liquid Loading in Hydraulic Fractures on Well Productivity, 2013 SPE Hydraulic Fracturing Technology Conference, Feb 04 - 06, 2013 2013, The Woodlands, TX, USA, SPE 163837-MS

- 58) Saffman, P.G. & Taylor, G. I. 1958 The penetration of fluid into a porous medium or Hele-Shaw cell. Proc. Roy. Soc. 245, 312-329.
- 59) McLean, J. W. and Saffman, P. G. The effect of surface tension on the shape of fingers in a Hele Shaw cell Volume 102 / January 1981, pp 455-469
- 60) Saffman, P.G, Taylor G (1958) Proc R Soc London Ser A 245:312
- 61) Homsy, G.M, Viscous fingering in porous media, Vol. 19: 271-311 (1987), <http://dx.doi.org/10.1146/annurev.fl.19.010187.001415>
- 62) Bensimon, D., Kadanoff, L.P., Liang, S., Shraiman, B. I., and Tang, C., "Viscous flows in two dimensions," Rev. Mod. Phys. 58, 977-999 (1986)
- 63) Chuoke, R.L., Meurs, P. van and Poel, C. van der, The Instability of Slow, Immiscible, Viscous Liquid-Liquid Displacements in Permeable Media, Petroleum Transactions, AIME, Volume 216, 1959, pages 188-194, Document ID 1141-G
- 64) Application of Integrated Reservoir Management and Reservoir Characterization to Optimize Infill Drilling, Quarterly Report September 13 - December 12, 1997 For U.S. Department of Energy Office of Fossil Energy
- 65) Cosse, R. 1993. "Basics of Reservoir Engineering". Institut Francais Du Petrole, Editions Technip, Paris, France
- 66) Stegent, N.A., Wagner, A.L., Mullen, J., Engineering a Successful Fracture-Stimulation Treatment in the Eagle Ford Shale, Tight Gas Completions Conference, 2-3 November 2010, San Antonio, Texas, USA, DOI: 10.2118/136183-MS

67) Wang, J.Y., Holditch, S.A., and McVay, D.A. 2010. Modeling Fracture-Fluid Cleanup in Tight-Gas Wells. SPE J. **15** (3): 783-793. SPE-119624-PA

68) Schlumberger glossary

http://www.glossary.oilfield.slb.com/en/Terms/d/displacement_efficiency.aspx

Appendix

This appendix presents detailed calculations used to obtain dimensionless time.

Step 1

Reduce the number of variables by grouping some variables which always exist together. For example gravity segregation is expressed as $\Delta\rho g$. Therefore we can replace ρ_w , ρ_{air} and g with one variable $\Delta\rho g$

The following are the experimental variables:

ΔP = Drawdown

d_p = Proppant diameter

t = Time

L = Length of experimental cell

W = Width of experimental cell

h = Thickness of experimental cell

μ_g = Injection gas viscosity

μ_L = Frac-fluid viscosity

$\Delta\rho g$ = Gravitational forces

$\sigma \cos \theta$ = Capillary forces

Step 2

Form the power product of all the variables listed above to obtain a dimensionless constant

$$(\Delta P)^{x_1} * (dp)^{x_2} * (t)^{x_3} * (L)^{x_4} * (\Delta \rho g)^{x_5} * (\sigma \cos \theta)^{x_6} * (\mu g)^{x_7} * (\mu L)^{x_8} * (h)^{x_9} * (W)^{x_{10}} = \text{Dimensionless constant} \quad (\text{A.1})$$

Step 3

Express each of the variables in terms of basic dimensional variables i.e. mass (M), length (L) and time (T).

$$[ML^{-1}T^{-2}]^{x_1} * [L]^{x_2} * [T]^{x_3} * [L]^{x_4} * [ML^{-2}T^{-2}]^{x_5} * [ML^{-2}]^{x_6} * [ML^{-1}T^{-1}]^{x_7} * [ML^{-1}T^{-1}]^{x_8} * [L]^{x_9} * [L]^{x_{10}} = \text{Dimensionless constant} \quad (\text{A.2})$$

Step 4

Since the right side of equation A2 is a dimensionless constant. Therefore, it can be represented as $[M^0L^0T^0]$. Now, equating the powers of mass, length and time on both sides gives us following linear homogenous equations. Equation 3.3, 3.4 and 3.5 are obtained by equating the powers of mass, length and time on both sides.

$$M: x_1 + x_5 + x_6 + x_7 + x_8 = 0 \quad (\text{A.3})$$

$$L: -x_1 + x_2 + x_4 - 2x_5 - 2x_6 - x_7 - x_8 + x_9 + x_{10} = 0 \quad (\text{A.4})$$

$$T: -2x_1 + x_3 - 2x_5 - x_7 - x_8 = 0 \quad (\text{A.5})$$

Equations 3.3, 3.4 and 3.5 can be represented in the form of a matrix as shown by equation 3.6

$$\begin{vmatrix} 1 & 0 & 0 & 0 & 1 & 1 & 1 & 1 & 0 & 0 \\ -1 & 1 & 0 & 1 & -2 & -2 & -1 & -1 & 1 & 1 \\ -2 & 0 & 1 & 0 & -2 & 0 & -1 & -1 & 0 & 0 \end{vmatrix} \begin{vmatrix} x1 \\ x2 \\ x3 \\ x4 \\ x5 \\ x6 \\ x7 \\ x8 \\ x9 \\ x10 \end{vmatrix} = \begin{vmatrix} 0 \\ 0 \\ 0 \end{vmatrix} \quad (\text{A.6})$$

Coefficients of equations A.3, A.4 and A.5 can be represented in the form of a matrix as shown by equation A.7

$$A = \begin{vmatrix} 1 & 0 & 0 & 0 & 1 & 1 & 1 & 1 & 0 & 0 \\ -1 & 1 & 0 & 1 & -2 & -2 & -1 & -1 & 1 & 1 \\ -2 & 0 & 1 & 0 & -2 & 0 & -1 & -1 & 0 & 0 \end{vmatrix} \quad (\text{A.7})$$

Next, we solve equation A.6 to obtain solution for the powers of variables which will give us a dimensionless constant. One obvious solution is a trivial solution of $x1 = x2 = x3 = x4 = x5 = x6 = x7 = x8 = x9 = x10 = 0$. But we want a non-trivial solution.

There is a detailed theory available to obtain non-trivial solution for set of linear homogenous equation such as A.6. However, we will apply a small part of that theory to obtain solution to our linear homogenous equation (A.6). The solution will give us a complete set of independent dimensionless groups. From equation A.6 it is seen that number of variables (10) is greater than number of equations (3). Thus we will have infinite number of solutions to equation A.6. We want these non-trivial solutions.

Rank (r) of matrix A is determined by largest r by r sub matrix whose determinant is non zero. According to Buckingham's π -theorem, the number of complete and independent dimensionless π groups is given by the number of variables minus the rank of the dimensional matrix. Therefore, if we can find the rank of matrix A we can predict the number of complete and independent solutions.

To determine the rank of matrix A, we first take a 3 by 3 sub-matrix of A and calculate its determinant. We take the first three columns of matrix A. The determinant of resulting sub-matrix is equal to 1 as shown in equation A.8.

$$\det \begin{vmatrix} 1 & 0 & 0 \\ -1 & 1 & 0 \\ -2 & 0 & 1 \end{vmatrix} = 1 \quad (\text{A.8})$$

Therefore, rank of matrix is 3. Hence there will be 10-3 or 7 complete and independent dimensionless groups.

Let us now use Gaussian elimination method to solve equation A.6. Gaussian elimination is a standard method used to solve linear algebraic equations. In Gaussian elimination simple row and column operations are performed to obtain an identity matrix. In this solution columns are carefully arranged so that there is no need to perform column operations. Thus, only row operations will be used to solve the equations.

Right hand side of equation A.6 is zero and it will remain zero even if we perform row operations. Hence we can ignore it in the calculations and only use the left hand side in the solution procedure. The left hand side of equation A.6 is illustrated in Table A.1

Table A.1: Calculation of identity matrix step 1

	ΔP	d_p	t	L	$\Delta \rho g$	$\frac{\sigma \cos}{\Theta}$	μ_g	μ_L	h	W
	x1	x2	x3	x4	x5	x6	x7	x8	x9	x10
M	1	0	0	0	1	1	1	1	0	0
L	-1	1	0	1	-2	-2	-1	-1	1	1
T	-2	0	1	0	-2	0	-1	-1	0	0

To solve equation A.6, add row 1 and row 2 and replace row 2 with the outcome.

The resulting left hand side is illustrated in Table A.2.

Table A.2: Calculation of identity matrix step 2

	ΔP	d_p	t	L	$\Delta \rho g$	$\frac{\sigma \cos}{\Theta}$	μ_g	μ_L	h	W
	x1	x2	x3	x4	x5	x6	x7	x8	x9	x10
M	1	0	0	0	1	1	1	1	0	0
L	0	1	0	1	-1	-1	0	0	1	1
T	-2	0	1	0	-2	0	-1	-1	0	0

Multiply row 1 by two and add it to row 3. Then, replace row 3 with resulting outcome. The resulting left hand side is illustrated in Table A.3.

Table A.3: Calculation of identity matrix step 3

	ΔP	d_p	t	L	$\Delta \rho g$	$\frac{\sigma \cos}{\Theta}$	μ_g	μ_L	h	W
	x1	x2	x3	x4	x5	x6	x7	x8	x9	x10
M	1	0	0	0	1	1	1	1	0	0
L	0	1	0	1	-1	-1	0	0	1	1
T	0	0	1	0	0	2	1	1	0	0

We now have 3 by 3 identity submatrix at the beginning of Table A.3. To complete the solution we will now bring right hand side into picture. The right hand side of the matrix has remained zero even after above mentioned row operations. Now we can solve 10 unknowns as follows:

$$x1 = -x5 -x6 -x7 -x8$$

$$x2 = -x4 +x5 +x6 -x9 -x10$$

$$x3 = -2x6 -x7 -x8$$

$$x4 = x4$$

$$x5 = x5$$

$$x6 = x6$$

$$x7 = x7$$

$$x8 = x8$$

$$x_9 = x_9$$

$$x_{10} = x_{10}$$

The above equations can be represented in the form of linear combination of the eigenvectors of the null space of the dimensionless matrix as shown below:

ΔP	x_1		0		-1		-1		-1		-1		0		0	
D_p	x_2		-1		1		1		0		0		-1		-1	
t	x_3		0		0		-2		-1		-1		0		0	
L	x_4	$=$	1	x_{4+}	0	x_{5+}	0	x_{6+}	0	x_{7+}	0	x_{8+}	0	x_{9+}	0	x_{10}
$\Delta \rho g$	x_5		0		1		0		0		0		0		0	
$\sigma \cos$	x_6		0		0		1		0		0		0		0	
Θ	x_7		0		0		0		1		0		0		0	
μg	x_8		0		0		0		0		1		0		0	
μL	x_9		0		0		0		0		0		1		0	
h	x_{10}		0		0		0		0		0		0		1	
W																

(A.9)

The variables associated with each exponential power are placed in column 1 of equation A.9. We can observe 10-3 i.e. 7 eigenvectors of the null space of A in equation A.9. The eigenvectors are as follows

$$\begin{array}{c}
e1 = \\
\left| \begin{array}{c} 0 \\ -1 \\ 0 \\ 1 \\ 0 \\ 0 \\ 0 \\ 0 \\ 0 \\ 0 \\ 0 \end{array} \right|
\end{array}
\begin{array}{c}
e2 = \\
\left| \begin{array}{c} -1 \\ 1 \\ 0 \\ 0 \\ 1 \\ 0 \\ 0 \\ 0 \\ 0 \\ 0 \\ 0 \end{array} \right|
\end{array}
\begin{array}{c}
e3 = \\
\left| \begin{array}{c} -1 \\ 1 \\ -2 \\ 0 \\ 0 \\ 1 \\ 0 \\ 0 \\ 0 \\ 0 \\ 0 \end{array} \right|
\end{array}
\begin{array}{c}
e4 = \\
\left| \begin{array}{c} -1 \\ 0 \\ -1 \\ 0 \\ 0 \\ 0 \\ 1 \\ 0 \\ 0 \\ 0 \\ 0 \end{array} \right|
\end{array}
\begin{array}{c}
e5 = \\
\left| \begin{array}{c} -1 \\ 0 \\ -1 \\ 0 \\ 0 \\ 0 \\ 0 \\ 1 \\ 0 \\ 0 \\ 0 \end{array} \right|
\end{array}
\begin{array}{c}
e6 = \\
\left| \begin{array}{c} 0 \\ -1 \\ 0 \\ 0 \\ 0 \\ 0 \\ 0 \\ 0 \\ 1 \\ 1 \\ 0 \end{array} \right|
\end{array}
\begin{array}{c}
e7 = \\
\left| \begin{array}{c} 0 \\ -1 \\ 0 \\ 0 \\ 0 \\ 0 \\ 0 \\ 0 \\ 0 \\ 1 \\ 1 \end{array} \right|
\end{array}$$

Step 5

Now we are ready to obtain 7 complete and independent dimensionless groups by making nontrivial solutions of equation A.6. Equation A.9 suggests that nontrivial solution can be obtained by arbitrarily choosing values of $x_4, x_5, x_6, x_7, x_8, x_9, x_{10}$. Let us choose $x_4 = 1$, and $x_5 = x_6 = x_7 = x_8 = x_9 = x_{10} = 0$. Therefore, the solution becomes

$$\begin{array}{c}
\left| \begin{array}{c} \Delta P \\ D_p \\ t \\ L \\ \Delta \rho g \\ \sigma \cos \\ \Theta \\ \mu g \\ \mu L \\ h \\ W \end{array} \right|
\end{array}
\begin{array}{c}
\left| \begin{array}{c} x_1 \\ x_2 \\ x_3 \\ x_4 \\ x_5 \\ x_6 \\ x_7 \\ x_8 \\ x_9 \\ x_{10} \end{array} \right|
\end{array}
= e1 =
\begin{array}{c}
\left| \begin{array}{c} 0 \\ -1 \\ 0 \\ 1 \\ 0 \\ 0 \\ 0 \\ 0 \\ 0 \\ 0 \end{array} \right|
\end{array}$$

Now, substitute the powers corresponding to each variable to obtain dimensionless π group.

$$\pi_1 = \frac{L}{D_p}$$

Similarly, to obtain next dimensionless group we substitute $x_5 = 1$, and $x_4 = x_6 = x_7 = x_8 = x_9 = x_{10} = 0$. The solution can be represented as follows

ΔP	x_1		-1
D_p	x_2		1
t	x_3		0
L	x_4	$= e_2 =$	0
$\Delta \rho g$	x_5		1
$\sigma \cos \Theta$	x_6		0
μg	x_7		0
μL	x_8		0
h	x_9		0
W	x_{10}		0

Now, substitute the powers corresponding to each variable to obtain second dimensionless π group.

$$\pi_2 = \frac{D_p * \Delta \rho g}{\Delta P}$$

Next, we substitute $x_6 = 1$, and $x_4 = x_5 = x_7 = x_8 = x_9 = x_{10} = 0$. The solution can be represented as follows

ΔP	x1	= e3 =	-1
Dp	x2		1
t	x3		-2
L	x4		0
$\Delta \rho g$	x5		0
$\sigma \cos \theta$	x6		1
μg	x7		0
μL	x8		0
h	x9		0
W	x10		0

Above solution can be represented as

$$\pi_3 = \frac{D_p * (\sigma \cos \theta)}{\Delta P * t^2}$$

For the next dimensionless group, we substitute $x7 = 1$, and $x4 = x5 = x6 = x8 = x9 = x10 = 0$. The solution can be represented as follows

ΔP	x1	= e4 =	-1
Dp	x2		0
t	x3		-1
L	x4		0
$\Delta \rho g$	x5		0
$\sigma \cos \theta$	x6		0
μg	x7		1
μL	x8		0
h	x9		0
W	x10		0

Above solution can be represented as

$$\pi_4 = \frac{\mu_g}{\Delta P * t}$$

For the next dimensionless group, we substitute $x_8 = 1$, and $x_4 = x_5 = x_6 = x_7 = x_9 = x_{10} = 0$. The solution can be represented as follows

ΔP	x_1	$= e_5 =$	-1
D_p	x_2		0
t	x_3		-1
L	x_4		0
$\Delta \rho g$	x_5		0
$\sigma \cos \Theta$	x_6		0
μg	x_7		0
μL	x_8		1
h	x_9		0
W	x_{10}		0

Above solution can be represented as

$$\pi_5 = \frac{\mu_L}{\Delta P * t}$$

For the next dimensionless group, we substitute $x_9 = 1$, and $x_4 = x_5 = x_6 = x_7 = x_8 = x_{10} = 0$. The solution can be represented as follows

ΔP	x_1	= e6 =	0
D_p	x_2		-1
t	x_3		0
L	x_4		0
$\Delta \rho g$	x_5		0
$\sigma \cos \Theta$	x_6		0
μg	x_7		0
μL	x_8		0
h	x_9		1
W	x_{10}		0

Above solution can be represented as

$$\pi_6 = \frac{h}{D_p}$$

For the next dimensionless group, we substitute $x_{10} = 1$, and $x_4 = x_5 = x_6 = x_7 = x_8 = x_9 = 0$. The solution can be represented as follows

ΔP	x_1	= e7 =	0
D_p	x_2		-1
t	x_3		0
L	x_4		0
$\Delta \rho g$	x_5		0
$\sigma \cos \Theta$	x_6		0
μg	x_7		0
μL	x_8		0
h	x_9		0
W	x_{10}		1

Above solution can be represented as

$$\pi_7 = \frac{W}{D_p}$$

Above dimensionless groups can be combined as follows to obtain dimensionless time.

$$t_d = \frac{\pi_1 * \pi_5 * \pi_6 * \pi_7}{\pi_2 * \pi_3^{0.5} * \pi_4}$$

$$t_d = \left(\frac{d_p^3}{L * W * h} \right) * \left(\frac{\mu_g}{\mu_L} \right) * \left(\frac{d_p * \Delta \rho g}{\Delta P} \right) * \left(\frac{\Delta P}{d_p * (\sigma \cos \theta)} \right)^{0.5} * t \quad (\text{A.10})$$